

**SYNTHESIS AND PHOTOCHEMISTRY OF A FEW
OLEFIN APPENDED DIBENZOBARRELENE
AND BISDIBENZOBARRELENE**

THESIS SUBMITTED TO THE
COCHIN UNIVERSITY OF SCIENCE AND TECHNOLOGY
IN PARTIAL FULFILMENT OF THE
REQUIREMENTS FOR THE DEGREE OF

DOCTOR OF PHILOSOPHY

IN

CHEMISTRY

IN THE FACULTY OF SCIENCE

BY

AMBILY MARY JACOB

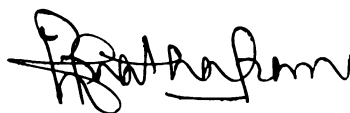
DEPARTMENT OF APPLIED CHEMISTRY
COCHIN UNIVERSITY OF SCIENCE AND TECHNOLOGY
COCHIN - 682 022

March 2008

CERTIFICATE

This is to certify that the thesis herewith is an authentic record of research work carried out by the author under my supervision, in partial fulfilment of the requirements for the degree of Doctor of Philosophy of Cochin University of Science and Technology, and further that no part thereof has been presented before for any other degree.

Kochi-22
12th March, 2008



Dr. Prathapan S.
(Supervising Guide)
Reader in Organic Chemistry
Department of Applied Chemistry
Cochin University of Science and
Technology
Kochi-682 022

DECLARATION

I hereby declare that the work presented in this thesis entitled: **“Synthesis and Photochemistry of a few Olefin appended Dibenzobarrelenes and Bisdibenzobarrelenes”** is original and was carried out by me independently under the supervision of Dr. Prathapan S., Reader in Organic Chemistry, Department of Applied Chemistry, Cochin University of Science and Technology, Kochi-682 022, India, and has not been included in any other thesis submitted previously for the award of any other degree.

Kochi-22
12th March, 2008


Ambily Mary Jacob

Acknowledgements

"In all thy ways acknowledge Him, and He shall direct thy paths" (Proverbs 3:6). I consider this opportunity as a golden moment in my life, to praise Lord Jesus Christ, the One who has brought me this far and sustained me throughout the years. If it were not for His love and provision, nothing would have been possible.

My utmost gratitude goes to my research supervisor Dr. S. Prathapan, Reader, Department of Applied Chemistry, Cochin University of Science and Technology, for giving me an opportunity to be in his research team, for his excellent guidance, valuable suggestions, outstanding support and for instilling in me a passion for research.

I am obliged to Prof. K. Girish Kumar, Head, Department of Applied Chemistry, Dr. M. R. Prathapachandrasekhar and Dr. S. Sugunan for providing the facilities to carry out the research work. Thanks are also due to Dr. P. A. Unnikrishnan for his concern and support at various stages of my research and Dr. Manoj N. Pillai for introducing me into the realm of photophysics. I acknowledge my sincere thanks to all the teaching and non-teaching staff of this department.

I offer my wholehearted thanks to Dr. A. C. Bhasikuttan, Scientific Officer, Bhabha Atomic Research Centre (BARC), Trombay, for helping me to conduct the photophysical studies. I am grateful to Dr. Guru Row, IISc, Bangalore for the X-ray crystallographic study. My heartfelt thanks to Dr. K. L. Sebastian, IISc, Bangalore, for helping me in utilizing the various facilities at IISc. Sincere thanks to Dr. R. Govindarajan, NIBRI, Lucknow, for the HPLC study.

I earnestly thank CDRI, Lucknow; IISc, Bangalore and STIC, Kochi for providing the necessary spectral and analytical data.

The financial support received from Department of Science and Technology, Delhi and from Council of Scientific and Industrial Research, Delhi is gratefully acknowledged.

I thank my senior lab mates, Jean John Vadakkān, Vidya Raman and Vishnuunni, for giving me an insight into the fundamentals of research. My wholehearted thanks to Rekha R. Mallia and Roshini K. Thumpakara, for the nice time we had together and for helping me to nurture my skills as an organic chemist. I also thank John P. R. and Samith, for their suggestions at various stages of my research. My appreciation to my juniors, Gisha, Jayakumar and Saino, for their timely assistance.

My days in Athulya Hostel with Maya, Radhika, Shali, Kochurani, Sreeja, Rinku, Nisha, Rehana and many more dear friends, will forever be cherished. I also take this opportunity to thank my friends in neighbouring labs especially Manju, Seena, Sreesha and Arun for their help during my research.

The boundless love, constant support and enduring prayers of my parents guides me throughout my life. I will forever remain indebted to them for transforming my dreams and aspirations into reality. To them I dedicate this thesis. To my loving sister Bindu, my best companion, I am especially grateful for her endless encouragement and vibrant support, be it physical or emotional.

To my in-laws, who are more like my parents, I remain indebted to them for their loving support. The last successful year of my doctoral studies was the outcome of their care, compassion and their value for education.

Finally, the person who has transformed my world, is my husband Rejie, whose motivation, sheer patience and whose belief in me more than I have myself, navigated me smoothly through the period of my doctoral studies and it is through him that I am able to fulfil my cherished dream of attaining my Ph.D.

Ambily Mary Jacob

CONTENTS

	Page	
ABSTRACT	1	
CHAPTER 1		
Diels-Alder Reaction, Di-π-methane Rearrangement and Energy Transfer Process in Organic Photochemistry: An Overview		
1.1	Abstract	
1.2	Introduction	10
1.3	Diels-Alder Reaction	11
1.3.1	The Diene and the Dienophile	12
1.3.2	Stereochemical Course of Diels-Alder Reactions	13
1.3.3	Frontier Orbital Interactions in Diels-Alder Reactions	16
1.3.4	Regioselectivity of Diels-Alder Reaction	18
1.3.5	Solvent Effects on Diels-Alder Reaction	20
1.3.6	Acceleration of Diels-Alder Reactions by Lewis Acid Catalysts	21
1.3.7	Effect of Pressure on Diels-Alder Reaction	22
1.3.8	Tandem Diels-Alder Reactions	22
1.3.9	Hetero Diels-Alder Reactions	25
1.3.10	Intramolecular Diels-Alder Reactions	26
1.4	Di- π -methane Rearrangement	27
1.4.1	Reaction Multiplicity	30
1.4.2	Regioselectivity of Di- π -methane Rearrangement	33
1.4.3	Regioselectivity Exhibited by Barrelene Related Molecules	35
1.4.4	Regioselectivity Exhibited by Dibenzobarrelenes	37
1.4.5	Photochemistry of Molecules Possessing Bisbarrelene Moieties	50
1.5	The Concept of Energy Transfer in Organic Photochemistry	52
1.5.1	Radiative Transfer	52
1.5.2	Radiationless Transfer	53
1.5.3	Quenching of Photochemical Reactions	54
1.5.4	Mechanistic Studies	55
1.5.5	Ideal Triplet Quencher	55
1.6	Outline of Research Problem and its Importance	57

	1.7	Objectives References	59
CHAPTER	2	Synthesis of 9-Olefin appended Anthracenes and Bisanthracenes	
	2.1	Abstract	
	2.2	Introduction	67
	2.3	Results and Discussion	70
	2.4	Experimental References	77
CHAPTER	3	Synthesis of Olefin appended Dibenzobarrelenes and Bisdibenzobarrelenes	
	3.1	Abstract	
	3.2	Introduction	87
	3.3	Results and Discussion	89
	3.4	Experimental References	103
CHAPTER	4	Preliminary Time-Resolved Fluorescence Studies of Some Olefin appended Dibenzobarrelenes and Bisdibenzobarrelenes Employing TCSPC Technique	
	4.1	Abstract	
	4.2	Introduction	116
	4.3	Results and Discussion	126
	4.4	Conclusion References	143
CHAPTER	5	Photochemistry of Olefin appended Dibenzobarrelenes and Bisdibenzobarrelenes	
	5.1	Abstract	
	5.2	Introduction	146
	5.3	Results and Discussion	155
	5.4	Conclusion	169
	5.5	Experimental References	170

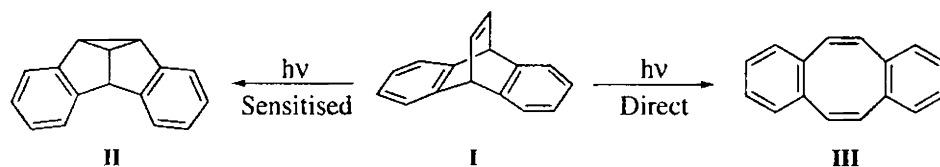
The thesis entitled: ‘**Synthesis and Photochemistry of a few Olefin appended Dibenzobarrelenes and Bisdibenzobarrelenes**’ is divided into 5 chapters.

In **Chapter 1**, the fundamental concepts of Diels-Alder reaction, di- π -methane rearrangement and energy transfer process in organic photochemistry is discussed. **Chapter 2** presents the synthesis of 9-olefin appended anthracenes and bisanthracenes. **Chapter 3** deals with the synthesis of olefin appended dibenzobarrelenes and bisdibenzobarrelenes. **Chapter 4** describes the preliminary time-resolved fluorescence studies of some olefin appended dibenzobarrelenes and bisdibenzobarrelenes. **Chapter 5** portrays the photochemistry of olefin appended dibenzobarrelenes and bisdibenzobarrelenes.

Chapter 1: Diels-Alder Reaction, Di- π -methane Rearrangement and Energy Transfer Process in Organic Photochemistry: An Overview

Ever since the discovery of di- π -methane rearrangement, dibenzobarrelenes, tailored with different substituents at various positions, have always been a tool to photochemists in unravelling the mechanisms of light induced reactions.

Dibenzobarrelenes (**I**) upon sensitised irradiation, the di- π -methane photoproduct, dibenzosemibullvalenes (**II**) are formed through the triplet excited state and (**I**) upon direct irradiation produce dibenzocyclooctatetraene (**III**) through the singlet excited state (Scheme A 1). But the absence of a clear line of demarcation between the singlet and triplet state reactivity of these bicyclic compounds, often results in a mixture of photoproducts from both the excited states.



Scheme A 1

Literature precedences indicate that olefins act as efficient triplet quenchers. In principle, we aimed at introducing a suitable π -system that can act as an intramolecular quencher for the dibenzobarrelene triplet, and moreover an olefin moiety at the bridgehead position opens up a tetra- π -methane system which could produce interesting photochemistry.

Two dibenzobarrelene moieties interlinked at the bridgehead position through a dienone moiety, creates a molecular architecture which might hold great potential in understanding the energy transfer process in bichromophoric systems.

Chapter 2: Synthesis of 9-Olefin appended Anthracenes and Bisanthracenes

As the first step in the synthesis of the targeted dibenzobarrelenes and bisdibenzobarrelenes, we synthesised the corresponding 9-alkenylanthracenes and bisanthracenes listed in Chart 1. Grignard reaction between anthrone and vinylmagnesium bromide gave 9-vinylanthracene **21a**, whereas the Grignard reaction between anthrone and allylmagnesium chloride gave 9-allylanthracene **21b** in appreciable yields. Wittig reaction between 9-anthraldehyde and benzyltriphenylphosphonium chloride gave 9-styrylanthracene **21c**. *trans,trans*-1,5-Bis(9-anthryl)-penta-1,4-dien-3-one **22** and *trans*-1-(9-anthryl)-1-buten-3-one **21d** were prepared through acid catalysed Claisen-Schmidt condensation of 9-anthraldehyde and acetone.

Base catalysed Claisen Schmidt condensation of 9-anthraldehyde and acetophenone, gave *trans*-3-(9-anthryl)-1-phenylprop-2-en-1-one **21e**. Claisen Schmidt condensation of 9-anthraldehyde and 2-butenone, under both acid and base catalysed conditions failed to generate **23** in synthetically viable yields. However, base catalysed Claisen Schmidt condensation of 9-anthraldehyde and cyclohexanone gave 2,6-bis(9-anthryl)cyclohexa-2,6-dien-1-one **24** in good yields.

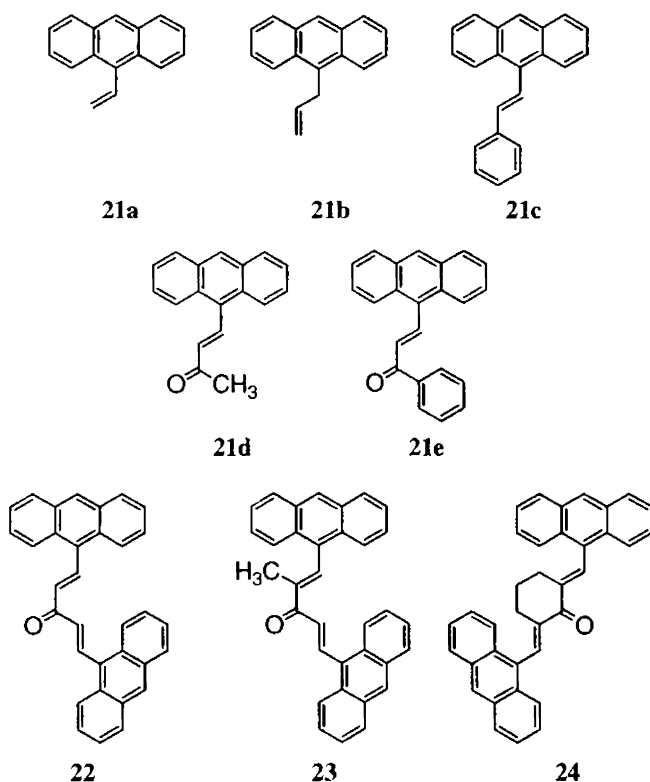
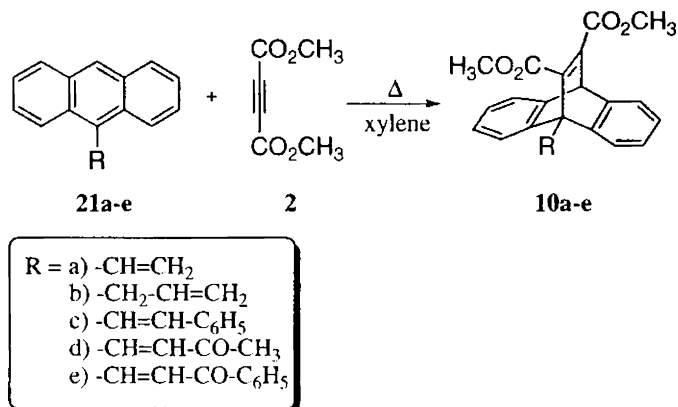


Chart 1

Chapter 3: Synthesis of Olefin appended Dibenzobarrelenes and Bisdibenzobarrelenes

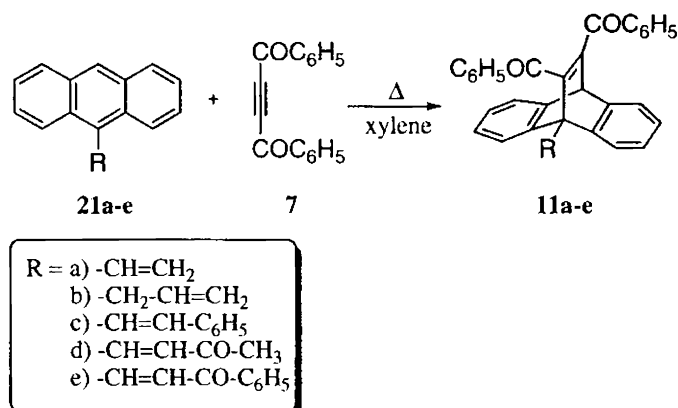
Diels-Alder reaction was used as the synthetic tool for the synthesis of

the target dibenzobarrelenes and bisdibenzobarrelenes. The corresponding 9-olefin appended dimethyl 9,10-dihydro-9,10-ethenoanthracene-11,12-dicarboxylate **10a-e** were obtained upon refluxing the 9-olefin appended anthracenes with dimethyl acetylenedicarboxylate (DMAD) in xylene for 8-10 h (Scheme A 2).



Scheme A 2

Diels-Alder reaction between the 9-olefin appended anthracenes and dibenzoyl acetylene (DBA) gave the corresponding 9-olefin appended 11,12-dibenzoyl-9,10-dihydro-9,10-ethenoanthracenes **11a-e** (Scheme A 3).



Scheme A 3

The novel bisdibenzobarrelenes **12,13** and **14,15** (Chart 2) were synthesised *via* the Diels-Alder reaction of the corresponding bisanthracenes as the bisdienes with DMAD or DBA as the dienophiles. All new compounds were fully characterised on the basis of spectral and analytical data.

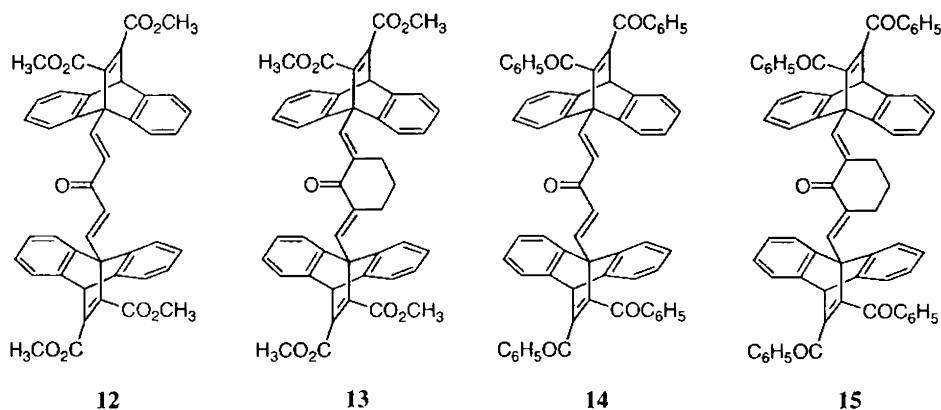


Chart 2

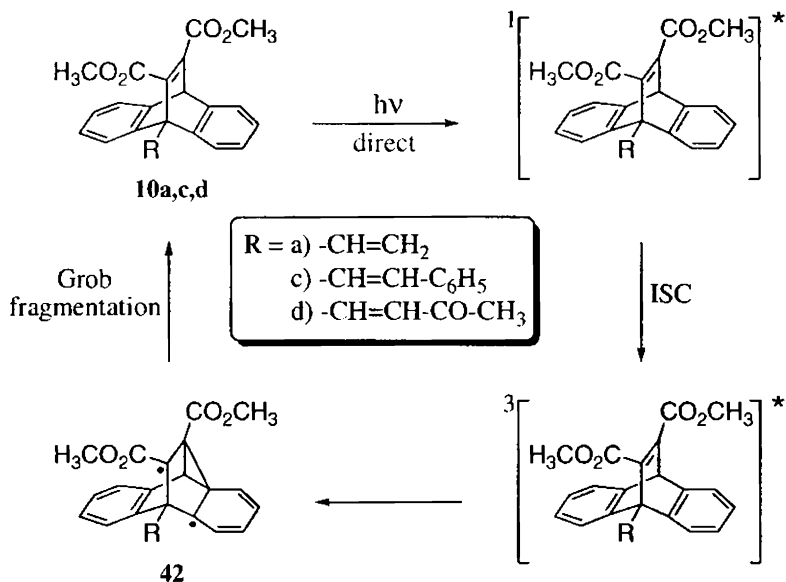
Chapter 4: Preliminary Time-Resolved Fluorescence Studies of Some Olefin appended Dibenzobarrelenes and Bisdibenzobarrelenes Employing TCSPC Technique

Time dependent fluorescence studies were conducted on some of these dibenzobarrelenes and bisdibenzobarrelenes using Time-Correlated Single-Photon Counting Spectrometer (TCSPC). The fluorescence λ_{max} showed marked sensitivity towards solvent polarity which establishes the formation of a charge transfer state in the excited state of the molecules. The fluorescence decay pattern showed a biexponential or triexponential decay which indicates complex processes involved in the deactivation of these compounds. The fluorescence quantum yield measurements, calculated using 4-(dimethylamino)benzonitrile as standard, indicate substantial interaction between the olefin appendages and the dibenzobarrelene units in the excited

state.

Chapter 5: Photochemistry of Olefin appended Dibenzobarrelenes and Bisdibenzobarrelenes

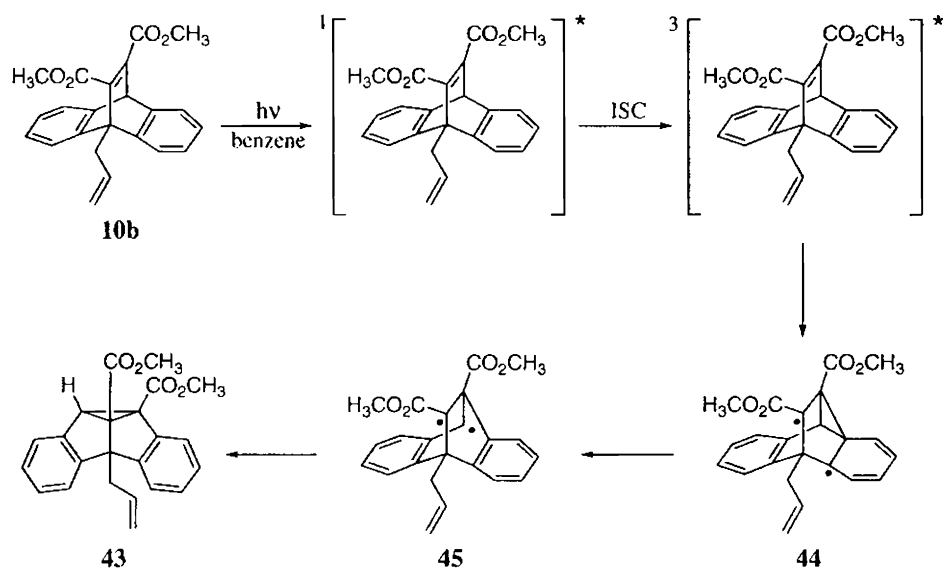
As the $S_0 \rightarrow S_1$ transition in dibenzobarrelenes takes place at 280 nm, all irradiations were carried out using RPR 300 nm lamps. Chemical literature reveals that carbomethoxy groups have an enhanced rate of intersystem crossing. A triplet mediated photoisomerization, in the case of **10a,c,d** could have resulted in the reversion of the 1,4-biradicals **42** to the ground state dibenzobarrelenes **10a,c,d** (Scheme A 4).



Scheme A 4

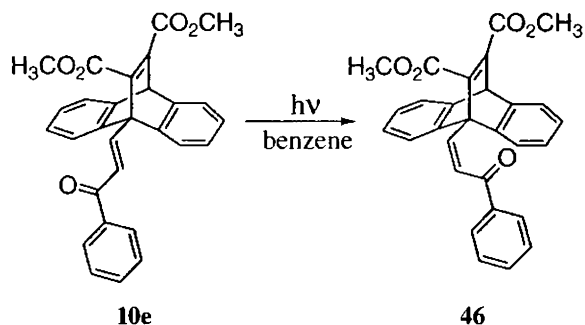
Irradiation of dimethyl 9-(prop-1-ene)-9,10-dihydro-9,10-ethenoanthracene-11,12-dicarboxylate **10b** gave the 4b-substituted dibenzosemibullvalene **43** as the photoproduct, *via* the di- π -methane

rearrangement shown in Scheme A 5.



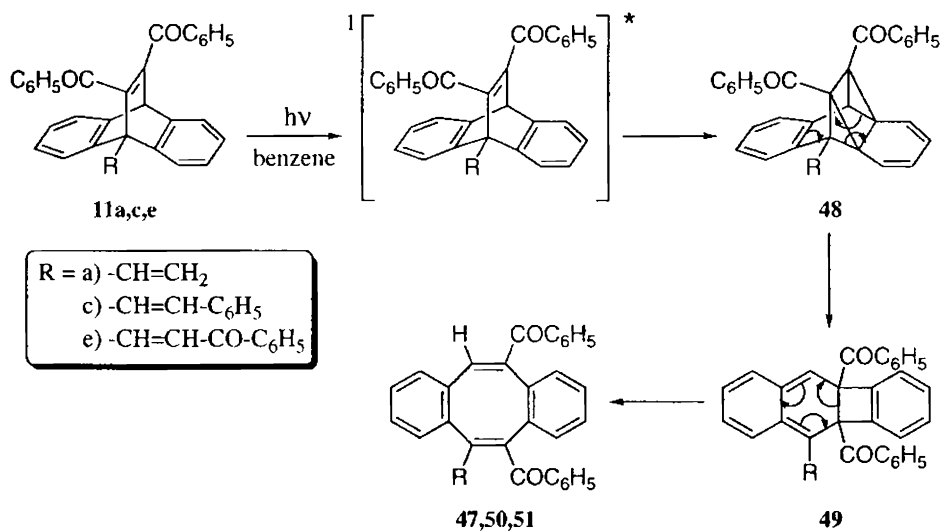
Scheme A 5

Irradiation of dimethyl 9-(1-phenylprop-2-en-1-one)-9,10-dihydro-9,10-ethenoanthracene-11,12-dicarboxylate **10e** led to *cis-trans* isomerisation of the olefin moiety as the only observed transformation, indicating efficient intramolecular quenching of the triplet excited state of the dibenzobarrelene by the bridgehead olefin (Scheme A 6).



Scheme A 6

Photochemistry of 11,12-dibenzoyl substituted dibenzobarrelenes indicated efficient triplet quenching in the case of **11a,c,e** bearing vinyl, styryl and 1-phenylprop-2-en-1-one respectively at the 9-position. In all the cases, singlet mediated cyclooctatetraene formation was observed. A probable route for the formation of dibenzocyclooctatetraenes **47,50,51** is shown in Scheme A 7. This result is in contrast to the preferential semibullvalene formation in the case of several 11,12-dibenzoyl-9,10-ethenoanthracenes reported earlier.



Scheme A 7

Photolysis of **11b** in benzene at 300nm, gave a complex mixture of photoproducts, which we were unable to isolate and identify.

Irradiation of **11d** in benzene at 300nm, gave a photoproduct having a lactone ring, as identified via the IR spectral analysis, but the photoproduct could not be separated and identified due to low yield and its structural identity has not been established.

Contrary to our expectations, irradiation of novel bisdibenzobarrelenes

12,13 and **14,15** synthesised by us did not give rise to any isolable products. Unchanged starting material was isolated in substantial amounts even after prolonged irradiation under different conditions.

Note: The numbers given to various compounds herein correspond to those given in respective chapters. All new compounds were fully characterised on the basis of spectral and analytical data. We have reported only the relevant data for the characterisation of novel compounds synthesised by us.

Diels-Alder Reaction, Di- π -methane Rearrangement and Energy Transfer Process in Organic Photochemistry: An Overview

1.1. Abstract

The present chapter outlines the fundamental concepts, based on which our investigations were formulated. The concepts considered here include Diels-Alder reaction, di- π -methane rearrangement and energy transfer process in organic photochemistry.

1.2. Introduction

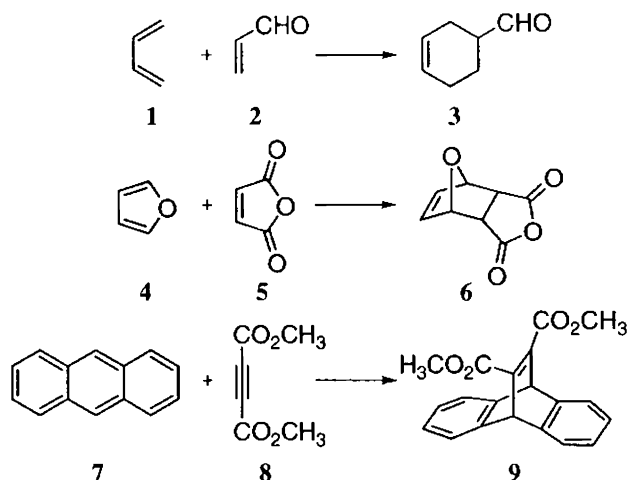
Organic chemistry is one of the prerequisites of modern science. Through organic synthesis, we are able to synthesise the most complicated natural products, which possess the exact three-dimensional structure of those isolated from nature. The realisation of the most difficult synthetic tasks would be a tremendous accomplishment to the intellectual expertise of the community of synthetic chemists.

Our investigations on the photochemical and photophysical behaviour of a few olefin-appended dibenzobarrelenes and bisdibenzobarrelenes, constitute the core of this thesis. The intention of appending various olefins at the bridgehead position of dibenzobarrelenes, was to assess its efficiency as an intramolecular quencher of triplet excited state of dibenzobarrelenes. The photobehaviour of the novel bisdibenzobarrelenes is yet to be explored. In this chapter an overview of the three basic building blocks of this thesis i.e., Diels-Alder reaction, di- π -methane rearrangement and energy transfer process

in organic photochemistry ^{is} ~~are~~ presented.

1.3. Diels-Alder Reaction

Diels-Alder reaction is one of the most versatile and useful processes in the repertoire of synthetic chemistry. [2+4] Cycloadditions are called Diels-Alder reactions in honor of Otto Diels and Kurt Alder, the chemists who carried out the first such reaction.¹ This cycloaddition consists of the addition of a "dienophile", which are olefinic and acetylenic compounds to the 1,4-positions of a conjugated diene system with the formation of a ~~six-membered~~ ^{cyclohexene} hydroaromatic ring.² Up to four stereocenters may be constructed in one Diels-Alder reaction and the great number of possible substrates gives the reaction great scope.



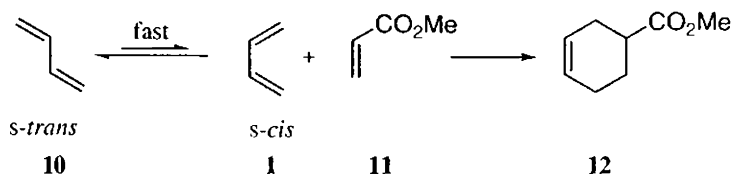
Scheme 1

Diels-Alder reaction is one of the most important synthetic routes for six-membered rings and it is one of the most important stereoselective C-C bond-forming reactions in general.³ The additions of various diene systems to dienophiles shown in Scheme 1 are typical examples of Diels-Alder reaction.

The olefinic dienophiles yield cyclohexene derivatives and the acetylenic dienophiles lead to derivatives of 1,4-dihydrobenzene.

1.3.1. The Diene and the Dienophile

The diene component in Diels-Alder reaction can be open chain or cyclic and it can have many different kinds of substituents. For the Diels-Alder reaction to occur, the diene must be able to adopt the *s-cis* conformation⁴ (Scheme 2). In butadiene, the *s-trans* conformer **10** is preferred over the *s-cis* conformation **1**. But only the *s-cis* conformer is capable of taking part in the Diels-Alder reaction.⁵



Scheme 2

Cyclopentadiene, a cyclic diene that is permanently in the *s-cis* conformation is exceptionally good at Diels-Alder reaction. But cyclic dienes that are permanently in the *s-trans* conformation and cannot adopt *s-cis* conformation, will not undergo Diels-Alder reaction at all.⁶ Furan, cyclohexadiene, cycloheptadiene, anthracene are some examples of dienes that are permanently in the *s-cis* conformation. 1,3-Butadienes with alkyl-, aryl-, alkoxy-, and trimethylsilyloxy substituents are some examples of acyclic dienes.

The dienophiles, active in Diels-Alder reaction can be divided into two main groups: ethylenic and acetylenic.⁷ In the ethylenic compounds, the double bond is usually conjugated with one or more unsaturated groups, but

simple ethylenes have also been found to undergo Diels-Alder reaction. The acetylenic compounds which have been employed contain the triple bond in conjugation with one or more carbonyl or cyanide groups.

Ethylenic Compounds



where $R = H, CH_3, C_6H_5$



Acetylenic Compounds



where $R = H, CH_3, C_6H_5$



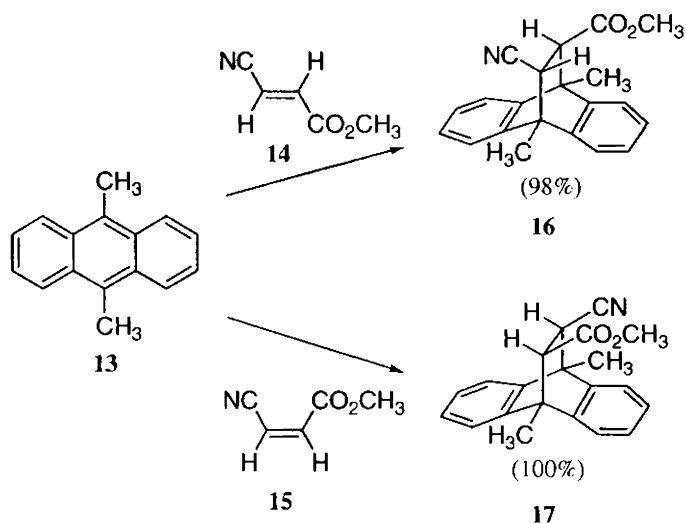
1.3.2. Stereochemical Course of Diels-Alder Reactions

Diels-Alder reaction exhibits pronounced stereochemical selectivity. The configuration of the adduct formed conforms to the following general principles⁸ commonly known as the "*cis*" principle and the Alder "*endo*" rule. In certain special cases, anomeric effect is also prominent.

1.3.2.1. The "*cis*" Principle

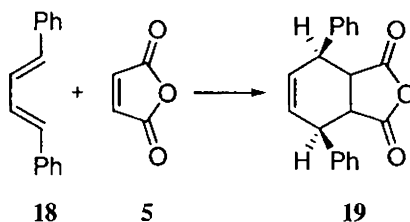
The addition of a dienophile to a diene is a purely *cis* addition. The relative positions of substituents are retained in the adduct. The reliability of the rule is one of the major factors in the importance of the Diels-Alder reaction in synthesis and in stereochemical studies. The almost universal strict *cis* addition can be readily explained by synchronous formation of the bonds between the two components in a one-step reaction.⁹ *cis*- or *trans*-Dienophiles react with dienes to give 1:1 adducts in which the *cis* or *trans* arrangement of

the substituents in the dienophile is retained, exhibiting the stereoselective nature of the Diels-Alder reaction. An illustrative example is shown for the reactions of the isomeric methyl β -cyanoacrylates **14** and **15** with 9,10-dimethylantracene¹⁰ **13** (Scheme 3).



Scheme 3

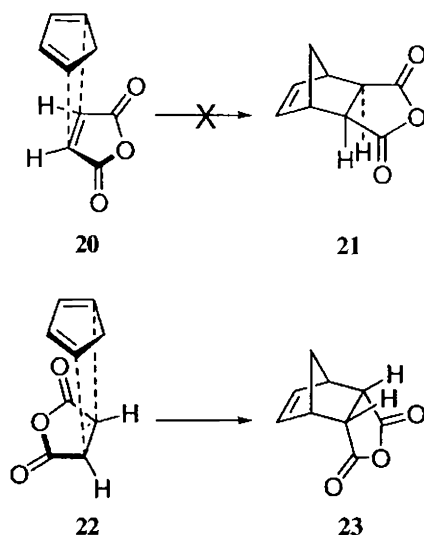
The *cis* principle applies also to substituents in the diene components, thereby exhibiting its stereospecificity with regard to the diene as shown in Scheme 4. In the 1:1 adduct **19**, which can be obtained almost quantitatively from *trans,trans*-1,4-diphenylbutadiene **18** and maleic anhydride **5** by refluxing in benzene, the phenyl groups are *cis* to each other.¹¹



Scheme 4

1.3.2.2. The Alder "endo" Rule

The title "endo" is derived from the strong propensity of most dienophile substituents to orient in the endo configuration in the bridged bicyclic adducts formed from cyclic dienes. The combination of cyclic dienes with cyclic dienophiles could in principle follow two courses. But in general, only one of these is actually realized. In the reaction of maleic anhydride with cyclopentadiene, two modes of addition are theoretically possible, leading to the formation of an "exo" adduct **21** or an "endo" compound **23** respectively. Actually, the endo configuration is produced exclusively.¹²



Scheme 5

After a "sandwich-like" preorientation of the reactants, the dienophile is added in such a way as to give a "maximum concentration" of double bonds⁸ in the transition state. The favoured orientation **22** corresponds to the maximum accumulation of double bonds. According to Alder and Stein, this includes not only the π systems directly involved in the reaction, but also those

of the "activating ligands". It has been calculated¹³ that the attractive forces between the two molecules are greater in the *endo* orientation than in the *exo* orientation. The principle of maximum accumulation of unsaturated centers point to the physical reality that electrostatic and electrodynamic attractive forces associated with the mobile electronic systems, not directly involved in the bond-forming processes lower the energy of intermediates such as **23** as compared with the type **21**.¹⁴

1.3.3. Frontier Orbital Interactions in Diels-Alder Reactions

Frontier molecular orbital¹⁵ (FMO) theory as first expressed by Fukui¹⁶ continues to be used extensively by synthetic organic chemists for the prediction of the reactivity and selectivity of many organic reactions. As pertains to the Diels-Alder reaction, predictions of reactivity and selectivity are normally based on the strength of a single FMO interaction between the diene and the dienophile, the so-called "dominant" interaction. The dominant interaction is usually taken to be the one involving the two frontier orbitals having the smallest energy gap between them.¹⁷ As shown in Figure 1, when the $\text{HOMO}_{\text{diene}} - \text{LUMO}_{\text{dienophile}}$ energy gap is least, the reaction is called a "normal Diels-Alder cycloaddition" (NDAC), while when the $\text{HOMO}_{\text{dienophile}} - \text{LUMO}_{\text{diene}}$ energy gap is smallest, the reaction is termed as "inverse-electron-demand Diels-Alder cycloaddition" (IEEDAC).

Dienophiles with conjugating groups are usually good for Diels-Alder reactions. Dienes react rapidly with electrophiles because their HOMOs are relatively high in energy, but simple alkenes have relatively high-energy LUMOs and do not react well with nucleophiles. The most effective modification is to lower the alkene LUMO energy by conjugating the double bond with an electron-withdrawing group such as carbonyl or nitro. This type of Diels-Alder reaction, involving an electron-rich diene and an electron-

deficient dienophile are referred to as Diels-Alder reactions with normal electron demand.¹⁹

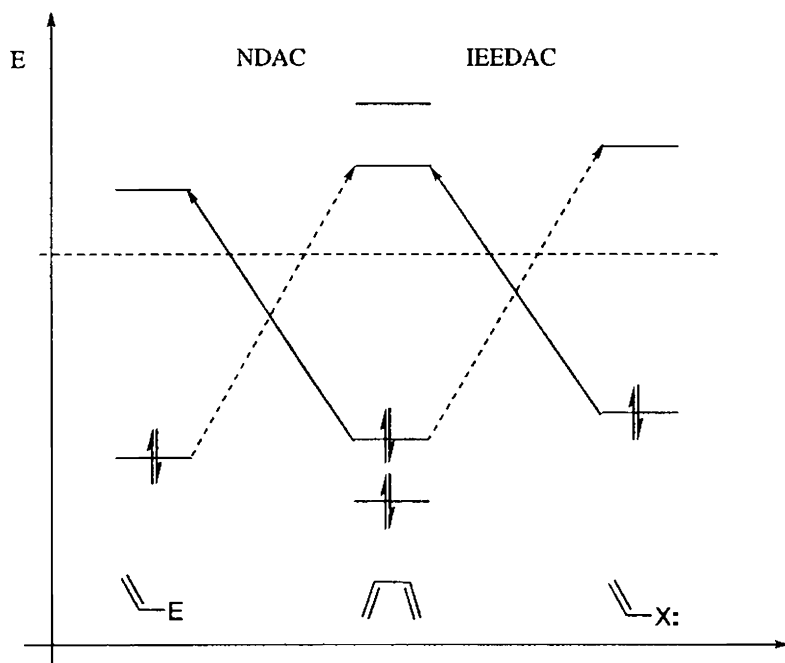
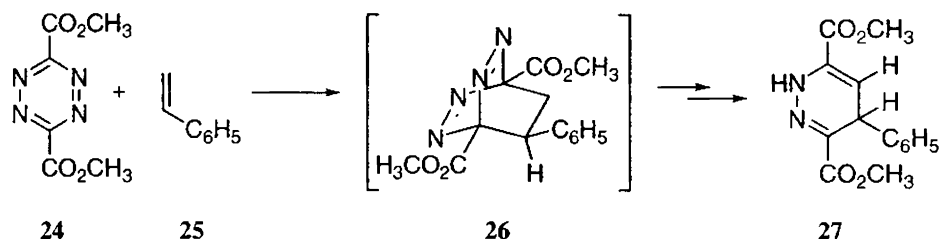


Figure 1. Frontier orbitals in normal and inverse electron-demand Diels-Alder cycloadditions¹⁸

Diels-Alder reactions may also occur when the electronic situation of the substrates is completely reversed, that is when electron-rich dienophiles react with electron-poor dienes. [4+2] Cycloadditions of this type are called Diels-Alder reactions with inverse electron demand.^{20,21} 1,3-Dienes that contain heteroatoms such as O and N in the diene backbone are the dienes of choice for this kind of cycloaddition. The reaction of 1,2,4,5-tetrazine-3,6-dicarboxylate **24** with styrene **25** producing 1,4-dihydropyridazines²² **27** is an example of inverse electron demand Diels-Alder reaction (Scheme 6).

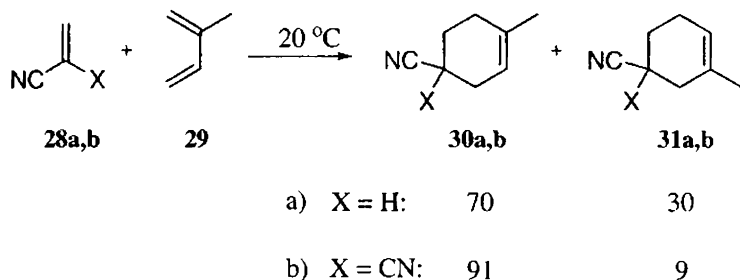


Scheme 6

1.3.4. Regioselectivity of Diels-Alder Reaction

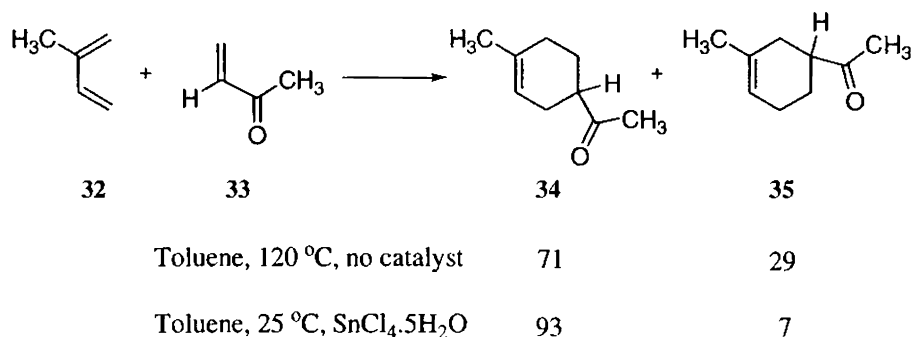
Constitutionally homogeneous cycloadducts are obtained through symmetrically substituted dienes and dienophiles. In contrast, when an unsymmetrical diene and an unsymmetrical dienophile combine in a Diels-Alder reaction, the reaction itself becomes unsymmetrical and it may afford two constitutionally isomeric cycloadducts. The specific regioisomeric behaviour of Diels-Alder reaction was interpreted through the application of simple perturbation theories.²³ The reaction remains concerted but, in the transition state, bond formation between the largest LCAO coefficients in the closest pair of frontier orbitals, in each partner is more advanced and this determines the regioselectivity of the reaction.^{24, 25}

1,3-Butadienes with alkyl substituents in the 2-position favour the formation of the so-called *para* products in their reactions with acceptor-substituted dienophiles (Scheme 7). The so-called *meta* product is formed in smaller amounts. This orientation selectivity increases if the dienophile carries two geminal acceptors. 2-Phenyl-1,3-butadiene exhibits a higher "*para*" selectivity in its reactions with every asymmetric dienophile than any 2-alkyl-1,3-butadiene does.¹⁹



Scheme 7

Catalysis by Lewis acids can influence the regiochemistry of Diels-Alder reactions. The reaction of but-3-en-2-one **33** with 2-methyl-1,3-butadiene **32** under non-catalytic conditions leads to a mixture of two adducts in the proportion 71:29.²⁶ Addition of tin tetrachloride, effects almost exclusive formation of the isomer **34** (Scheme 8). The complexing of dienes and dienophiles by Lewis acids changes the energetic position and the structure of the frontier orbitals²⁷ and thus it affects the regiochemistry (*vide infra*).



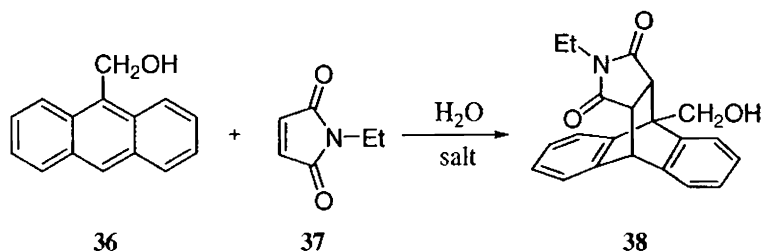
Scheme 8

Apart from the dominant HOMO-LUMO interactions, secondary orbital interactions are as additional modifying factors for the regioselectivity of Diels-Alder reaction.²⁸ They are supposed to enhance the orientation

behaviour indicated by primary interactions.

1.3.5. Solvent Effects on Diels-Alder Reaction^{29,30}

Pericyclic reactions with chargeless transition states, were considered to be insensitive to solvent effects.³¹ The pioneering discovery of Rideout and Breslow in 1980, reveals the dramatic acceleration of Diels-Alder reactions in aqueous solutions.³² The rates of Diels-Alder reactions have been accelerated by factors up to 1.3×10^4 in aqueous solution as compared to organic solvents. The principal effect was ascribed to hydrophobic association of the diene with the dienophile. Blokzijl and Engberts suggested that "enforced hydrophobic interaction" due to a decrease in the overall hydrophobic surface area during the activation process is a key factor in determining the rate acceleration in water.³³ Other interpretations of the acceleration of Diels-Alder reactions beyond the former two primary effects involve micellar effects, internal pressure, solvophobicity and enhanced hydrogen bonding to the transition state.



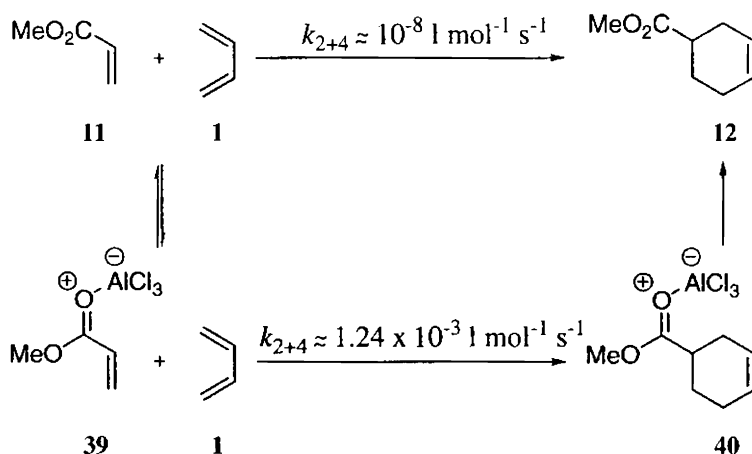
Scheme 9

A striking example is the Diels-Alder reaction of anthracene-9-carbinol **36** with *N*-ethylmaleimide **37** (Scheme 9).³⁴ The second order rate constant of the reaction, when carried out in water at 45 °C was over 200 times larger than in acetonitrile, showing^{ed} the expected effects of dissolved salts. With 4.86 M

lithium chloride the rate in water at 45 °C of the aforementioned reaction, increases by 2.5 fold; lithium chloride is a solute which increases hydrophobic effects, decreasing the solubility of hydrocarbons in water.

1.3.6. Acceleration of Diels-Alder Reactions by Lewis Acid Catalysts³⁵

Yates *et al.*³⁶ were the first to recognize the significant increase in the reaction rates of Diels-Alder reactions upon the addition of a catalytic amount of AlCl_3 . Further studies showed that Lewis acids like BF_3 , SnCl_4 , TiCl_4 also catalysed the reaction.³⁷ An additional advantage of Lewis acid catalysed Diels-Alder reaction is that the reaction temperature can be lowered by more than 100 °C with no decrease in rate.



Scheme 10

The catalytic action is due to complex formation between the Lewis acid and the polar groups of the activating substituents in the dienophile (e.g. in maleic anhydride, ethyl maleate etc) or in the diene⁹ (reaction of tetraphenyl cyclopentadienone with ethylene). The Lewis acid catalysed Diels-Alder reaction of methyl acrylate **11** with butadiene **1** is 10^5 times faster than in the

absence of Lewis acid (Scheme 10). The Lewis acid coordinates at the Lewis base side of the dienophile, for example, at the carbonyl oxygen of methyl acrylate, making the carbonyl group even more electron-withdrawing and thus more reactive.

According to the FMO theory, a Lewis acid that binds to the electron-withdrawing group of the dienophile catalyses the reaction by lowering the LUMO of the dienophile. In the presence of Lewis acids, *cis-trans* isomeric dienophiles give diastereoisomeric adducts just as in the uncatalysed reaction, revealing that Lewis acid catalysed Diels-Alder reactions also are pure *cis* additions.³⁸

1.3.7. Effect of Pressure on Diels-Alder Reaction³⁹⁻⁴¹

Pressure exerts an exceptionally large accelerating effect on Diels-Alder reaction⁴² and this phenomenon has been exploited both for mechanistic⁴³ and for synthetic purposes.⁴⁴ This effect is particularly important for gaseous reactants, for example, ethylene adds smoothly to dimethyl cyclohexa-1,3-diene-1,4-dicarboxylate at 165 °C/1000 atm.⁴⁵ The reaction of naphthalene with maleic anhydride at 10⁴ atm gives the 1:1 adduct in 78% yield, whereas at 1 atm and otherwise identical conditions the yield is only 1%.⁴⁶

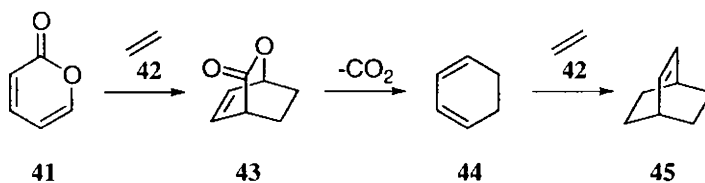
1.3.8. Tandem Diels-Alder Reactions

In the context of chemical reactions, "tandem" means two reactions which follow one another. The construction of multiple carbon-carbon bonds in a single chemical step represents an efficient method for the synthesis of complex molecular structures.⁴⁷ The intramolecular arene-olefin cyclization, applied by Wender⁴⁸ for the direct synthesis of a series of polycyclic

compounds is an excellent example of the utility of tandem Diels-Alder reaction.

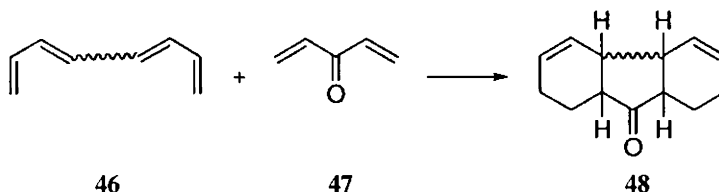
The nature by which the reaction cascades follow one another can be classified into two different ways: Interrupted and Uninterrupted cycloaddition.⁴⁹ An example of the interrupted cycloaddition is the extrusion of carbon dioxide from a pyrone Diels-Alder adduct **43** to generate a second diene moiety, 1,3-cyclohexadiene **44**, which can undergo a second cycloaddition reaction to give **45** as shown in Scheme 11. The uninterrupted cycloadditions can be further classified into (a) reaction sequences in which both diene-dienophile pairs are present in the starting compounds (Scheme 12) and (b) a sequential pathway in which the first cycloaddition opens up a new diene or dienophile which can then undergo a second cycloaddition reaction (Scheme 13).

Interrupted Biscycloaddition



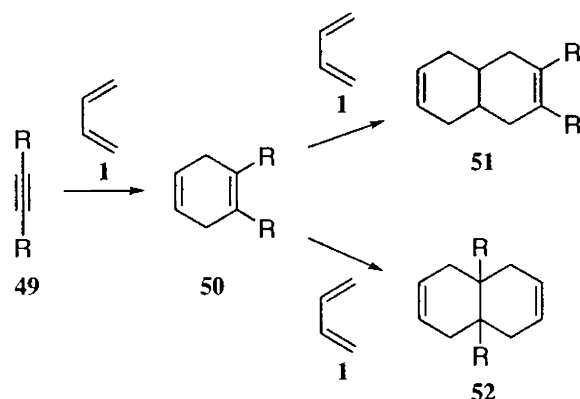
Scheme 11

Uninterrupted "Simultaneous"



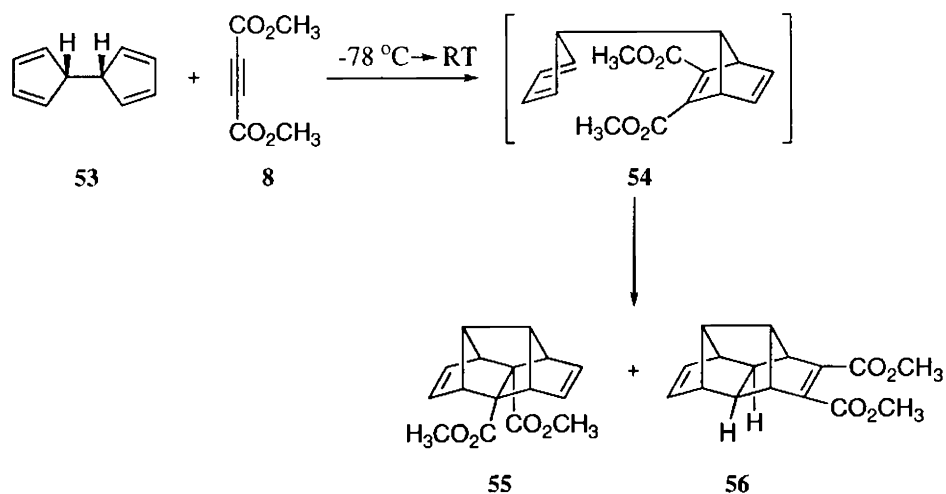
Scheme 12

Uninterrupted "Sequential"



Scheme 13

The most important application of this methodology is the Diels-Alder reaction of bicyclic bisdienes, which facilitate the synthesis of a variety of bridged polycyclic ring systems.



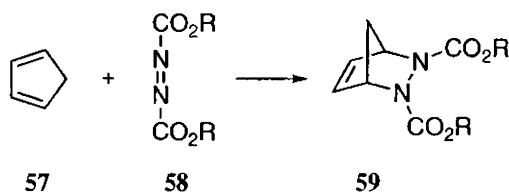
Scheme 14

Intermolecular Diels-Alder reaction of the bicyclic bisdiene 53 with dimethyl acetylenedicarboxylate 8 leads to the formation of a bimolecular

adduct **54**, which can then undergo intramolecular cycloaddition to give the bridged tetracyclic products **55** and **56**, in appreciable yield (Scheme 14).⁵⁰ This reaction termed as a "domino" Diels-Alder reaction, served as the cornerstone in the synthesis of dodecahedrane by Paquette.⁵¹

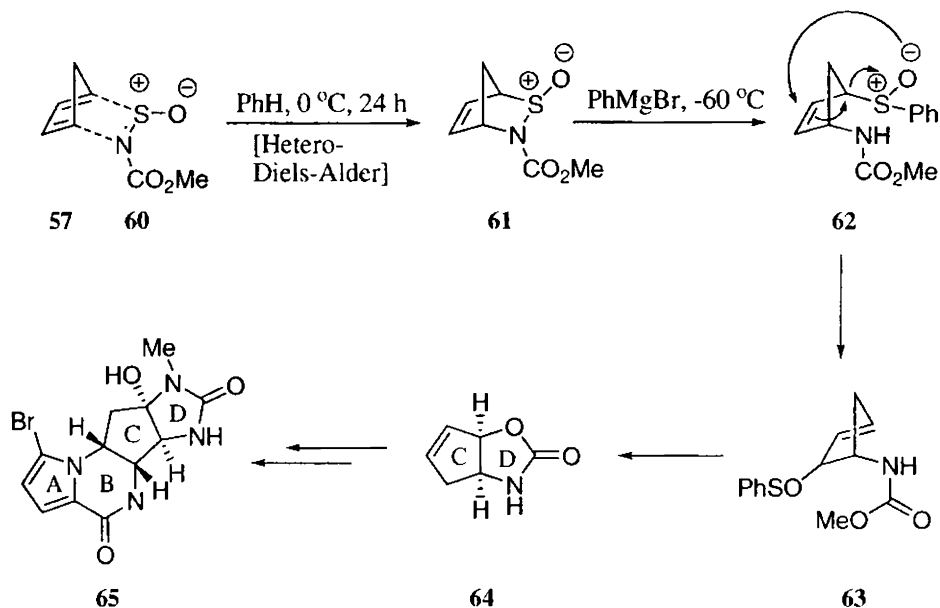
1.3.9. Hetero Diels-Alder Reactions

In hetero Diels-Alder reactions, those molecular systems are involved in which one or more atoms of the diene or the dienophile are heteroatoms, leading to the formation of heterocyclic systems. In the production of commercially useful organic intermediates and medicines,⁵² this technique has become an inevitable tool. In hetero Diels-Alder reactions, carbonyl compounds, nitroso compounds, nitrile group, imino group, alkyl azodicarboxylate etc can function as dienophiles, when they are activated by a strong electronegative group in conjugation with the double or triple bond.⁵³ The formation of the heterocyclic system **59** from cyclopentadiene **57** and azocarboxylic ester **58** is one of the earliest examples of synthesis by the Hetero Diels-Alder reaction⁵⁴ (Scheme 15).



Scheme 15

Hetero Diels-Alder reaction is a sharp synthetic tool in the field of natural product total synthesis.⁵⁵ The power of this hetero Diels-Alder based methodology is elegantly illustrated in the total synthesis of agelastatin A⁵⁶ **65** (Scheme 16).

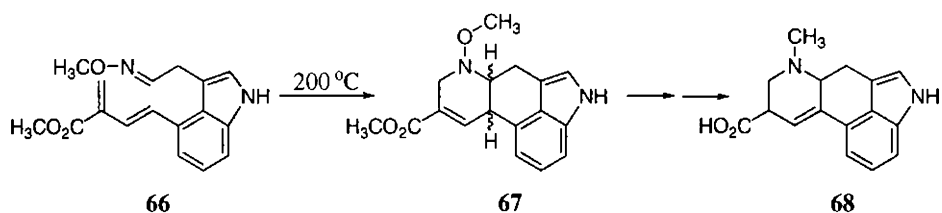


Scheme 16

1.3.10. Intramolecular Diels-Alder Reactions

In the intramolecular Diels-Alder reaction,^{57, 58} two rings are formed in one step. In addition to the six-membered ring formed by the [4+2] cycloaddition the product contains a second ring, the size of which depends on the length of the chain connecting diene and dienophile.⁵⁹ When compared to intermolecular Diels-Alder reaction, the two reacting functionalities are part of the same molecule in intramolecular Diels-Alder reaction, thus exhibiting less negative activation entropies and increased reaction rates under mild conditions. The constraints imposed by the connecting chain, together with the lower reaction temperatures, results in pronounced regio- and stereoselectivity. One of the most striking observations in the intramolecular Diels-Alder reaction is the fact that considerable strain can be accommodated in the product. So even substantial ring strain does not deter the reaction.⁶⁰

Intramolecular Diels-Alder reaction has become a most versatile method for the synthesis of polycyclic structures, particularly natural products. The special interest in it is the selective introduction of stereochemistry. The synthesis of a precursor molecule **67** of the alkaloid, lysergic acid **68** employing intramolecular Diels-Alder reaction⁶¹ is shown in Scheme 17.



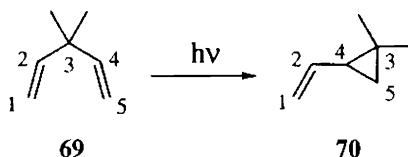
Scheme 17

1.4. Di- π -methane Rearrangement

Since the discovery of di- π -methane rearrangement by Zimmerman and Grunewald in 1966,⁶² this rearrangement has attracted much attention from organic chemists because of its importance in organic synthesis as well as its interesting mechanistic aspects. In view of the pioneering and extensive contributions of Zimmerman and coworkers to illustrate the generality of di- π -methane rearrangement, this rearrangement is also referred to as the Zimmerman rearrangement. The variants of di- π -methane rearrangement are the oxa-di- π -methane rearrangement,⁶³ in which one of the two π -moieties is a carbonyl group and the aza-di- π -methane rearrangement⁶⁴ has a C-N double bond function as one of the π groups.

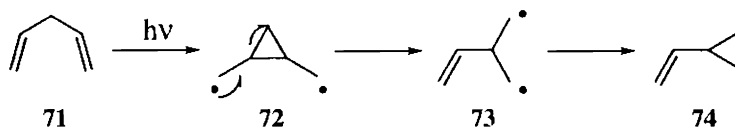
Di- π -methane rearrangement occurs on photolysis of molecules having two π moieties bonded to a single sp^3 -hybridised carbon atom. The rearrangement leads to a π -substituted cyclopropane. Formally, it involves migration of one π moiety originally bonded to the methane carbon C-3 to C-4

of the other π moiety with concomitant bonding between C-3 and C-5, resulting in the three-membered ring formation.⁶⁵

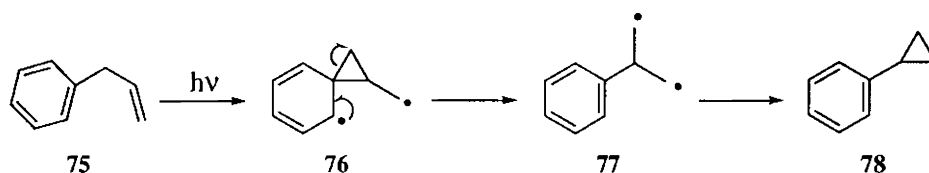


Scheme 18

Studies have shown that one basic mechanism^{66, 67} describes the skeletal change in the di- π -methane rearrangement. The mechanism is depicted in simple resonance terms in Scheme 19, where two vinyl groups are present. Scheme 20 depicts di- π -methane rearrangement in a molecular system where one of the two π -substituents is a phenyl group. These resonance structures, which have proved useful in describing photochemical mechanisms, are not necessarily intermediates but are approximations of species along the reaction coordinate, simply depicted by points on the energy hypersurface leading from excited state of reactant to ground state of product.⁶⁸

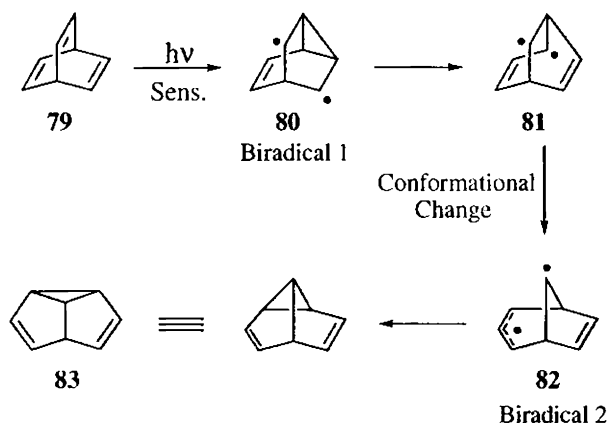


Scheme 19



Scheme 20

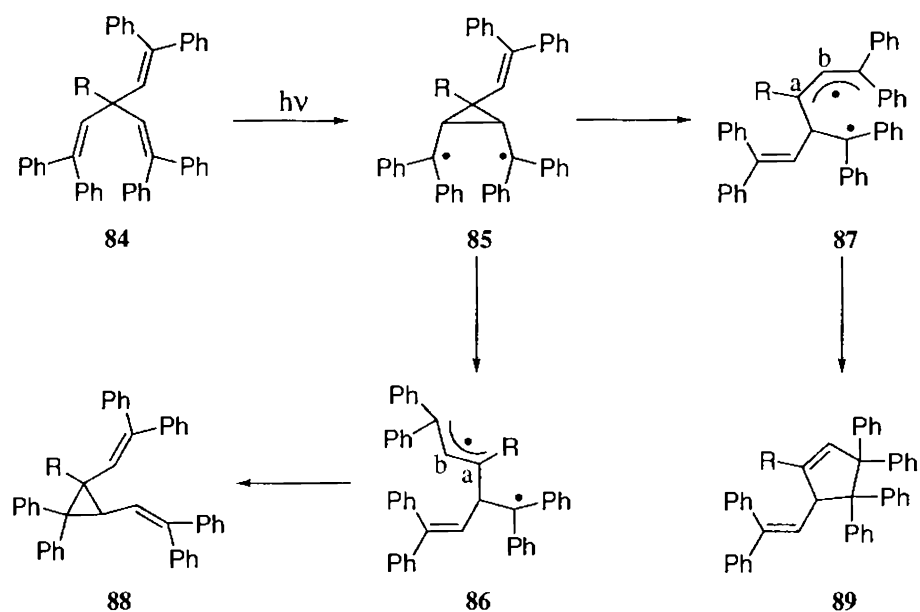
The photochemical conversion of barrelene **79** to semibullvalene **83** using acetone sensitisation,⁶⁹ prompted Zimmerman *et al.* to the reaction mechanism and to the generality of the di- π -methane rearrangement. The details of the molecular reorganisation occurring were demonstrated using hexadeuteriobarrelene,⁷⁰ in which the bridgehead carbons were undeuteriated. The pathway followed during di- π -methane rearrangement is depicted in Scheme 21. Interaction of orbitals at C-2 and C-4 of an electronically excited pentadiene, leads to the stabilization of the excited species, thus accounting for the vinyl-vinyl bonding in the initial steps of di- π -methane rearrangement.⁷¹



Scheme 21

The reactants with three π groups attached to the central carbon mechanistically are capable of affording both di- π -methane and tri- π -methane photoproducts.⁷² Scheme 22 shows the mechanism of the di- π -methane rearrangement and its potential diversion to a tri- π -methane pathway. In this, on excitation of **84**, the singlet or triplet bridges to give cyclopropyldicarbonyl diradical **85**. Opening of this species tends to give transoid (bond a-b) allylic diradical **86** as consequence of less steric interference. This species closes to

afford π -substituted cyclopropane product **88** characteristic of a di- π -methane rearrangement. In contrast, if cyclopropyldicarbonyl diradical opening were to lead to cisoid allylic diradical **87**, closure to tri- π -methane product **89** may compete with 1,3-closure to di- π -methane product **88**. Thus tri- π -methane rearrangement exhibits a parallelism with the di- π -methane rearrangement in the initial π - π bridging step with a preference for the more delocalised cyclopropyldicarbonyl diradical.⁷³



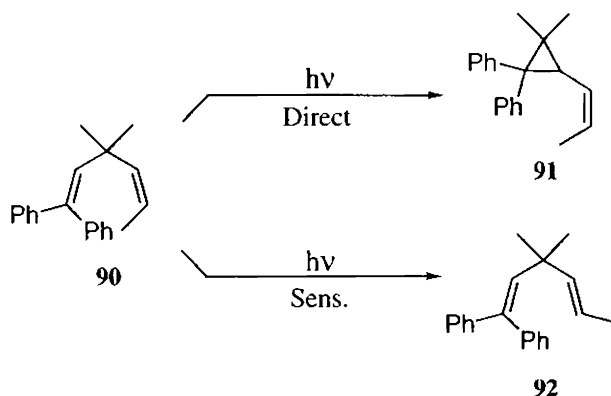
Scheme 22

1.4.1. Reaction Multiplicity

Di- π -methane rearrangement displays a photochemistry where the excited singlet and triplet states exhibit different intramolecular reactivity. Studies on numerous molecular systems led to the generalisation that acyclic di- π -methane reactants rearrange effectively from their singlet excited states,

whereas bicyclic di- π -methane systems prefer to rearrange via their triplet excited states.⁶⁷ Sensitisers used in di- π -methane rearrangement are mainly acetophenone, benzophenone and xanthone, which generate the triplet excited state of the di- π -methane reactant. At times, the singlet excited states produced without a sensitizer, might undergo intersystem crossing to their triplet excited states.

A noteworthy example of di- π -methane rearrangement in acyclic molecular systems is the rearrangement of 3,3-dimethyl-1,1-diphenyl-1,4-hexadiene **90** (Scheme 23).

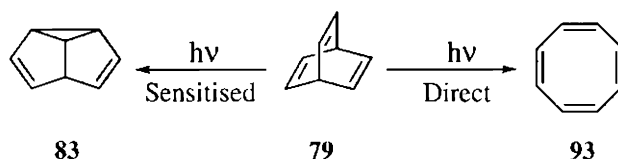


Scheme 23

This diene rearranges on direct irradiation through the singlet excited state to give vinylcyclopropane **91**. In contrast, sensitised irradiation through the triplet excited state leads to the *cis-trans* isomerisation of the diene (Scheme 23). The "free rotor effect" operates in the decay of the triplet excited states of those molecules, in which double bonds are not incorporated in a ring structure or not inhibited from free rotation.^{74,75}

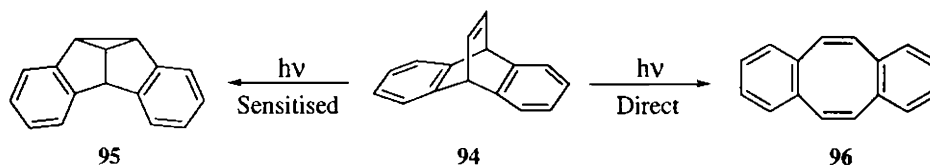
Triplet multiplicity is preferred for the di- π -methane rearrangements in rigidly constrained systems i.e., in structures which prohibit free rotation about

the π bonds. Zimmerman and coworkers⁶² have shown that barrelene **79**, which contains π moieties within rigidly structured environments, rearranges by the di- π -methane pathway to semibullvalene **83** solely by acetone sensitisation. The triplet excited states of bicyclic systems are incapable of "free rotor" energy dissipation due to their rigid structures, thus paving way for the conversion of the triplets to π -substituted cyclopropanes. The singlet excited states of many cyclic systems have potentially available facile alternative pericyclic processes which compete with di- π -methane rearrangement. Direct irradiation of barrelene **79** leads to cyclooctatetraene **93** by an electrocyclic $[2\pi + 2\pi]$ addition followed by a retro $2\pi + 2\pi$ fission⁷⁶ (Scheme 24).



Scheme 24

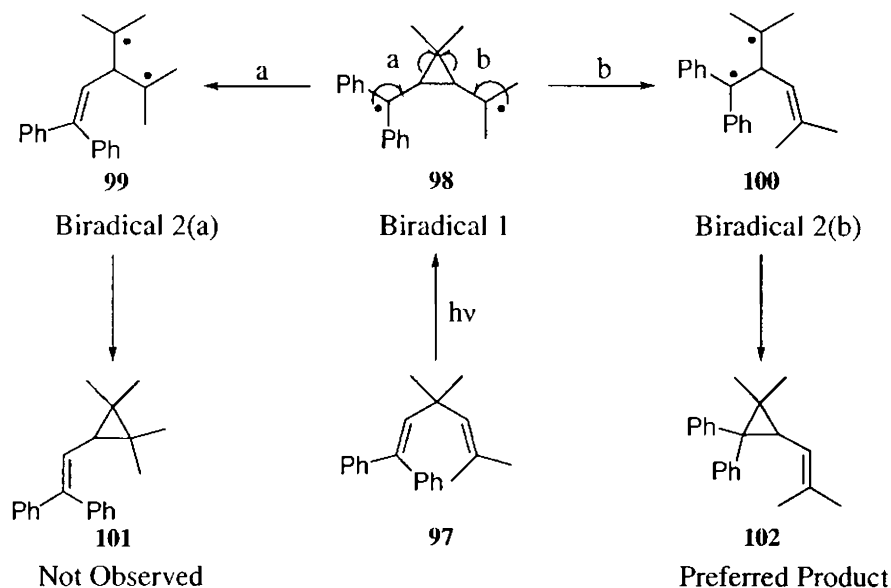
Dibenzobarrelenes **94** upon direct irradiation produce dibenzocyclooctatetraene **96** through the singlet excited state⁷⁷ and upon sensitised irradiation, the di- π -methane photoproduct, dibenzosemibullvalenes **95** are formed through the triplet excited state⁸⁴ (Scheme 25).



Scheme 25

1.4.2. Regioselectivity of Di- π -methane Rearrangement

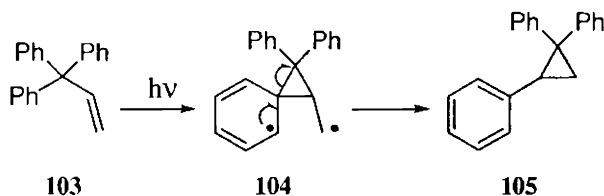
Di- π -methane rearrangement exhibits strong regioselectivity in an unsymmetric di- π -methane system i.e., the marked preference for migration of one of the two different π moieties attached to the methane carbon.



Scheme 26

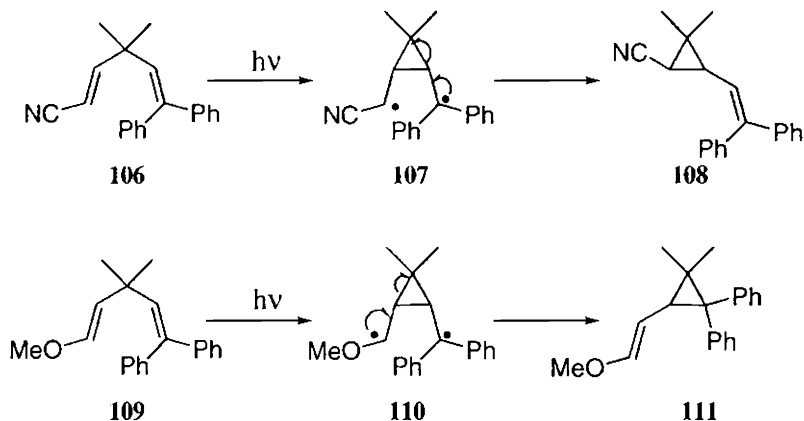
An illustrious example is found in the direct irradiation of 3,3,5-trimethyl-1,1-diphenyl-1,4-hexadiene **97** which leads to only one of the two *a priori* possible products⁷⁴ (Scheme 26). The regioselectivity exhibited in the photoproduct is understood on the basis of "biradical 1" undergoing three-ring opening preferentially by mechanism **b** rather than **a**. The cyclopropyldicarbonyl diradical opens up in such a way as to produce the more stable of two alternative 1,3-biradicals, in this case the one with benzhydryl delocalization is retained. The overall process can be summarised as a

preferential formation of that regioisomer which has the less delocalising group on the residual double bond. The regioselectivity of aryl-vinyl di- π -methane systems operate in such a way as to regenerate the aromatic system in the three-membered ring opening process as shown in Scheme 27.⁷⁸



Scheme 27

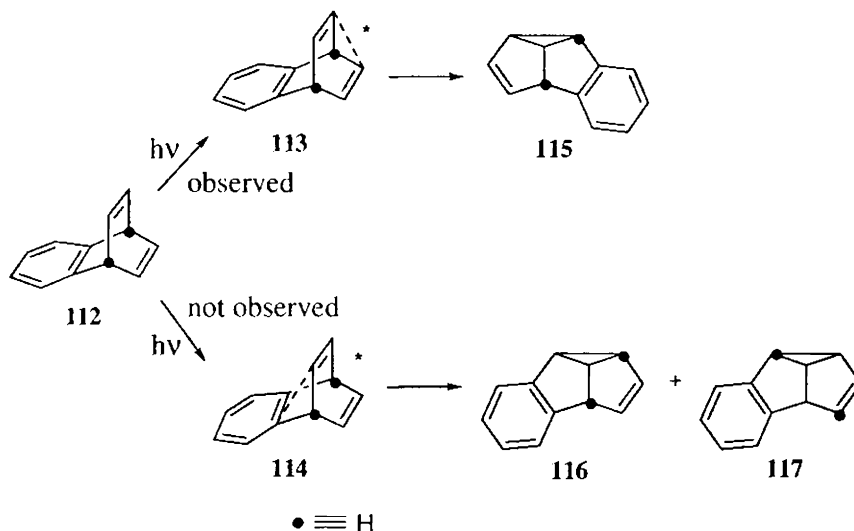
When heteroatom-bearing substituents are involved, then there is a strong tendency for electron donors to appear on the residual π -bond of the photoproduct and electron-withdrawing groups to be found on the cyclopropane product ring⁶⁵ (Scheme 28). This suggests that the carbonyl carbons in the cyclopropyldicarbonyl diradicals are electron rich and as the diradical opens its three-membered ring this negative charge is dissipated on the carbon developing π -bond character. Thus, with an electron-donating group present, there is driving force for the carbonyl carbon bearing this donor to be that involved in ring opening and in becoming the π -bonded carbon. Conversely, for electron-withdrawing substituents there is an advantage that the carbonyl carbon retains its electron-rich character and not being the one generating the π bond.



Scheme 28

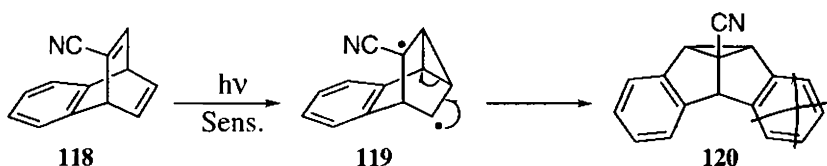
1.4.3. Regioselectivity Exhibited by Barrelene Related Molecules

In barrelene related molecules, we encounter "tri- π -methane" reactants, in which the three π -systems are bonded to a single "methane carbon". Non-equivalence in the three bridges, raises the question of which two π -systems will bond. Zimmerman and coworkers observed a preferential bonding between the two vinyl bridges rather than between benzo and vinyl bridges in the case of benzobarrelene,^{70,79} 2,3-naphthobarrelene⁸⁰ and related molecules. In the case of benzobarrelene (Scheme 29), the initial interaction between vinyl chromophores leads to a system **113** isoconjugate with triplet butadiene and so of lower triplet energy ($E_T = ca. 58 \text{ kcal/mol}$)⁷¹ than the species formed by vinyl-benzo interaction **114** and resembling styrene ($E_T = ca. 64 \text{ kcal/mol}$).¹² One exception is that of 1,2-naphthobarrelene where α -naphtho-vinyl bridging is preferred.⁸⁰



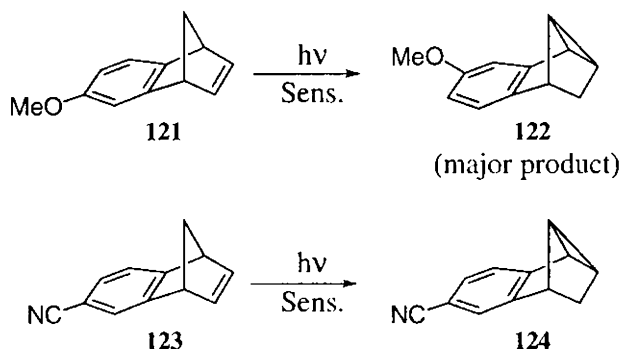
Scheme 29

A different variation in regioselectivity is encountered in systems where the two π -moieties are bonded to "methane carbons" at both ends, opening up two possible sites for the initial π - π bridging. A similar situation occurs in the rearrangement of 2-cyanobarrelene **118** studied by Bender⁸¹ (Scheme 30). Here the initial bridging occurs between two vinyl groups to leave the cyano group at an odd-electron center. Isotopic labeling ruled out benzo-vinyl bridging. The odd-electron not stabilised by the cyano group is utilised in the three-membered ring opening, leading to the observed photoproduct **120**.



Scheme 30

Paquette^{82,83} has shown that the photochemistry of substituted benzonorbornadienes, follow a similar regioselectivity. Scheme 31 illustrates that in methoxy-benzonorbornadiene, benzo-vinyl bridging occurs distal to the methoxy group while in the cyanobenzonorbornadiene, benzo-vinyl bridging takes place proximate to the cyano group. The regioselectivity is similar to that observed with electron-donating and -withdrawing substituents on acyclic di- π -methane systems, thus drawing the generalisation that electron donors avoid positioning themselves in conjugation with the carbonyl centers of the cyclopropyldicarbonyl biradicals and electron-withdrawing groups lead to stabilisation when so situated.

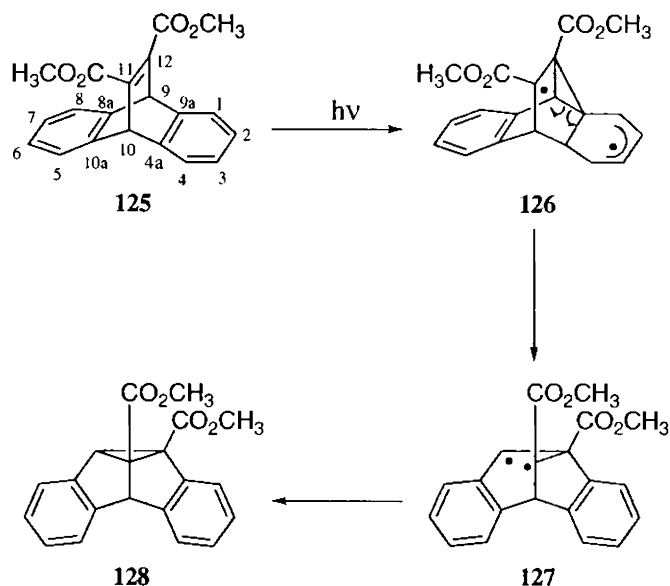


Scheme 31

1.4.4. Regioselectivity Exhibited by Dibenzobarrelenes (9,10-Ethanoanthracenes)

The photochemical studies conducted on several dibenzobarrelenes by Ciganek⁸⁴ and Friedman⁷⁷ indicated that electronic effects are important in determining the course of initial bonding in di- π -methane rearrangement. In fact Ciganek was the first to recognise the modest effect of the bridgehead substituent group on the bridging regioselectivity of di- π -methane

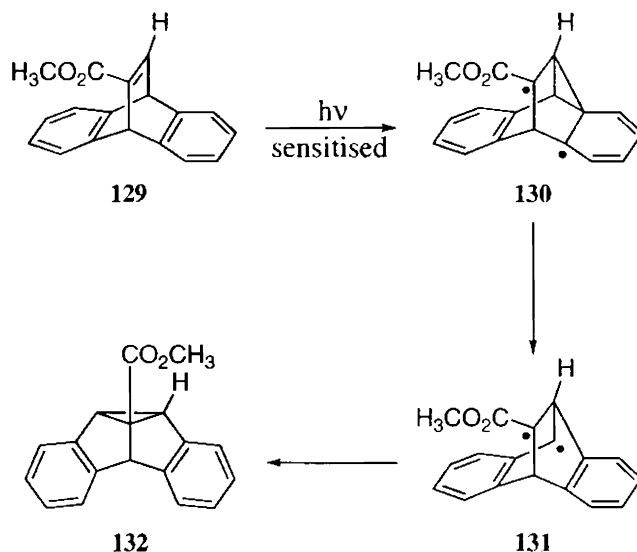
rearrangement. The mechanism⁸⁵ (Scheme 32) in the case of dibenzobarrelene **125** (applicable to all dibenzobarrelenes) is thought to involve (a) initial bonding between positions 9a and 12 ("benzo-vinyl" bridging) to afford the 1,4-biradical **126**, (b) cyclopropane ring cleavage to give 1,3-biradical **127** and (c) 1,3-biradical closure to form the dibenzosemibullvalene **128**. In Scheme 32, there are three additional pathways (II-IV) for a total mechanistic degeneracy of four, path I and II leading to one enantiomer of **128**, and paths III and IV giving the other.



Scheme 32

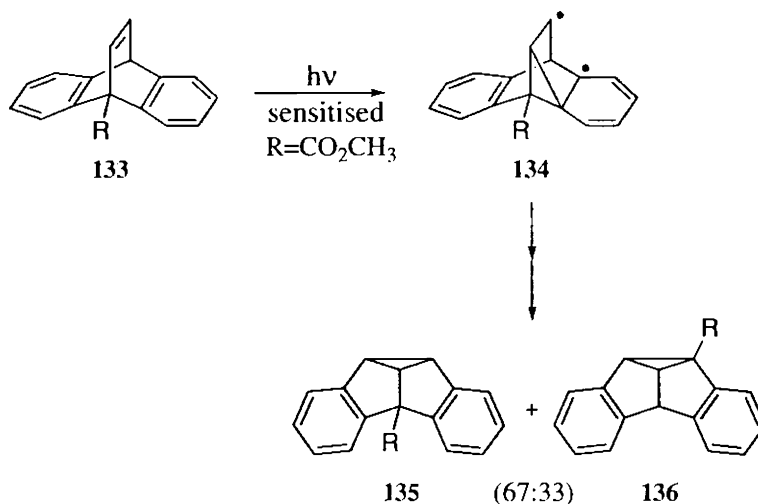
- Path I : Initial 9a-12 bonding
 Path II : Initial 10a-11 bonding
 Path III : Initial 4a-11 bonding
 Path IV : Initial 8a-12 bonding

In Scheme 33, the reactivity seen in the formation of the major dibenzosemibullvalene product **132**, from the irradiation of acetone or benzene solution of dibenzobarrelene **129**, could be readily explained on the basis of odd-electron stabilisation by the carbomethoxy group.⁷¹



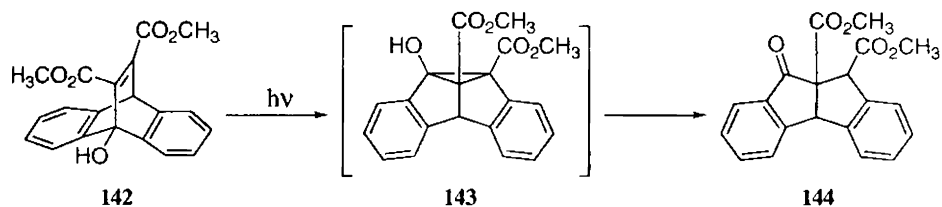
Scheme 33

In the dibenzobarrelene system **133**, substituted with methoxycarbonyl at the bridgehead position, unfavourable bridging at the end nearer to the group occurred, which was interpreted as arising from a reluctance to have the electronegative group held by a bond which becomes heavy in s character⁷¹ (Scheme 34).



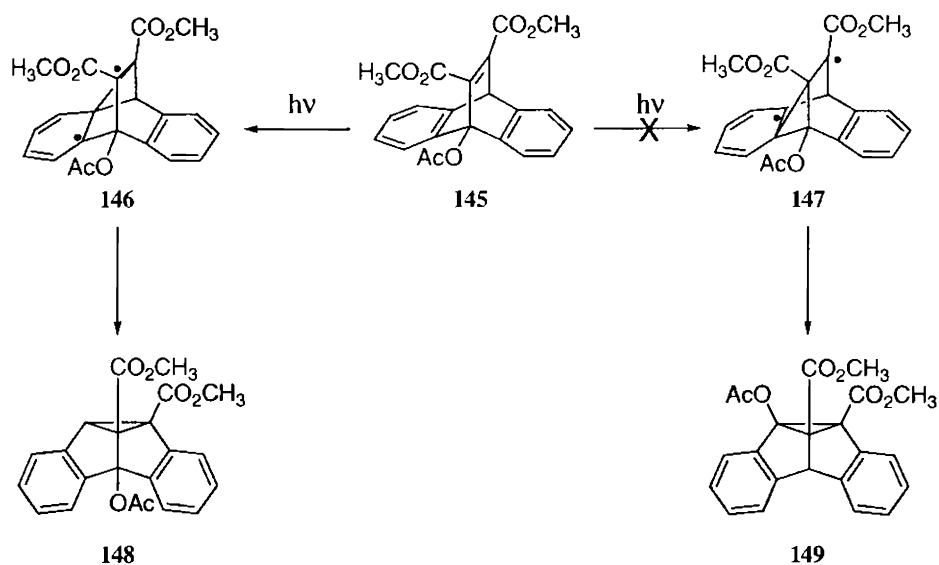
Scheme 34

Iwamura *et al.*⁸⁶ has disclosed the effect of a wider range of substituents at the methane position on the bridging selectivity in di- π -methane systems. As depicted in Scheme 35, there are two possible termini capable of competitive vinyl benzo bridging in the excited triplet states (path a and path b). These bridging regioselectivities would be interpreted in terms of the relative stability of the initially formed cyclopropyldicarbonyl diradicals 138 and 139. Experimental and theoretical studies show that π -electron acceptors such as CN, CO_2CH_3 and CHO at the bridgehead position, should stabilise the cyclopropane ring and thus favours bridging through path a, while π -electron donors such as OCH_3 should destabilise the cyclopropane ring and therefore favour path b.



Scheme 36

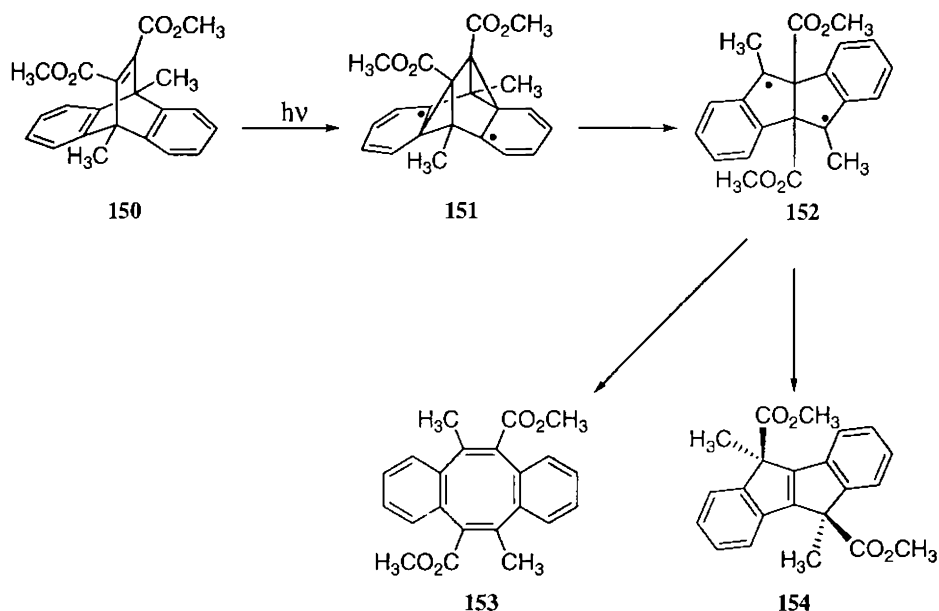
9-Acetydibenzobarrelene **145** upon irradiation in acetone⁸⁷ gave the dibenzosemibullvalene **148**. Scheme 37 shows that the electronegativity effect will favour the formation of **146** which will have only one electronegative substituent on the incipient cyclopropane ring compared with two in **147**.



Scheme 37

Scheffer and coworkers were the first to report the tri- π -methane rearrangement pathway for the photoisomerisation of dibenzobarrelenes.⁸⁸ They have observed that dimethyl 9,10-dimethyl-9,10-dihydro-9,10-

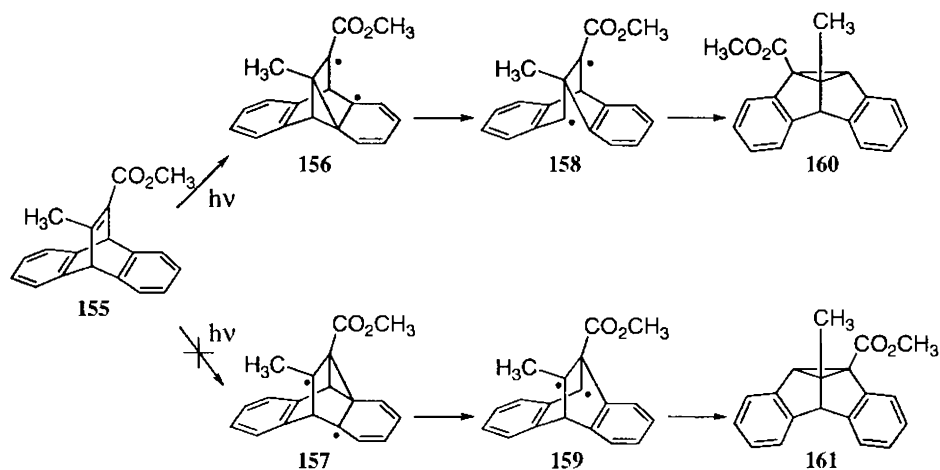
ethenoanthracene-11,12-dicarboxylate **150**, reacts from its singlet state in an unexpected manner to give photoproducts **153** and **154**, through the intermediacy of the bis-benzylic diradical **152** (Scheme 38). The involvement of a similar diradical intermediate was postulated in the photoisomerisation of dimethyl 9-chloromethyl-9,10-dihydro-9,10-ethenoanthracene-11,12-dicarboxylate.⁸⁹



Scheme 38

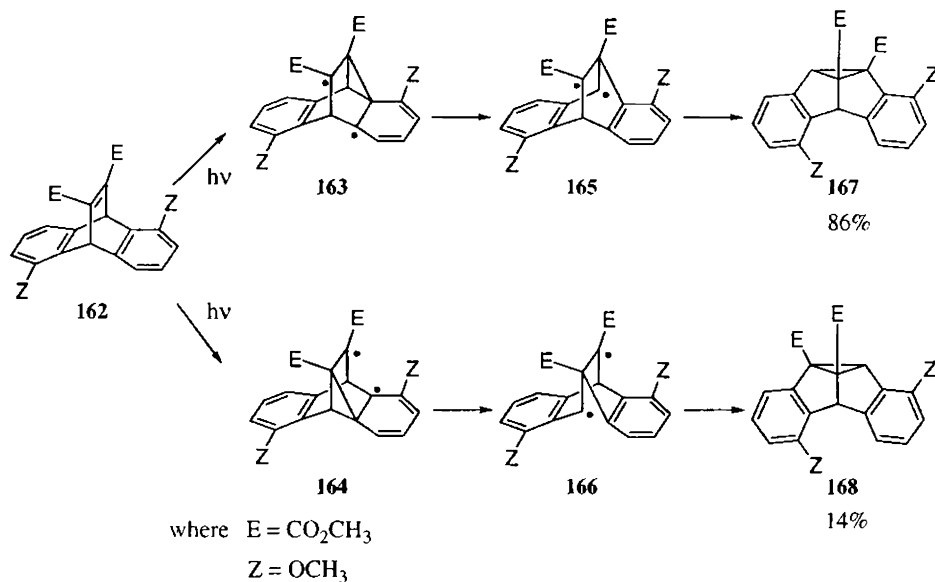
Scheffer *et al.*⁹⁰ reported some studies on the influence that vinyl and aryl substituents have on the photochemistry of the dibenzobarrelene system. Disubstituted compounds such as **155** were prepared in order to analyse the intramolecular competition between two different vinyl substituents (Scheme 39). The photochemical results were in accord with the idea put forward by Zimmerman,⁹¹ that the radical termini of the cyclopropyldicarbinyl diradicals (**156** and **157**) become electron rich during the di- π -methane rearrangement, as

a result both the polar nature as well as the radical-stabilising ability of the substituents are important in determining regioselectivity. As an example, though the radical stabilising abilities of the methyl and ester groups are probably equal, the photoproduct **160** is formed exclusively owing to the preference for the radical to be formed next to the electron-withdrawing ester group rather than the electron-donating methyl substituent.



Scheme 39

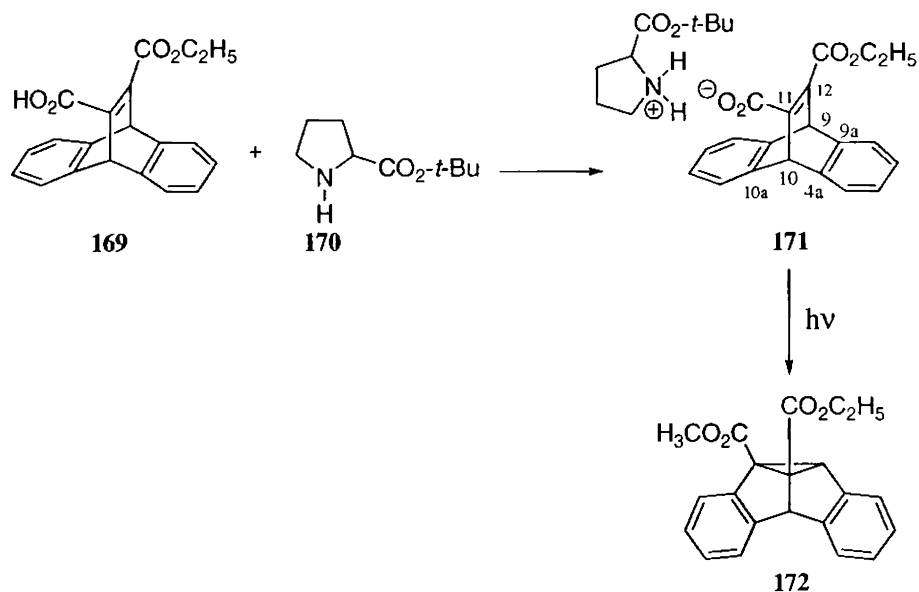
Aryl substituent effects⁹⁰ were briefly investigated in the 1,5-disubstituted dibenzobarrelene system **162** (Scheme 40). Although photolysis of such compounds can lead to regioisomeric di- π -methane products, results showed the initial benzo-vinyl bridging occurring preferentially ortho to the methoxy substituent.



Scheme 40

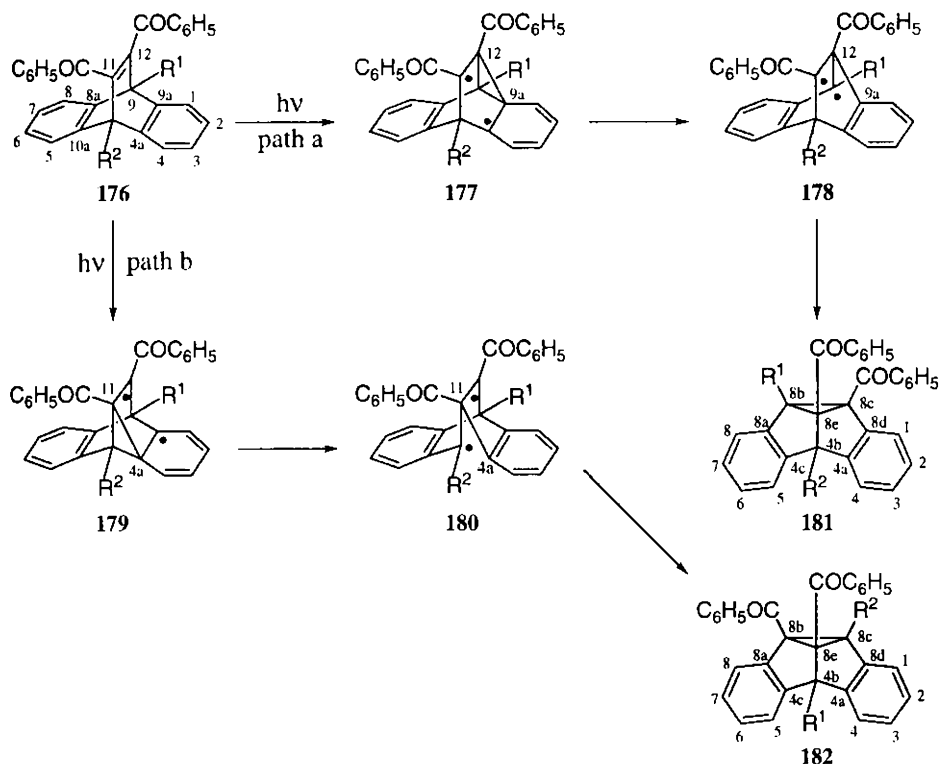
Scheffer and coworkers have shown that the solid state reactions of dibenzobarrelenes lead to greater regio-, stereo- and enantioselectivity compared to their solution phase reactions.⁸⁵ They have shown that the enantioselectivity of several dibenzobarrelenes can be enhanced through the "ionic auxiliary" concept.⁹² In this approach, the chromophore is linked to a sensitizer or a heavy atom, followed by the solid state irradiation of the salts, resulting in increased yields of the triplet photoproduct. An example is the irradiation of the salt **171** formed between the dibenzobarrelene ester-acid **169** and the *tert*-butyl ester of (*S*)-proline, **170** (Scheme 41). Irradiation of crystals of **171**, followed by acidic work-up to remove the ionic chiral auxiliary and the esterification of the resulting carboxylic acid with diazomethane gave exclusively the regioisomer **172**.⁹³ The factors for the preferential enantioselectivity is an intramolecular steric effect in which the substituents on the vinyl group tend to remain far apart during the "benzo-vinyl" bridging.

Due to the less steric interference, bridging occurs between C(11) and C(4a) as compared to C(11)-C(10a) bridging.



Scheme 41

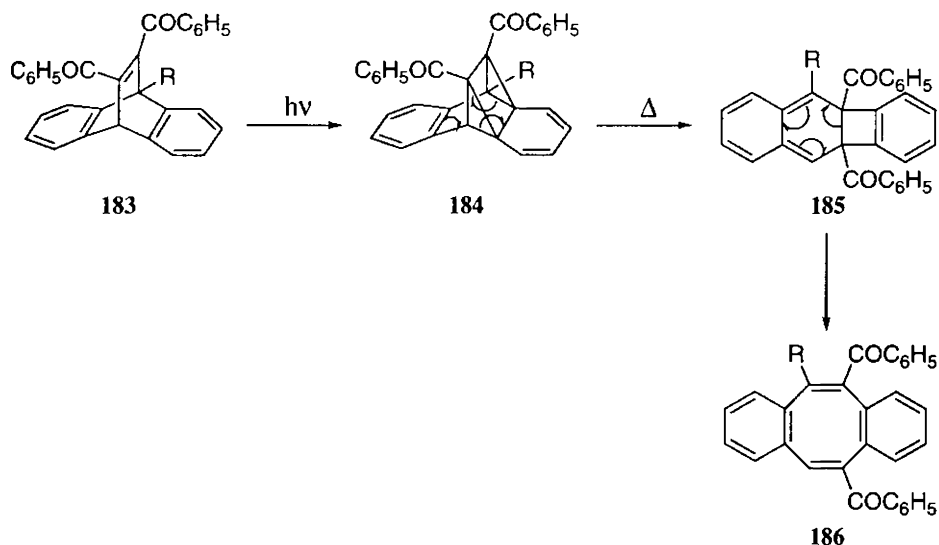
Ihmels and coworkers⁹⁴ conducted a recent study showing that the photochemical properties of a chromophore are modified by alkali metal ions through crown ether complexation. The dibenzobarrelene **173**, which is annulated with a crown ether, complexes with alkali metals such as sodium, potassium and caesium, on treatment with NaBF_4 , KBF_4 and CsBF_4 respectively. Irradiation of **173** alone or its alkali metal complexes in acetonitrile or benzene, leads preferentially to the dibenzocyclooctatetraene **174** as the photoproduct. In contrast, the solid state irradiation of the alkali metal complexes of **173** leads exclusively to the dibenzosemibullvalene **175**, which is attributed to a cation effect (Scheme 42).



Scheme 43

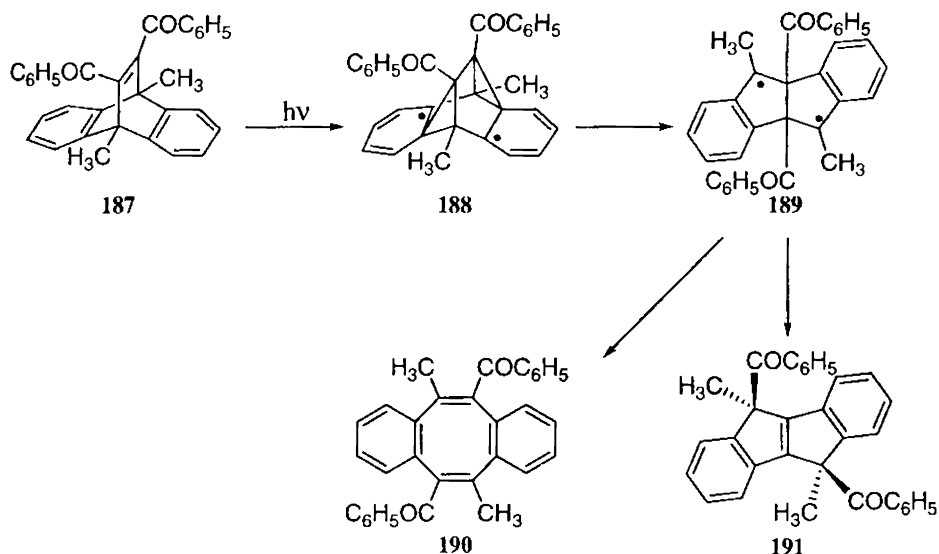
Photochemical studies suggest that dibenzocyclooctatetraene formation takes place through the singlet excited states of dibenzobarrelenes, involving an initial intramolecular [2+2] cycloaddition.⁹⁹ Although there is a greater propensity for the formation of triplet state mediated products in most of the 11,12-dibenzoyl-substituted dibenzobarrelenes, George and coworkers found that the corresponding dibenzocyclooctatetraenes are also formed. When the bridgehead positions are substituted by isopropyl, cyclopentyl or cyclohexyl groups, substantial amounts of dibenzocyclooctatetraenes are formed.¹⁰⁰ A probable route to the formation of dibenzocyclooctatetraenes are shown in Scheme 44. The reaction is assumed to proceed through the initially formed

[2+2] adduct **184**, which rearranges to **185** and ultimately to dibenzocyclooctatetraene **186**.



Scheme 44

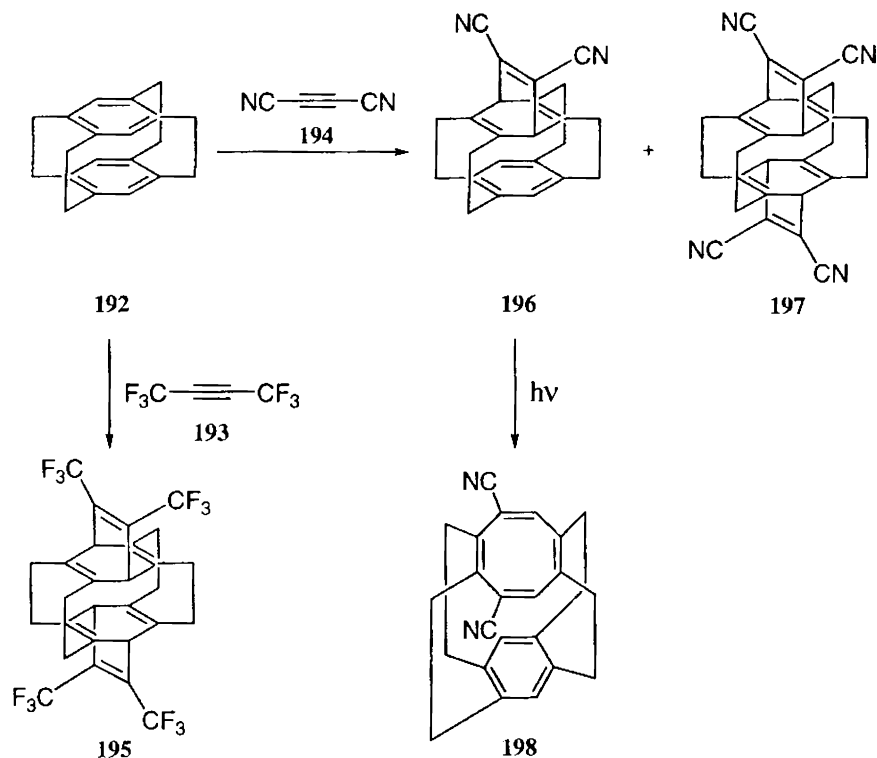
Instances of tri- π -methane rearrangement leading to dibenzocyclooctatetraenes with C_2 symmetry, occurred in certain 11,12-dibenzoyl substituted dibenzobarrelenes. Irradiation of 11,12-dibenzoyl-9,10-dimethyl-substituted dibenzobarrelene **187**, in benzene and under complete absence of oxygen, gave a mixture of the dibenzocyclooctatetraene **190** and the dibenzopentalene derivative **191** (Scheme 45).¹⁰¹ The mechanism involves the excitation of **187** leading to the diradical intermediate **188**, through a tri- π -methane route.⁸⁸ Further transformation of **188** will result in the benzylic 1,4-diradical **189**. A Grob type fragmentation¹⁰² of **189**, will lead to dibenzocyclooctatetraene **190** whereas rearrangements involving benzoyl group migration would give the dibenzopentalene derivative **191**.



Scheme 45

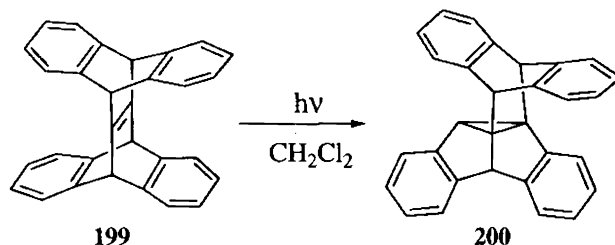
1.4.5. Photochemistry of Molecules Possessing Bisbarrelene Moieties

Gray *et al.*¹⁰³ reported the synthesis of [2.2.2.2](1,2,4,5)cyclophane **192** and its Diels-Alder reaction with dienophiles such as perfluoro-2-butyne **193** and dicyanoacetylene **194** to give the corresponding mono- and bisbarrelene adducts. Irradiation of **196** in THF with a low pressure mercury lamp gave a cyclophane **198** having a cyclooctatetraene moiety for one deck. The irradiation of the bisbarrelenes **195** and **197** gave complex mixtures of products, which they were unable to isolate and identify (Scheme 46).



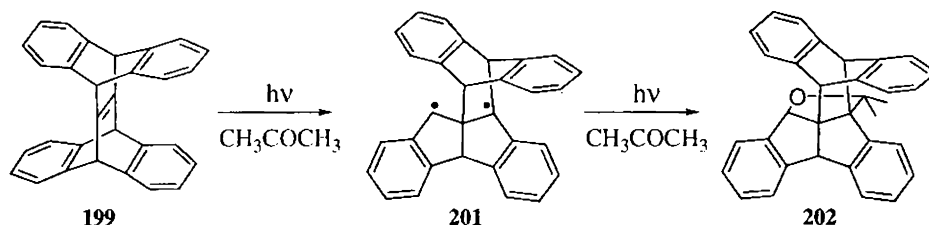
Scheme 46

Dehydrojanusene¹⁰⁴ **199**, a molecule possessing two dibenzobarrelene units, upon photosensitisation with benzophenone in methylene chloride using a Hanovia 450-W medium-pressure mercury lamp, gave high yields of the photoproduct **200**. (Scheme 47).



Scheme 47

With acetone as solvent, an addition product **202**, of acetone to photoproduct **200** was also formed (Scheme 48).



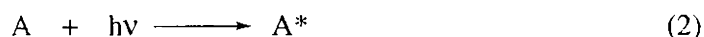
Scheme 48

1.5. The Concept of Energy Transfer in Organic Photochemistry

Electronic energy transfer has become a powerful tool for sighting new photochemical reactions, for elucidating mechanisms of photochemical reactions and for obtaining information about molecular excited states. The term energy transfer¹⁰⁵ as used in photochemistry, refers to any transfer of energy from an excited molecule to other species. The energy acceptor may itself be promoted to an excited electronic state or the electronic energy may be donated to a host system as vibrational, rotational or translational energy. The energy transfer process may involve two steps with the intermediacy of a photon (radiative transfer) or may be one-step radiationless process requiring some direct interaction of the excited donor with the acceptor.

1.5.1. Radiative Transfer

Radiative transfer of electronic energy involves the possibility of reabsorption of donor emission by an acceptor. The process requires two steps with the intermediacy of a photon (Equations 1 and 2).



No direct interaction of the donor with the acceptor is involved. Only energies corresponding to that part of the emission spectrum of the donor that overlaps with the absorption spectrum of the acceptor can be transferred.

1.5.2. Radiationless Transfer

In this context, the process of electronic energy transfer involves non-radiative transfer of electronic excitation from an excited donor molecule D^* to an acceptor molecule A .¹⁰⁶ The transfer may be an intermolecular process, which can be described in terms of a bimolecular quenching process as in Equation 3.



The asterisk denotes an electronic excited state and the bimolecular quenching rate constant k_q is related to an intermolecular energy rate constant k_{ET} by

$$k_{ET} = k_q [A] \quad (4)$$

In most cases k_{ET} is attributed to two possible contributions. The long-range Coulombic contribution was formulated by Galanin¹⁰⁷ and by Forster¹⁰⁸ in terms of dipole-dipole interaction. This is particularly suitable for describing inter-electronic energy transfer (inter-EET) in solution whenever conditions for favourable spectroscopic overlap between the emission of D^* and the absorption of A are met.

The second contribution to EET can be realised whenever these conditions are not fulfilled. A short range exchange interaction, as formulated by Dexter,¹⁰⁹ can then facilitate EET.

Intra-EET processes in bichromophoric molecules are usually described in terms of the process



where the excitation energy is transferred from an excited donor D* chromophore moiety to a ground state acceptor moiety A, resulting in quenching of D* fluorescence and sensitisation of A. B denotes a molecular spacer bridge connecting the two chromophores. This bridge may play a role in promoting the transfer process. In all EET processes, a resonance matching between the energy of the initial state of the system and that of its final state is required.

Without electronic energy transfer, the photosynthesis process in plants might not be efficient at all. Excitation transfers are important controlling factors in radiation chemistry and photochemistry of nucleic acids and proteins.

1.5.3. Quenching of Photochemical Reactions

The process of quenching is considered as the transfer of electronic-energy from the substrate to a quencher molecule. Either the excited singlet or the triplet state of the substrate can be quenched. The classical triplet quenching scheme is shown in Figure 2.

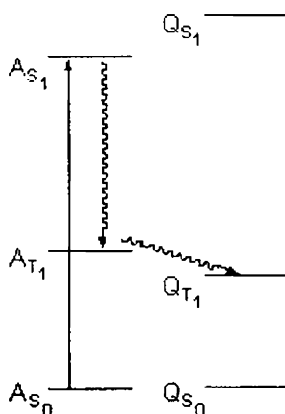


Figure 2. Classical triplet quenching scheme¹⁰⁵

1.5.4. Mechanistic Studies

The only way the quencher can interact with the compound of interest is as an acceptor of its triplet excitation energy. The quencher does not compete for the exciting light. If a particular photoproduct is formed in the absence but not in the presence of the triplet quencher, then its formation must involve a triplet state precursor. An easy way to determine whether or not triplet state quenching is occurring is sometimes afforded by the use of quenchers such as olefins and conjugated dienes, which undergo detectable reactions such as isomerisations and dimerisations from their triplet states.

There are cases in which the same product arises by two or more paths, some of which involve a triplet state intermediate. The triplet quencher can block only the paths involving the triplet state intermediate, so the products arising from paths not involving the triplet state will survive.

1.5.5. Ideal Triplet Quencher

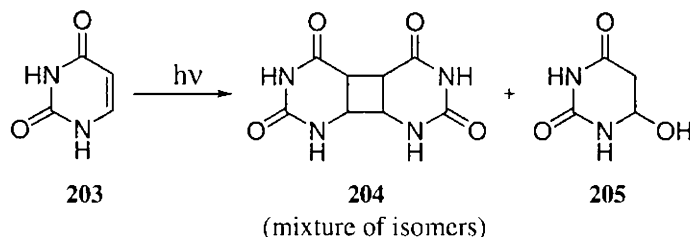
The ideal triplet quencher possesses a lowest lying excited singlet state

which lies much higher than that of the substrate and a triplet state which lies lower than the lowest lying triplet state of the substrate. Interaction of the quencher and excited substrate should lead only to electronic energy transfer. The excited quencher should be chemically inert and should be capable of shedding excitation energy very quickly.

Compounds with relatively low-lying triplet states and large singlet-triplet splittings are prime candidates for useful triplet quenchers. Two kinds of compounds, (a) olefins, conjugated dienes and higher polyenes and (b) aromatic hydrocarbons generally fulfill these requirements.

1.5.5.1. An Example of the Use of Quencher

The photolysis of uracil **203** in aqueous solution leads to dimers **204** and the photohydration product **205** (Scheme 49).



Scheme 49

Addition of 2,4-hexadienol¹¹⁰ or oxygen¹¹¹, which act as triplet quenchers, leads to quenching of dimer production but has no effect on the photohydration. This demonstrates that the dimers arise by way of the uracil triplet state but that the photohydration reaction does not involve the triplet state.

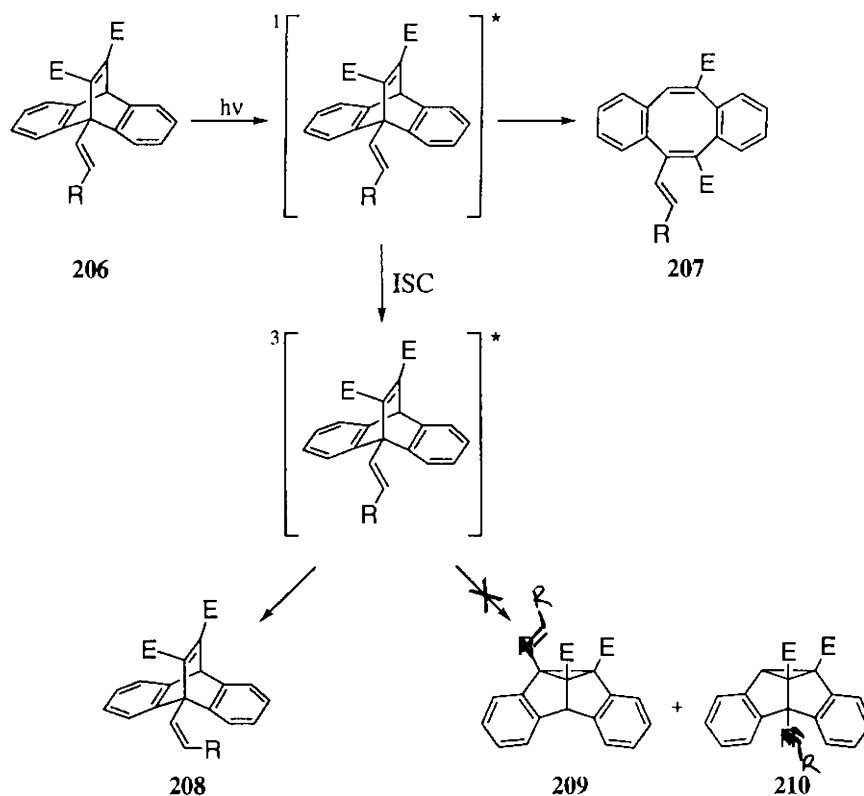
1.6. Outline of Research Problem and its Importance

The exemplary synthetic chemist of all times, Nature has marvelously synthesised its chemical substances with utmost efficiency and remarkable selectivity. Nature puts forth a herculean task to the brand of organic chemists in mimicking her incredible synthetic skills. As a humble venture, we aimed at obtaining selectivity in a selected organic photochemical reaction.

Bicyclo[2.2.2]octa-2,5,7-triene, trivially known as "barrelene", was the key molecule, which Howard E. Zimmerman used in unlocking the mechanism of the well-known photochemical rearrangement, the di- π -methane rearrangement. Dibenzobarrelenes, similar to the photochemical behaviour of barrelenes, exhibit dissimilar photoreactivity from its singlet and triplet excited states. But the absence of a clear line of demarcation between the singlet and triplet state reactivity of these bicyclic compounds, often results in a mixture of photoproducts from both the excited states.

In an attempt to investigate the conditions for obtaining selectivity in photochemical reactions, we chose dibenzobarrelenes as the precursor molecule. Literature precedences indicate that olefins act as efficient triplet quenchers. In principle, we aimed at introducing a suitable π -system that can act as an intramolecular quencher for the dibenzobarrelene triplet. In order to exploit the true potential of this possibility, it is important to fine-tune the triplet energy of the olefin unit. This entails the synthesis of several alkenylbarrelenes having strategically-positioned olefin units possessing a range of triplet energies for identifying the structural features for efficient intramolecular quenching. Carbomethoxy ester and benzoyl functionalities were appended at the vinylic positions of the dibenzobarrelenes, as they would act as efficient intramolecular intersystem crossing catalysts.

Our research target is outlined in the following scheme (Scheme 50).



Scheme 50

Dibenzobarrelenes upon excitation to the singlet excited state, dibenzocyclooctatetraene is formed whereas excitation to the triplet excited state produces dibenzosemibullvalene. With the notion that olefins are efficient triplet quenchers, we intend to quench the triplet excited state of the dibenzobarrelenes from forming triplet mediated photoproducts, through the *cis-trans* isomerisation of the bridgehead olefin appendages; thereby inducing a selectivity in the photochemical reaction.

Studies have shown that molecular systems with three olefin moieties

bonded to an sp^3 hybridised carbon atom, have the potentiality of undergoing both the di- π -methane and tri- π -methane rearrangement. In this context, our synthesis of bridgehead olefin appended dibenzobarrelenes, opens up the venue for both the rearrangements as well as for hitherto unknown photochemical transformations.

The molecular architecture of the novel bisdibenzobarrelenes is such that they hold tremendous potential to exhibit interesting photochemistry and photophysics. They are ideal molecules for investigating the modes of energy transfer in bichromophoric molecular systems.

1.7. Objectives

1. To synthesise 9-olefin appended anthracenes and bisanthracenes
2. To synthesise bridgehead olefin appended 11,12-dicarbomethoxy substituted dibenzobarrelenes
3. To synthesise bridgehead olefin appended 11,12-dibenzoyl substituted dibenzobarrelenes
4. To synthesise bisdibenzobarrelenes
5. Preliminary fluorescence studies of some synthesised dibenzobarrelenes and bisdibenzobarrelenes employing Time-Correlated Single-Photon Counting (TCSPC) Technique
6. Photochemistry of dibenzobarrelenes to assess the role of the bridgehead olefin moieties and the photochemistry of the novel bisdibenzobarrelenes

References

1. Diels, O.; Alder, K. *Ann.* **1928**, *460*, 98.
 2. Kloetzel, M. *Organic Reactions* **1967**, *4*, 1.
 3. Corey, E. J. *Angew. Chem. Int. Ed.* **2002**, *41*, 1650.
 4. Sauer, J. *Angew. Chem. Int. Ed.* **1966**, *5*, 211.
 5. Craig, D.; Shipman, J. J.; Fowler, R. B. *J. Am. Chem. Soc.* **1961**, *83*, 2885.
 6. Martin, J. G.; Hill, R. K. *Chem. Rev.* **1961**, *61*, 537.
 7. Holmes, H. L. *Organic Reactions* **1948**, *4*, 60.
 8. Alder, K.; Stein, G. *Angew. Chem.* **1937**, *50*, 510.
 9. Sauer, J. *Angew. Chem. Int. Ed.* **1967**, *6*, 16.
 10. Sauer, J.; Wiest, H.; Mielert, A. *Chem. Ber.* **1964**, *97*, 3183.
 11. Alder, K.; Schumacher, M. *Liebigs Ann. Chem.* **1951**, *571*, 87.
 12. Stockmann, H. *J. Org. Chem.* **1961**, *26*, 2025.
 13. Wassermann. *J. Chem. Soc.* **1935**, 1511.
 14. Woodward, R. B.; Katz, T. J. *Tetrahedron* **1959**, *5*, 70.
 15. Fleming, I. *Frontier Orbitals and Organic Chemical Reactions*; Wiley: London; **1976**.
 16. Fukui, K. *Acc. Chem. Res.* **1971**, *4*, 57.
 17. Fukui, K. *Acc. Chem. Res.* **1981**, *14*, 363.
 18. Spino, C.; Rezaei, H.; Dory, Y. L. *J. Org. Chem.* **2004**, *69*, 757.
 19. Bruckner, R. *Advanced Organic Chemistry. Reaction Mechanisms*; Academic Press: USA **2002**.
 20. Bachmann, W. E.; Deno, N. C. *J. Am. Chem. Soc.* **1949**, *71*, 3062.
 21. Boger, D. L.; Robarge, K. D. *J. Org. Chem.* **1988**, *53*, 3373.
 22. Avram, M.; Dinulescu, I. G.; Marica, E.; Nenitzescu, C. D. *Chem. Ber.* **1962**, *95*, 2248.
-

-
23. Houk, K. N. *J. Am. Chem. Soc.* **1973**, *95*, 4092.
 24. Eisenstein, O.; Lefour, J. M.; Anh, N. T. *Chem. Commun.* **1971**, 969.
 25. Eisenstein, O.; Lefour, J. M.; Anh, N. T.; Hudson, R. F. *Tetrahedron* **1977**, *33*, 523.
 26. Lutz, E. F.; Bailey, G. M. *J. Am. Chem. Soc.* **1964**, *86*, 3899.
 27. Houk, K. N.; Strozier, R. W. *J. Am. Chem. Soc.* **1973**, *95*, 4094.
 28. Hoffmann, R.; Woodward, R. B. *J. Am. Chem. Soc.* **1965**, *87*, 4388.
 29. Jun-Li, C. *Chem. Rev.* **1993**, *93*, 2023.
 30. Cativiela, C.; Garcia, J. I.; Mayoral, J. A.; Salvatella, L. *Chem. Soc. Rev.* **1996**, 209.
 31. Gajewski. *J. Org. Chem.* **1992**, *57*, 5500.
 32. Rideout, D. C.; Breslow, R. *J. Am. Chem. Soc.* **1980**, *102*, 7816.
 33. Otto, S.; Blokzijl, W.; Engberts, J. B. F. N. *J. Org. Chem.* **1994**, *59*, 5372.
 34. Breslow, R.; Maitra, U.; Rideout, D. *Tetrahedron Lett.* **1983**, *24*, 1901.
 35. Kagan, H. B.; Riant, O. *Chem. Rev.* **1992**, *92*, 1007.
 36. Yates, P.; Eaton, P. *J. Am. Chem. Soc.* **1960**, *82*, 4436.
 37. Fray, G. I.; Robinson, R. *J. Am. Chem. Soc.* **1961**, *83*, 249.
 38. Sauer, J.; Lang, D.; Wiest, H. *Chem. Ber.* **1964**, *97*, 3208.
 39. Asano, T.; le Noble, W. *Chem. Rev.* **1978**, *78*, 407.
 40. Sera, A.; Ohara, M.; Kubo, T.; Itoh, K.; Yamada, H.; Mikata, Y. *J. Org. Chem.* **1988**, *53*, 5460.
 41. Kotsuki, H.; Kondo, A.; Nishizawa, H.; Ochi, M.; Matsuoka, K. *J. Org. Chem.* **1981**, *46*, 5454.
 42. Raistrick, B.; Sapiro, R. H.; Newitt, D. M. *J. Chem. Soc.* **1939**, 1761.
 43. Grieger, R. A.; Eckert, C. A. *J. Am. Chem. Soc.* **1970**, *92*, 2918.
 44. Dauben, W. G.; Krabbenhoft, H. O. *J. Org. Chem.* **1977**, *42*, 282.
-

-
45. Kauer, J. C.; Benson, R. E.; Parshall, G. W. *J. Org. Chem.* **1965**, *30*, 1431.
 46. Jones, W. H.; Mangold, D.; Plieninger, H. *Tetrahedron* **1962**, *18*, 267.
 47. Tietze, L. F.; Biefuss, U. *Angew. Chem.* **1993**, *32*, 131.
 48. Wender, P.; Howbert, J. *J. Am. Chem. Soc.* **1981**, *103*, 688.
 49. Jeffrey, D. W. *Chem. Rev.* **1996**, *96*, 167.
 50. Paquette, L.; Wyratt, M.; Berk, H.; Moerch, R. *J. Am. Chem. Soc.* **1978**, *100*, 5845.
 51. Paquette, L.; Ternansky, R. J.; Balogh, D.; Kentgen, G. *J. Am. Chem. Soc.* **1983**, *105*, 5446.
 52. Stork, G.; van Tamelen, E. E.; Friedman, L. J.; Burgstahler, A. *J. Am. Chem. Soc.* **1951**, *73*, 4501.
 53. Needleman, S. B.; Changkuo, M. C. *Chem. Rev.* **1962**, *62*, 405.
 54. Diels, O.; Blom, J.; Koll, W. *Ann.* **1925**, *443*, 242.
 55. Nicolaou, K. C.; Snyder, S. A.; Montagnon, T.; Vassilikogiannakis, G. *Angew. Chem. Int. Ed.* **2002**, *41*, 1668.
 56. Stein, D.; Anderson, G. T.; Chase, C. E.; Kok, Y.; Weinreb, S. M. *J. Am. Chem. Soc.* **1999**, *121*, 9574.
 57. Brieger, G.; Bennett, J. N. *Chem. Rev.* **1980**, *80*, 63.
 58. Grieco, P. A.; Parker, D. T. *J. Org. Chem.* **1988**, *53*, 3325.
 59. Ciganek, E. *Organic Reactions* **1984**, *32*, 1.
 60. Oppolzer, W. *Angew. Chem. Int. Ed. Engl.* **1977**, *16*, 10.
 61. Oppolzer, W.; Francotte, E.; Baltig, K. *Helv. Chim. Acta* **1981**, *64*, 478.
 62. Zimmerman, H. E.; Grunewald, G. L. *J. Am. Chem. Soc.* **1966**, *88*, 183.
 63. Schuster, D. I. In *Rearrangements in Ground and Excited States*; DeMayo, P., Ed.; Academic Press: New York, **1980**; Vol. 3, p. 167.
-

64. Armesto, D. In *CRC Handbook of Organic Photochemistry and Photobiology*; Horspool, W. M., Soon, P. S., Ed.; CRC Press: New York, **1995**.
 65. Zimmerman, H. E. In *Rearrangement in Ground and Excited States*; Vol. 3, DeMayo, P., Ed.; Academic Press: New York, **1980**.
 66. Zimmerman, H. E.; Binkley, R. W.; Givens, R. S.; Sherwin, M. A. *J. Am. Chem. Soc.* **1967**, *89*, 3932.
 67. Zimmerman, H. E.; Mariano, P. S. *J. Am. Chem. Soc.* **1969**, *91*, 1718.
 68. Zimmerman, H. E.; Schuster, D. I. *J. Am. Chem. Soc.* **1961**, *83*, 4486.
 69. Zimmerman, H. E.; Armesto, D. *Chem. Rev.* **1996**, *96*, 3065.
 70. Zimmerman, H. E.; Givens, R. S.; Pagni, R. M. *J. Am. Chem. Soc.* **1968**, *90*, 6096.
 71. Hixson, S. S.; Mariano, P. S.; Zimmerman, H. E. *Chem. Rev.* **1973**, *73*, 531.
 72. Zimmerman, H. E.; Novak, T. *J. Org. Chem.* **2003**, *68*, 5056.
 73. Zimmerman, H. E.; Cirkva, V. *Org. Lett.* **2000**, *2*, 2356.
 74. Zimmerman, H. E.; Pratt, A. C. *J. Am. Chem. Soc.* **1970**, *92*, 6259.
 75. Zimmerman, H. E.; Pratt, A. C. *J. Am. Chem. Soc.* **1970**, *92*, 6267.
 76. Zimmerman, H. E.; Binkley, R. W.; Givens, R. S.; Grunewald, G. L.; Sherwin, M. A. *J. Am. Chem. Soc.* **1969**, *91*, 3316.
 77. Rabideau, P. W.; Hamilton, J. B.; Friedman, L. *J. Am. Chem. Soc.* **1968**, *90*, 4465.
 78. Griffin, G. W.; Marcantonio, F. M.; Kristinsson, H. *Tetrahedron Lett.* **1965**, 2951.
 79. Zimmerman, H. E.; Givens, R. S.; Pagni, R. M. *J. Am. Chem. Soc.* **1968**, *90*, 4191.
-

-
80. Zimmerman, H. E.; Bender, C. O. *J. Am. Chem. Soc.* **1970**, *92*, 4366.
 81. Bender, C. O.; Brooks, D. W.; Cheng, W.; Dolman, D.; O'Shea, S. F.; Shugarman, S. *Can. J. Chem.* **1979**, *56*, 3027.
 82. Paquette, L. A.; Cottrell, D. M.; Snow, R. A.; Gifkins, K. B.; Clardy, J. *J. Am. Chem. Soc.* **1975**, *97*, 3275.
 83. Paquette, L. A.; Cottrell, D. M.; Snow, R. A. *J. Am. Chem. Soc.* **1977**, *99*, 3723.
 84. Ciganek, E. *J. Am. Chem. Soc.* **1966**, *88*, 2882.
 85. Chen, J.; Scheffer, J. R.; Trotter, J. *Tetrahedron* **1992**, *48*, 3251.
 86. Iwamura, M.; Tukada, H.; Iwamura, H. *Tetrahedron Lett.* **1980**, *21*, 4865.
 87. Richards, K. E.; Tillman, R. W.; Wright, G. J. *Aust. J. Chem.* **1975**, *28*, 1289.
 88. Pokkuluri, P. R.; Scheffer, J. R.; Trotter, J. *J. Am. Chem. Soc.* **1990**, *112*, 3676.
 89. Chen, J.; Pokkuluri, P. R.; Scheffer, J. R.; Trotter, J. *J. Photochem. Photobiol. A.* **1991**, *57*, 21.
 90. Rattray, G.; Yang, J.; Gudmundsdottir, A. D.; Scheffer, J. R. *Tetrahedron Lett.* **1993**, *34*, 35.
 91. Zimmerman, H. E., in *Organic Photochemistry*, ed. Padwa, A., Marcel Dekker, New York, **1991**, Vol. *11*, ch. 1, p. 1.
 92. Gamlin, J. N.; Jones, R.; Leibovitch, M.; Patrick, B.; Scheffer, J. R.; Trotter, J. *Acc. Chem. Res.* **1996**, *29*, 203.
 93. Gudmundsdottir, D.; Scheffer, J. R. *Tetrahedron Lett.* **1990**, *31*, 6807.
 94. Ihmels, H.; Schneider, M.; Waidelich, M. *Org. Lett.* **2002**, *4*, 3247.
-

95. Ramaiah, D.; Sajimon, M. C.; Joseph, J.; George, M. V. *Chem. Soc. Rev.* **2005**, *34*, 48.
 96. Kumar, C. V.; Murthy, B. A. R. C.; Lahiri, S.; Chackachery, E.; Scaiano, J. C.; George, M. V. *J. Org. Chem.* **1984**, *49*, 4923.
 97. Murthy, B. A. R. C.; Pratapan, S.; Kumar, C. V.; Das, P. K.; George, M. V. *J. Org. Chem.* **1985**, *50*, 2533.
 98. Sajimon, M. C.; Ramaiah, D.; Muneer, M.; Ajithkumar, E. S.; Rath, N. P.; George, M. V. *J. Org. Chem.* **1999**, *64*, 6347.
 99. Scheffer, J. R.; Yang, J., in *CRC Handbook of Organic Photochemistry and Photobiology*, ed. Horspool, W. M. and Sean, P. S., CRC Press, Boca Raton, FL, USA, 1995, ch. 16, p. 204.
 100. Pratapan, S.; Ashok, K.; Cyr, D. R.; Das, P. K.; George, M. V. *J. Org. Chem.* **1987**, *52*, 5512.
 101. Asokan, C. V.; Kumar, S. A.; Das, S.; Rath, N. P.; George, M. V. *J. Org. Chem.* **1991**, *56*, 5890.
 102. Grob, C. A. *Angew. Chem.* **1969**, *81*, 543.
 103. Gray, R.; Boekelheide, V. *J. Am. Chem. Soc.* **1979**, *101*, 2128.
 104. Bartlett, P. D.; Kimura, M.; Nakayama, J.; Watson, W. H. *J. Am. Chem. Soc.* **1979**, *101*, 6332.
 105. Lamola, A. A.; Turro, N. J. in *Energy Transfer and Organic Photochemistry*, Vol. XIV, Interscience Publishers, New York, 1969, ch. 2, p.18.
 106. Speiser, S. *Chem. Rev.* **1996**, *96*, 1953.
 107. Galanin, M. D. *Sov. Phys. JETP* **1955**, *1*, 317.
 108. Forster, Th. *Discuss. Faraday Soc.* **1959**, *27*, 7.
 109. Dexter, D. L. *J. Chem. Phys.* **1953**, *21*, 836.
-

110. Lamola, A. A.; Mittal, J. P. *Science* **1966**, *154*, 1560.
111. Greenstock, C. L.; Brown, I. H.; Hunt, J. W.; Johns, H. E. *Biochem. Biophys. Res. Commun.* **1967**, *27*, 431.

Synthesis of 9-Olefin appended Anthracenes and Bisanthracenes

2.1. Abstract

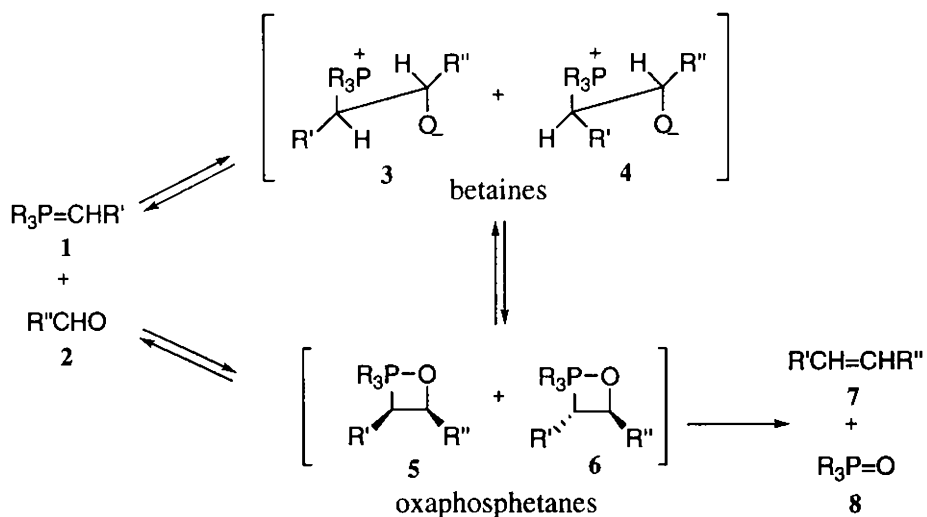
The target of synthesising various bridgehead olefin appended dibenzobarrelenes and some novel bisdibenzobarrelenes, led us to the synthesis of the appropriate alkenylanthracenes and bisanthracenes as precursor molecules. Diels-Alder reaction was the synthetic tool for the preparation of the target olefin appended dibenzobarrelenes and bisdibenzobarrelenes. This chapter attempts to throw light on our endeavours in synthesising the various 9-alkenylanthracenes and bisanthracenes.

2.2. Introduction

The role of an olefin moiety in the photochemistry of various photoactive molecules has intrigued photochemists. On the grounds of literature precedences, the notion that olefin moieties could quench triplet excited states,^{1,2} prompted us to the synthesis of various bridgehead olefin appended dibenzobarrelenes. Moreover, the functional role of a π -moiety at the bridgehead position of the dibenzobarrelenes, is yet to be assessed, as it would fabricate a tetra- π -methane system. The photochemistry and photophysics of the novel bisdibenzobarrelenes, could unravel new interesting aspects. We synthesised several 9-alkenylanthracenes and bisanthracenes by employing Wittig reaction, Grignard reaction and Claisen-Schmidt reaction.

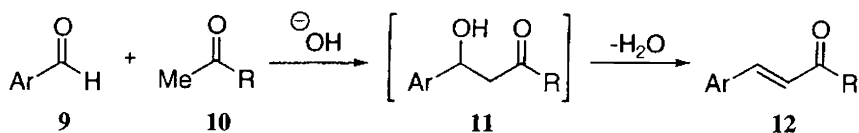
Wittig reaction³ helped to usher in the modern era of organic synthesis, the paramount important entities of positional selectivity, stereoselectivity and

chemoselectivity, under the control of the synthetic chemist. Conventional Wittig reaction entails the reaction of a phosphonium ylide with an aldehyde or ketone to yield the corresponding alkene, the overall consequence being the substitution of the C=O bond for a C=C bond.^{4,5} The attractiveness of Wittig reaction is in the high selectivity for (*Z*)- or (*E*)-alkenes, depending on the type of ylide, type of carbonyl compound or reaction conditions. The mechanism of Wittig reaction is commonly expressed in terms of two steps: (1) nucleophilic addition of the phosphorus ylide to the carbonyl compound to give a betaine species and (2) irreversible decomposition of the betaine to give alkene and phosphine oxide.⁶ (Scheme 1).



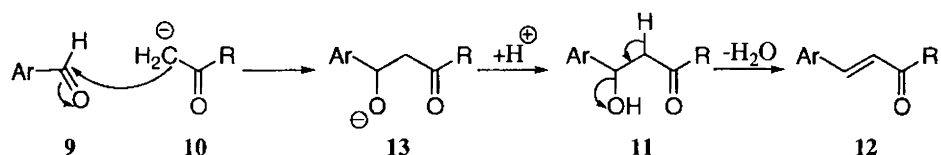
Scheme 1

The condensation of aromatic aldehydes with aliphatic or mixed alkyl aryl ketones in the presence of a relatively strong base to form α,β -unsaturated ketones is termed as the Claisen-Schmidt reaction^{7,8} (Scheme 2). This reaction has been widely used in organic synthesis.^{9,10} Claisen-Schmidt condensation can also be catalysed by acid.¹¹



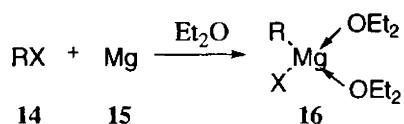
Scheme 2

The first step is a condensation of the aldol type, involving the nucleophilic addition of enolate ion derived from the methyl ketone to the carbonyl-carbon of the aromatic aldehyde. Dehydration of the hydroxyketone to form the conjugated unsaturated carbonyl compound occurs spontaneously (Scheme 3).¹² There exists a pronounced preference for the formation of a *trans* double bond in the Claisen-Schmidt condensation of methyl ketones.¹³



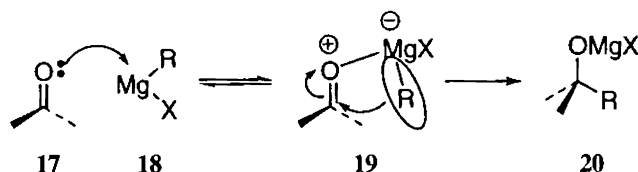
Scheme 3

The Grignard reaction is an organometallic chemical reaction involving alkyl- or aryl-magnesium halides, also called Grignard reagents with electrophiles.¹⁴ Grignard reagents, which are among the most versatile and important reagents in organic chemistry, are reactive carbon nucleophiles. It is an important tool in the formation of carbon-carbon bonds. The reaction of magnesium metal with an alkyl or aryl halide in diethyl ether is the classical method of synthesis of Grignard reagent¹⁵ (Scheme 4).



Scheme 4

The strong Lewis acid-base complex formation between the ether molecules and the magnesium atom is the reason behind the stability and solubility of Grignard reagents in ether.¹⁶ Its reaction with the carbonyl group of an aldehyde, ketone or ester is represented as a nucleophilic addition process as shown in Scheme 5.



Scheme 5

2.3. Results and Discussion

As precursor molecules for the synthesis of some bridgehead olefin-appended dibenzobarrelenes, we targeted the synthesis of the following 9-alkenyl anthracenes: 9-vinylanthracene (**21a**), 9-allylanthracene (**21b**), 9-styrylanthracene (**21c**), *trans*-1-(9-anthryl)-1-buten-3-one (**21d**) and *trans*-3-(9-anthryl)-1-phenylprop-2-en-1-one (**21e**). The bisanthracenes *trans,trans*-1,5-bis(9-anthryl)penta-1,4-dien-3-one (**22**), 1,5-bis(9-anthryl)-2-methylpenta-1,4-dien-3-one (**23**) and 2,6-bis(9-anthryl)cyclohexa-2,6-dien-1-one (**24**) were chosen for the synthesis of the corresponding bisdibenzobarrelenes (Chart 1).

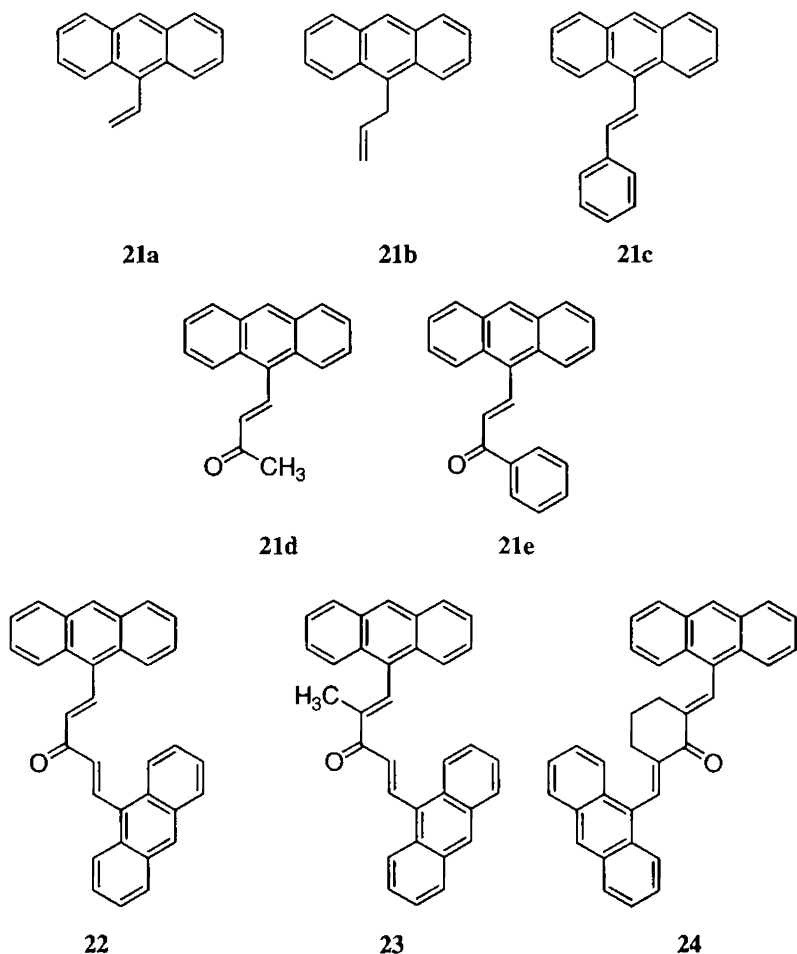
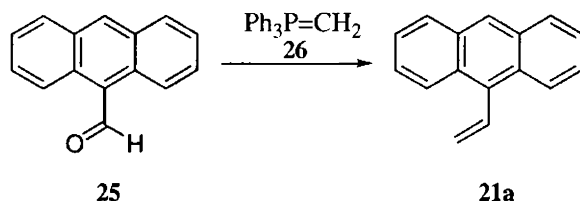


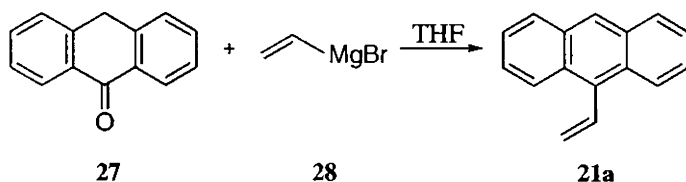
Chart 1

Wittig reaction was employed for the preparation of the 9-alkenyl anthracenes **21a** and **21c**. The reaction of 9-anthraldehyde **25** with methyltriphenylphosphonium iodide¹⁷ **26** in dichloromethane in the presence of 50% NaOH solution resulted in low yields of **21a**¹⁸ (Scheme 6).



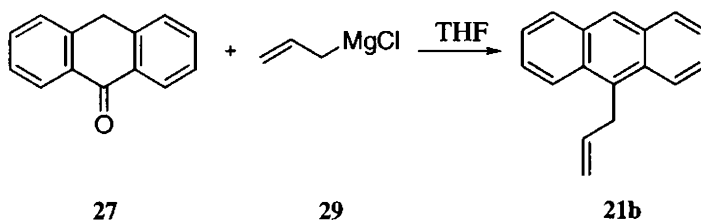
Scheme 6

Grignard reaction between anthrone **27** and vinylmagnesium bromide **28** by refluxing in THF for 4 h, followed by acid hydrolysis and dehydration with P_2O_5 , yielded **21a** in appreciable amount¹⁹ (Scheme 7).



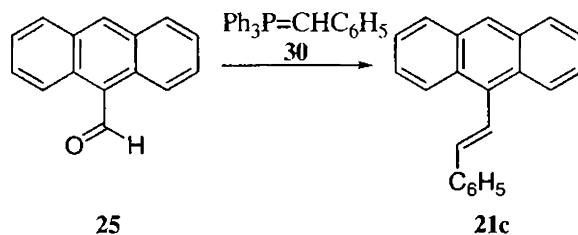
Scheme 7

The Grignard reaction between anthrone **27** and allylmagnesium chloride **29**, gave good yield of **21b**¹⁹ (Scheme 8).



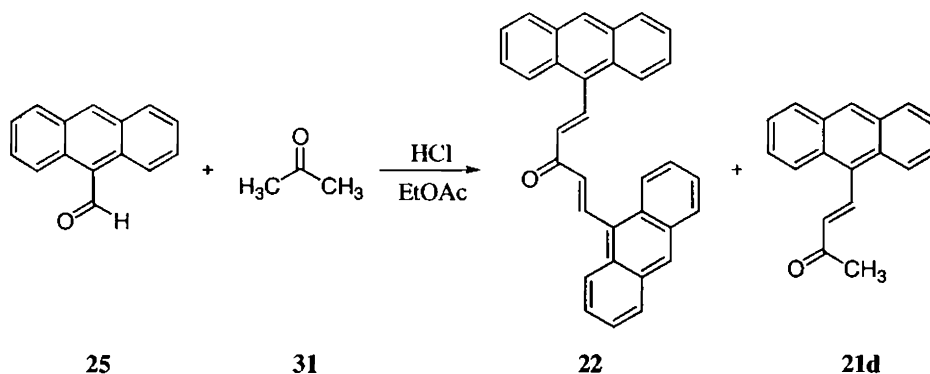
Scheme 8

The Wittig reaction of 9-anthraldehyde **25** and benzyltriphenylphosphonium chloride¹⁷ **30** in dichloromethane in the presence of 50% NaOH solution, resulted in good yield of **21c**²⁰ (Scheme 9).



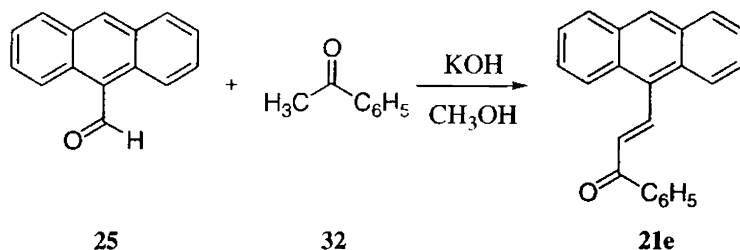
Scheme 9

Acid-catalysed Claisen-Schmidt condensation was utilised for the synthesis of the 9-alkenyl anthracene **21d** and the bisanthracene **22**. A solution of 9-anthraldehyde **25** and acetone **31** (1:10) in ethyl acetate was saturated with hydrogen chloride gas and stirred for 24 h at room temperature²¹ (Scheme 10). Bisanthracene **22**, precipitated from the reaction mixture, whereas **21d** was isolated from the reaction mixture by column chromatography.



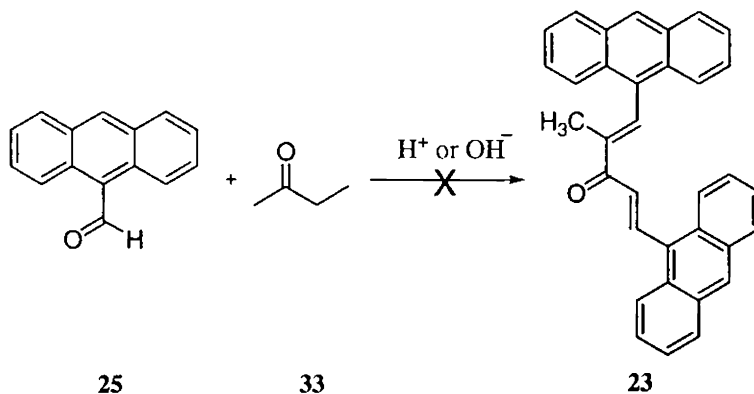
Scheme 10

Base-catalysed Claisen-Schmidt condensation between the aromatic aldehyde **25** and the methyl ketone **32** in methanol by stirring for 48 h at 60 °C, resulted in the formation of the α,β -unsaturated carbonyl compound **21e**.²²(Scheme 11).



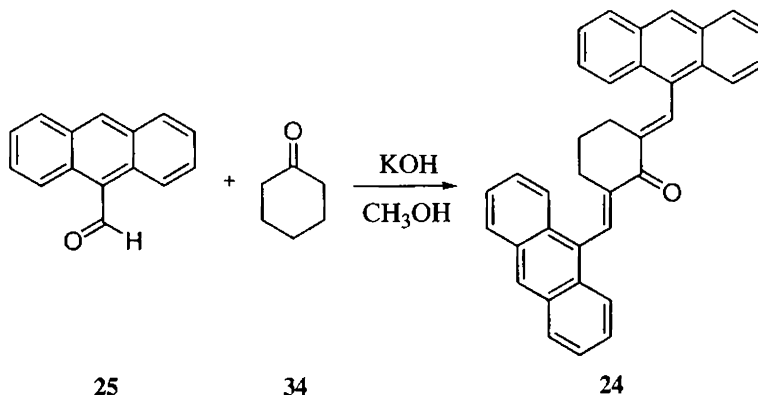
Scheme 11

The acid catalysed as well as the base catalysed Claisen-Schmidt condensation of 9-anthraldehyde **25** and 2-butanone **33**, carried out in varying molar ratios, did not lead to the successful isolation of bisanthracene **23** (Scheme 12).



Scheme 12

The bisanthracene **24**, was prepared in appreciable yields through the base catalysed Claisen-Schmidt condensation of 9-anthraldehyde **25** and cyclohexanone **34**, in methanol at 60 °C for 6 h. The precipitated **24** was further purified by recrystallisation from dichloromethane-methanol mixture (Scheme 13).



Scheme 13

The structure of alkenyl anthracenes **21a-e** and bisanthracenes **22-24** were established on the basis of analytical results and spectral data. The physical data of **21a** was identical to the data reported in literature.¹⁸ The UV absorption spectra of **21a** and **21b** is dominated by the anthracene residue. In the ¹H NMR spectrum of **21a**, the doublet of doublets at δ 5.66 and at δ 6.04 indicates the methylene protons of the olefinic moiety. The region from δ 7.46 to δ 8.40 depicts the aromatic region and also the methine proton of the vinylic moiety. The signal at δ 8.40, signifying the proton at C-10 clearly depicts a 9-substituted anthracene moiety.

In the ¹H NMR spectrum of **21b**, the two distorted triplets at δ 4.40 and δ 4.42 indicate the methylene protons connected to the sp³ hybridised carbon of the substituent moiety. The doublet of a doublet at δ 5.00 and at δ 5.10 with *J* values of 16.8 Hz and 9.9 Hz respectively, depicts the methylene protons connected to the sp² hybridised carbon of the substituent functionality. The multiplet, spread over from δ 6.17 to δ 6.30, indicates the methine proton of the olefin moiety. The aromatic hydrogens are depicted from δ 7.46 to δ 8.40. The mass spectrum of **21b** showed the molecular ion peak at *m/z* 218.

The UV absorption spectra of **21c**, **21d** and **21e** indicates the presence of extended conjugation in the anthracene residues. The ^1H NMR spectrum of **21c** indicates, a 9-styrylanthracene possessing *E*-geometry, which was ascertained through the physical data reported in literature.²⁰ The vinylic protons of the styryl moiety, appear in ^1H NMR spectrum, as doublets at δ 6.95 and δ 7.92, both having $J_{AX} = 16.56$ Hz, establishes the *E*-geometry of the olefinic bond. The aromatic region is depicted from δ 7.25 to δ 8.41. The ^{13}C NMR spectrum shows peaks from δ 124.87 to δ 137.26, confirming the structure of **21c**.

A strong peak at 1665 cm^{-1} in the IR spectrum of **21d** depicts an α,β -unsaturated keto group. A singlet at δ 2.55 in the ^1H NMR spectrum of **21d** shows the presence of the methyl protons of the vinylic moiety. The vinylic protons which appear as doublets at δ 6.70 ($J_{AX} = 16.5$ Hz) and at δ 8.47 ($J_{AX} = 16.8$ Hz), confirms the *E*-configuration of the olefin. The aromatic protons are spread over the region from δ 7.45 to δ 8.32. The ^{13}C NMR spectrum shows a peak at δ 27.97 depicting the sp^3 hybridised carbon of the methyl moiety and the keto functionality appears at δ 197.80.

The α,β -unsaturated keto group in **21e** is indicated in the IR spectrum, by the strong peak at 1653 cm^{-1} . The doublets at δ 7.21 and δ 8.81 in the ^1H NMR spectrum with $J_{AX} = 16.1$ Hz, indicate the *E*-geometry of the double bond. The peaks from δ 7.50 to δ 8.50 depict the aromatic protons of **21e**. The keto functionality appears at δ 189.68 in the ^{13}C NMR spectrum.

The UV absorption spectra of bisanthracenes **22** and **24** clearly signify the presence of extended conjugation. The physical data obtained for **22** was identical to that reported in literature.²¹ The peak at 1668 cm^{-1} in the IR spectrum of **22**, shows a conjugated keto group and the peak at 1614 cm^{-1} is

indicative of a conjugated olefinic bond. The *E*-geometry of the olefinic bond of **22** was ascertained through the ^1H NMR spectrum, where the doublet at δ 8.82 procures a *J* value of 15.8 Hz. The peaks from δ 7.49 to δ 8.50 depict the aromatic protons and the peaks of the other vinylic proton remain embedded in this region. The peak of the aromatic H-10 is seen as a singlet at δ 8.50. In the ^{13}C NMR spectrum, the peaks at δ 141.1 and at δ 141.8 indicate the β and β' carbon of the dienone system. The signal at δ 188.0 depicts the carbonyl function.

In the IR spectrum of **24**, the peak at 1669 cm^{-1} symbolises the keto group of the dienone functionality. The ^1H NMR spectrum shows a quintet at δ 1.45, denoting the two geminal hydrogens at position 4 of the cyclohexanone moiety. The geminal hydrogens at position 3 and 5 of the cyclohexanone, appear as a triplet at δ 2.21. The singlet at δ 7.96 indicates the vinylic proton of the dienone moiety of cyclohexanone, furthermore proving that **24** is a symmetric molecule. The multiplets from δ 7.46 to δ 8.49 establish the aromatic protons of **24**. The molecular ion peak at m/z 475 ($M^+ + 1$) in the FAB mass spectrum, ascertains the structural identity of the novel bisanthracene **24**.

2.4. Experimental

2.4.1. General Procedures

All melting points are uncorrected and were determined on a Neolab melting point apparatus. All reactions and chromatographic separations were monitored by thin layer chromatography (TLC). Aluminium sheets coated with silica (Merck) were used for thin layer chromatography. Visualisation was achieved by exposure to iodine vapour or UV radiation. Column chromatography was carried out with slurry-packed silica (Qualigens 60-120

mesh). Absorption spectra were recorded using Shimadzu 160A spectrometer and infrared spectra were recorded using ABB Bomem (MB series) FT-IR spectrophotometer respectively. The ^1H and ^{13}C NMR spectra were recorded at 300 and 75 MHz on a Bruker FT-NMR spectrometer with tetramethylsilane (TMS) as internal standard. Chemical shifts are reported in parts per million (ppm) downfield of tetramethylsilane. Elemental analysis was performed on Elementar Systeme (Vario ELIII) at Regional Sophisticated Instrumentation Centre (STIC), Kochi.

2.4.2. Starting Materials: Anthrone, vinylmagnesium bromide and allyl chloride were purchased from Sigma-Aldrich and were used as obtained. Acetone, acetophenone and cyclohexanone were purchased from S. D. Fine Chemicals.

2.4.2.1. 9-Anthraldehyde (25): Prepared by a known procedure (52%, mp 104-106 °C).²³

2.4.2.2. Methyltriphenylphosphonium iodide (26): Prepared by a known procedure (86%, mp >280 °C).¹⁷

2.4.2.3. Benzyltriphenylphosphonium chloride (30): Prepared by a known procedure (88%, mp >300 °C).¹⁷

2.4.3. Synthesis of 9-Olefin appended Anthracenes (21a-e)

2.4.3.1. 9-Vinylanthracene (21a):

(A) Wittig Reaction: A solution of 9-anthraldehyde **25** (4.12 g, 0.02 mol) in dry THF (80 mL), was added to the stirred mixture of methyltriphenylphosphonium iodide **26** (24.24 g, 0.06 mol) in dry THF (120 mL) under nitrogen atmosphere. The reaction mixture was stirred at room

temperature for 5 h. Aqueous solution of NaOH (50%), was then added from a dropping funnel. The reaction mixture was stirred for another 30 minutes, poured into water and extracted with dichloromethane. The organic layer was separated, washed with water and dried over anhydrous MgSO₄. The solvent was removed under reduced pressure and the product formed was separated by column chromatography and purified by recrystallisation from a mixture of hexane and dichloromethane (3:2).

(B) Grignard Reaction: A solution of anthrone **27** (15.0 g, 0.08 mol) dissolved in dry THF (200 mL), was added to a mixture of vinylmagnesium bromide (11.80 g, 0.09 mol) **28** in dry THF (80 mL), maintained at 55 °C. The mixture was refluxed for 4 h, cooled and then hydrolysed with 50 mL of 4N HCl. The organic layer was extracted with 70 mL of benzene. The extract was washed with water and dried with anhydrous Na₂SO₄. The filtrate was added at room temperature to P₂O₅ (10 g) in 250 mL of anhydrous benzene with stirring over a 40 h period. Subsequently the filtrate was evaporated to dryness, giving a crude solid, which was purified by column chromatography over silica gel using hexane as eluant.

Compound 21a: (A) Wittig reaction yielded 12% and (B) Grignard reaction yielded 70% of **21a**; mp 65 °C; IR ν_{\max} (KBr) 3075 cm⁻¹ (=CH₂), 3043 cm⁻¹ (=CH), 1625 cm⁻¹ (C=C); UV λ_{\max} (CH₃CN) 250 (ϵ 73,000), 330 (ϵ 2,500), 385 (ϵ 4,900); ¹H NMR (CDCl₃) δ 5.66 (1H, dd, J_{trans} = 17.7 Hz, J_{gem} = 2.1 Hz, vinylic), 6.04 (1H, dd, J_{cis} = 11.4 Hz, J_{gem} = 2.1 Hz, vinylic), 7.46-8.40 (10H, m, aromatic and vinylic). Anal. Calcd for C₁₆H₁₂: C, 94.08; H, 5.92. Found: C, 94.51; H, 5.52.

2.4.3.2. 9-Allylanthracene (21b): A solution of allyl chloride (7.7 g, 0.1 mol) in dry THF (40 mL) was added dropwise during 1 h to a mixture of metal

Mg ribbon (2.43 g, 0.1 mol) and dry THF (10 mL) at 55 °C. After the Mg had disappeared, a solution of anthrone **27** (15.0 g, 0.08 mol) dissolved in dry THF (200 mL) was added to the Grignard reagent. The mixture was refluxed for 4 h, cooled and then hydrolysed with 50 mL of 4N HCl. The organic layer was extracted with 70 mL of benzene. The extract was washed with water and dried with anhydrous Na₂SO₄. The filtrate was added at room temperature to P₂O₅ (10 g) in 250 mL of anhydrous benzene with stirring over a 40 h period. Subsequently the filtrate was evaporated to dryness, giving a crude solid, which was purified by column chromatography over silica gel using hexane as eluant.

Compound 21b: (90%); mp 44-46 °C; IR ν_{\max} (KBr) 3077 cm⁻¹ (=CH₂), 3048 cm⁻¹ (=CH), 1635 cm⁻¹(C=C), 1443 cm⁻¹ (sp³ CH₂); UV λ_{\max} (CH₃CN) 255 (ϵ 77,500), 350 (ϵ 4,200), 365 (ϵ 5,700), 385 (ϵ 5,400); ¹H NMR (CDCl₃) δ 4.38 (2H, two distorted t, CH₂, J_{vic} = 5.7 Hz, J_{gem} = 1.8 Hz), 5.01 (1H, dd, J_{trans} = 16.8 Hz, vinylic), 5.09 (1H, dd, J_{cis} = 9.9 Hz, vinylic), 6.17-6.30 (1H, m, vinylic), 7.46-8.40 (9H, m, aromatic); MS m/z 218 (M^+), and other peaks. Anal. Calcd for C₁₇H₁₄: C, 93.54; H, 6.46. Found: C, 93.82; H, 6.67.

2.4.3.3. 9-Styrylanthracene (21c): A mixture of 9-anthraldehyde **25** (4.12 g, 0.02 mol) and benzyltriphenylphosphonium chloride **30** (8.00 g, 0.02 mol) in dichloromethane (35 mL) was stirred vigorously at room temperature for about 5 mts. 50% aqueous solution of NaOH, was then added from a dropping funnel, at the rate of 1 drop per 7 seconds. The reaction mixture became a clear brown solution, it was stirred for another 30 minutes, poured into water and extracted with dichloromethane. The organic layer was separated, washed with water twice and dried over anhydrous MgSO₄. Solvent was removed under reduced pressure and the pasty residue obtained was recrystallised from

1-propanol, to obtain shining yellow plates of **21c**.

Compound 21c: (67%); mp 131 °C; IR ν_{\max} (KBr) 3024 cm^{-1} (=CH), 1621 cm^{-1} (C=C); UV λ_{\max} (CH₃CN) 270 (ϵ 19,800), 300 (ϵ 7,900), 350 (ϵ 1,100), 390 (ϵ 60,000); ¹H NMR (CDCl₃) δ 6.95 (1H, d, J_{AX} = 16.56 Hz, vinylic), 7.25-8.41 (14H, m, aromatic), 7.92 (1H, d, J_{AX} = 16.56 Hz, vinylic); ¹³C NMR (CDCl₃) δ 124.87, 125.12, 125.41, 125.98, 126.43, 126.56, 127.96, 128.65, 128.78, 129.71, 131.48, 132.72, 137.26. Anal. Calcd for C₂₂H₁₆: C, 94.25; H, 5.75. Found: C, 94.47; H, 5.42.

2.4.3.4. *trans*-1-(9-Anthryl)-1-buten-3-one (21d): A solution of 9-anthraldehyde **25** (4.12 g, 0.02 mol) and acetone **31** (11.6 g, 0.20 mol) in ethyl acetate (50 mL) was saturated with hydrogen chloride gas. After stirring for 24 h at room temperature, the precipitate was removed by filtration. Vacuum evaporation of filtrate left an oily residue from which **21d** was isolated by column chromatography over silica gel (elution with 1:1 hexane-dichloromethane mixture). The product thus obtained was further purified by recrystallisation from absolute ethanol.

Compound 21d: (42%); mp 109-110 °C; IR ν_{\max} (KBr) 1665 (C=O) cm^{-1} ; UV λ_{\max} (CH₃CN) 260 (ϵ 20,000), 340 (ϵ 8,500), 390 (ϵ 35,200), 420 (ϵ 76,100); ¹H NMR (CDCl₃) δ 2.55 (3H, s, CH₃), 6.70 (1H, d, J_{AX} = 16.5 Hz, vinylic), 7.45-8.50 (9H, m, aromatic), 8.47 (1H, d, J_{AX} = 16.8 Hz, vinylic); ¹³C NMR (CDCl₃) δ 27.97, 125.03, 125.38, 126.39, 127.17, 128.44, 128.90, 129.20, 129.33, 131.24, 134.06, 135.87, 140.39, 197.80. Anal. Calcd for C₁₈H₁₄O: C, 87.78; H, 5.73. Found: C, 87.53; H, 5.17.

2.4.3.5. *trans*-3-(9-Anthryl)-1-phenylprop-2-en-1-one (21e): A mixture of 9-anthraldehyde **25** (4.12 g, 0.02 mol), acetophenone **32** (2.44 g, 0.02 mol)

and potassium hydroxide pellets (1.80 g, 0.03 mol) in methanol (30 mL) was stirred at 60 °C for 48 h and later kept in refrigerator for 48 h. The solid product that separated out was filtered and purified by recrystallisation from a mixture (1:2) of hexane and dichloromethane to give **21e**.

Compound 21e: (60%); mp 120 °C; IR ν_{\max} (KBr) 1653 (C=O) cm^{-1} ; UV λ_{\max} (CH₃CN) 250 (ϵ 27,400), 330 (ϵ 6,400), 380 (ϵ 39,800), 420 (ϵ 81,700); ¹H NMR (CDCl₃) δ 7.21 (1H, d, J_{AX} = 16.16 Hz, vinylic), 7.50-8.50 (14H, m, aromatic), 8.81 (1H, d, J_{AX} = 16.08 Hz, vinylic); ¹³C NMR (CDCl₃) δ 125.29, 125.41, 126.42, 128.41, 128.73, 128.90, 129.64, 130.17, 131.08, 131.32, 133.05, 137.92, 141.88, 189.68. Anal. Calcd for C₂₃H₁₆O: C, 89.58; H, 5.23. Found: C, 90.20; H, 5.04.

2.4.4. Synthesis of Bisanthracenes 22-24

2.4.4.1. *trans,trans*-1,5-Bis(9-anthryl)penta-1,4-dien-3-one (22): A solution of 9-anthraldehyde **25** (4.12 g, 0.02 mol) and acetone **31** (11.6 g, 0.20 mol) in ethyl acetate (50 mL) was saturated with hydrogen chloride gas. After stirring for 24 h at room temperature, the orange crystalline precipitate was removed by filtration and recrystallised by Soxhlet extraction with dichloromethane to obtain **22**.

Compound 22: (46%); mp 292 °C; IR ν_{\max} (KBr) 1668 (C=O) cm^{-1} ; UV λ_{\max} (CH₂Cl₂) 260 (ϵ 44,300), 340 (ϵ 1,090), 385 (ϵ 13,400), 420 (ϵ 89,000); ¹H NMR (CDCl₃) δ 7.49-8.50 (10H, m, aromatic and vinylic), 8.82 (1H, d, J_{AX} = 15.8 Hz, vinylic); ¹³C NMR (CDCl₃) δ 125.29, 125.43, 125.76, 126.43, 127.74, 128.41, 128.73, 128.92, 129.65, 131.11, 131.35, 133.05, 134.28, 141.11, 141.89, 187.8. Anal. Calcd for C₃₃H₂₂O: C, 91.21; H, 5.10. Found: C, 91.43; H, 5.28.

2.4.4.2. 1,5-Bis(9-anthryl)-2-methylpenta-1,4-dien-3-one (23):

(A) Acid-catalysed Claisen-Schmidt Condensation: A solution of 9-anthraldehyde **25** (4.12 g, 0.02 mol) and 2-butanone **33** (0.72 g, 0.01 mol) in ethyl acetate (50 mL) was saturated with hydrogen chloride gas. After stirring for 24 h at room temperature, the solvent was removed under reduced pressure and the filtrate was subject to column chromatography over silica gel (elution with 1:1 hexane-dichloromethane mixture). As the product mixture showed the characteristics of an intractable mixture, the isolation of **23** was unsuccessful.

The experiment was repeated with varying molar ratios of the reactants **25** and **33**, but did not lead to the isolation of **24**.

(B) Base-catalysed Claisen-Schmidt Condensation: A mixture of 9-anthraldehyde **25** (4.12 g, 0.02 mol), 2-butanone **33** (0.72 g, 0.01 mol) and potassium hydroxide (1.12 g, 0.02 mol) in methanol (50 mL) was stirred at 60 °C for 24h and later kept in refrigerator for 24h. The solid product that separated out was identified as 9-anthraldehyde **25** and the filtrate showed the characteristics of an intractable mixture.

The experiment was repeated with varying molar ratios of the reactants **25** and **33**, but did not lead to the isolation of **24**.

2.4.4.3. 2,6-Bis(9-anthryl)cyclohexa-2,6-dien-1-one (24): A mixture of 9-anthraldehyde **25** (4.12 g, 0.02 mol), cyclohexanone **34** (0.98 g, 0.01 mol) and potassium hydroxide pellets (1.12 g, 0.02 mol) in methanol (50 mL) was stirred at 60 °C for 6 h and later kept in refrigerator for 24 h. The solid product that separated out was filtered and purified by recrystallisation from a mixture (1:2) of hexane and dichloromethane to give **24**.

Compound 24: (43%); mp >280 °C; IR ν_{\max} (KBr) 1669 (C=O) cm^{-1} ; UV λ_{\max} (CH_2Cl_2) 260 (ϵ 65,900), 345 (ϵ 14,700), 380 (ϵ 30,000), 410 (ϵ 30,600); ^1H NMR (CDCl_3) δ 1.45 (2H, quintet), 2.21 (4H, triplet), 7.46-8.49 (9H, m, aromatic), 7.96 (1H, s, vinylic); FAB-MS m/z 475 ($M^+ + 1$), and other peaks. Anal. Calcd for $\text{C}_{36}\text{H}_{26}\text{O}$: C, 91.11; H, 5.52. Found: C, 91.84; H, 5.23.

References

1. Kochevar, I. H.; Wagner, P. J. *J. Am. Chem. Soc.* **1970**, *92*, 5742.
2. Matura, T.; Kitaura, Y. *Tetrahedron* **1969**, *25*, 4487.
3. Wittig, G.; Schollkopf, U. *Chem. Ber.* **1954**, *87*, 1318.
4. Maryanoff, B. E.; Reitz, A. B. *Chem. Rev.* **1989**, *89*, 863.
5. Pommer, H. *Angew. Chem., Int. Ed. Engl.* **1977**, *16*, 423.
6. Schneider, W. P. *Chem. Commun.* **1969**, 785.
7. Claisen, L.; Claparede, A. *Ber.* **1881**, *14*, 2460.
8. Schmidt, J. G. *Ber.* **1881**, *14*, 1459.
9. Wayne, W.; Adkins, H. *J. Am. Chem. Soc.* **1940**, *62*, 3401.
10. Marvel, C. S.; King, W. B. *Org. Syn.* **1944**, *1*, 252.
11. Stiles, M.; Wolf, D.; Hudson, G. V. *J. Am. Chem. Soc.* **1959**, *81*, 628.
12. Vogel, A. I. *A Text Book of Practical Organic Chemistry*; English Language Book Society and Longman Group Ltd.: London; **1996**; p 1032.
13. House, H. O. *Modern Synthetic Reactions*; 2nd ed.; Benjamin: Menlo Park, California; **1972**.
14. Carey, F. A.; Sundberg, R. J. *Advanced Organic Chemistry Part B: Reactions and Synthesis*; 3rd ed; Plenum Press, New York and London; **1990**.
15. Ashby, E. C.; Duke, R. B.; Neuman, H. M. *J. Am. Chem. Soc.* **1967**, *89*, 1964.
16. Bruckner, R. *Advanced Organic Chemistry. Reaction Mechanisms*; Academic Press: USA. **2002**.
17. Wittig, G.; Schoelkopf, U. *Org. Syn.* **1960**, *40*, 66.
18. Hawkins, E. G. E. *J. Chem. Soc.* **1957**, 3858.

19. Mosnaim, D.; Nonhebel, D. C.; Russell, J. A. *Tetrahedron* **1969**, *25*, 3485.
20. Vogel, A. I. *A Text Book of Practical Organic Chemistry*; English Language Book Society and Longman Group Ltd.: London; **1996**; p 500.
21. Becker, H.-D.; Anderson, K. *J. Org. Chem.* **1983**, *48*, 4542.
22. Russell, A.; Happoldt, W. B., Jr. *J. Am. Chem. Soc.* **1942**, *64*, 1101.
23. Fieser, L. F.; Hartwell, J. L.; Jones J. E. *Org. Syn.* **1955**, Coll. Vol., 3, 98.

Synthesis of Olefin appended Dibenzobarrelenes and Bisdibenzobarrelenes

3.1. Abstract

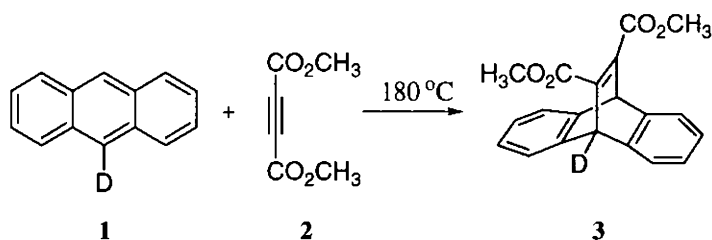
Ever since the discovery of di- π -methane rearrangement, dibenzobarrelenes, tailored with different substituents at various positions, have always been a tool to photochemists in unravelling the mechanisms of light induced reactions. Our intention of analysing the role of a π -moiety at the bridgehead position of the dibenzobarrelene, was synthetically envisaged via the Diels-Alder reaction. Bisdibenzobarrelenes were synthesised through tandem Diels-Alder reaction. Various alkenylanthracenes and bisanthracenes were employed as dienes and the dienophiles used were dimethyl acetylenedicarboxylate and dibenzoylacetylene. In this chapter, we report our venture in synthesising the various olefin appended dibenzobarrelenes and bisdibenzobarrelenes.

3.2. Introduction

Diels-Alder reaction, the most powerful of synthetic reactions, presents a convenient and highly stereospecific route to the ubiquitous six-membered ring.¹⁻²⁰ The true power and effectiveness of the Diels-Alder reaction had only began to be realized with the applications of the process to the total synthesis of many complex natural products.²¹ Different versions of the Diels-Alder reaction have arisen, including intramolecular [4+2] cycloadditions²², hetero Diels-Alder reactions²³, pressure accelerated Diels-Alder reactions²⁴, Lewis acid accelerated Diels-Alder reactions²⁵, Diels-Alder reactions in aqueous

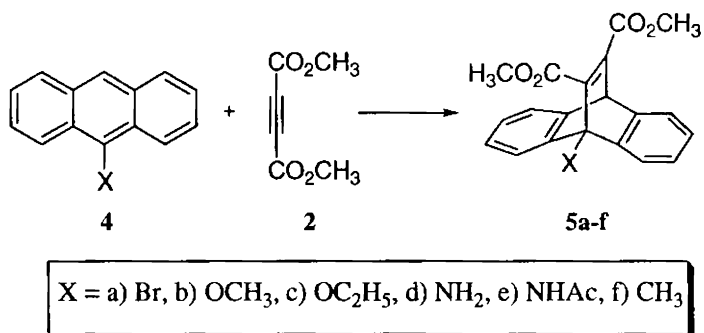
media,²⁶ etc. If one chemical reaction had to be selected from all those in the repertoire of synthetic organic chemists as the most useful and powerful synthetic construction, Diels-Alder reaction would be the logical choice. Its application not only leads to a strong increase in molecular complexity, but also can result in structures that lend themselves to additional amplification of complexity by the use of other powerful synthetic reactions.

Organic photochemists found Diels-Alder reaction, a highly efficient and useful method in the synthesis of many photoactive compounds, especially dibenzobarrelenes. Paquette *et al.* synthesised dimethyl 9-deuterio-9,10-dihydro-9,10-ethenoanthracene-11,12-dicarboxylate **3**, through the neat reaction of anthracene-9-*d* **1** and dimethyl acetylenedicarboxylate **2** at 180 °C, in appreciable yield²⁷ (Scheme 1).



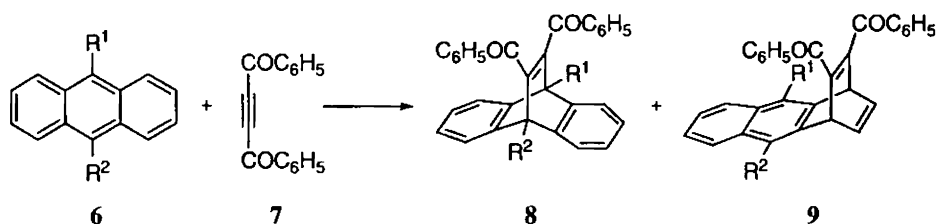
Scheme 1

Richards *et al.* prepared a series of 9-substituted dimethyl 9,10-dihydro-9,10-ethenoanthracene-11,12-dicarboxylates **5a-f**, by refluxing a solution of the appropriate 9-substituted anthracene **4** and dimethyl acetylenedicarboxylate **2** in a suitable solvent²⁸ (Scheme 2).



Scheme 2

George *et al.* conveniently prepared several 11,12-dibenzoyl-substituted dibenzobarrelenes, through the Diels-Alder addition of appropriately substituted anthracenes **6** with dibenzoylacetylene (DBA) **7**, either thermally or in the presence of Lewis acid catalysts such as aluminium chloride.²⁹⁻³² Depending on the substituents and reaction conditions, the reaction yields either 11,12-dibenzoyl-substituted dibenzobarrelene **8** or a mixture of **8** and dibenzoyl-substituted naphthobarrelene **9** (formed through addition across the 1,4 positions of anthracene)³³ (Scheme 3).



Scheme 3

3.3. Results and Discussion

The synthesis of various olefin appended dibenzobarrelenes and some bisdibenzobarrelenes were carried out through Diels-Alder reaction.

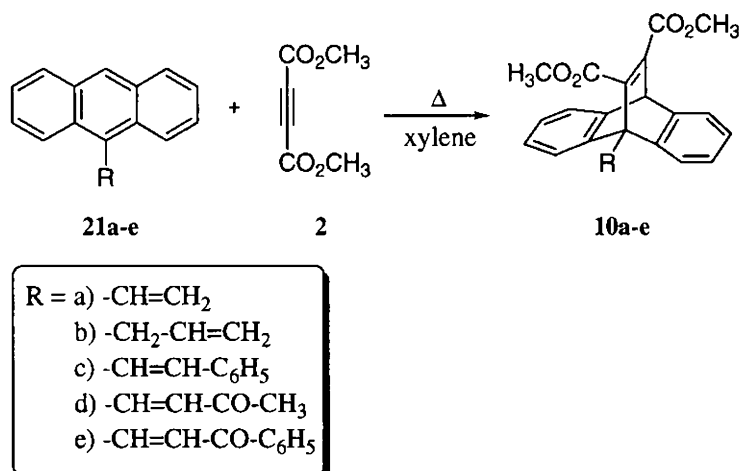
Introduction of a vinyl substituent at the bridgehead position of dibenzobarrelenes, for example, will provide a tetra- π -methane system capable of exhibiting interesting photochemistry. It is also interesting to investigate the role of a 9-allyl substituent in controlling the photochemistry of dibenzobarrelenes. In principle, we could even introduce a suitable π -system that can act as an intramolecular quencher for the barrene triplet. In order to exploit the true potential of this possibility, it is important to fine-tune the triplet energy of the olefin unit. This entails the synthesis of several alkenylbarrelenes having strategically-positioned olefin units possessing a range of triplet energies for identifying the structural features for efficient intramolecular quenching. The photochemistry of the novel bisdibenzobarrelenes is yet to be explored. We employed some selected 9-alkenyl anthracenes and bisanthracenes as dienes and dimethyl acetylenedicarboxylate and dibenzoylacetylene as dienophiles.

The dibenzobarrelenes synthesised by us are dimethyl 9-(1-ethene)-9,10-dihydro-9,10-ethenoanthracene-11,12-dicarboxylate (**10a**), dimethyl 9-(prop-1-ene)-9,10-dihydro-9,10-ethenoanthracene-11,12-dicarboxylate (**10b**), dimethyl 9-(2-phenylethene)-9,10-dihydro-9,10-ethenoanthracene-11,12-dicarboxylate (**10c**), dimethyl 9-(but-3-en-2-one)-9,10-dihydro-9,10-ethenoanthracene-11,12-dicarboxylate (**10d**), dimethyl 9-(1-phenylprop-2-en-1-one)-9,10-dihydro-9,10-ethenoanthracene-11,12-dicarboxylate (**10e**), 9-(1-ethene)-11,12-dibenzoyl-9,10-dihydro-9,10-ethenoanthracene (**11a**), 9-(prop-1-ene)-11,12-dibenzoyl-9,10-dihydro-9,10-ethenoanthracene (**11b**), 9-(2-phenylethene)-11,12-dibenzoyl-9,10-dihydro-9,10-ethenoanthracene (**11c**), 9-(but-3-en-2-one)-11,12-dibenzoyl-9,10-dihydro-9,10-ethenoanthracene (**11d**), and 9-(1-phenylprop-2-en-1-one)-11,12-dibenzoyl-9,10-dihydro-9,10-ethenoanthracene (**11e**).

In continuation, we synthesised a few novel bisbarrelenes such as **12-15**. The engineered dibenzobarrelenes and bisdibenzobarrelenes were obtained in appreciable yields.

3.3.1. Diels-Alder Reaction of 9-Alkenylanthracenes (**21a-e**) with Dimethyl acetylenedicarboxylate (DMAD)

The Diels-Alder reaction between 9-alkenylanthracenes **21a-e** with dimethyl acetylenedicarboxylate (DMAD) **2**, yielded the corresponding olefin appended dibenzobarrelenes **10a-e** under suitable conditions (Scheme 4).



Scheme 4

The structures of the Diels-Alder adducts **10a-e** were established on the basis of literature precedence, analytical results and spectral data. Dibenzobarrelene **10a**, exhibited the ester carbonyl stretching peaks at 1712 and 1732 cm⁻¹. In the ¹H NMR spectrum, two singlets were observed at δ 3.75 and δ 3.80, indicating the two methoxy groups. The singlet at δ 5.67 shows the bridgehead proton. The presence of vinylic moiety was ascertained

through the doublet of doublets at δ 5.66 and δ 6.09 and the multiplet at δ 6.71-6.81. The multiplets from δ 7.03-7.55 establish the aromatic protons of the adduct. The ^{13}C NMR spectrum showed peaks at δ 52.09 and δ 52.13 representing the two methoxy carbon. The peak at δ 50.54 indicates the tertiary bridgehead carbon and the peak at δ 58.35 represents the quaternary bridgehead carbon. The peaks from δ 122.75 to δ 156.28 indicate the vinylic and aromatic protons of **10a**. The ester carbonyl peaks appear at δ 163.73 and δ 167.46. The molecular ion peak at m/z 347 ($M^+ + 1$) in the FAB mass spectrum, confirms the identity of **10a**. The elemental analysis result gave acceptable data.

In the IR spectrum of **10b**, the stretching frequencies of the ester carbonyls appear at 1713 and 1728 cm^{-1} . The methoxy carbons appear as singlets at δ 3.73 and δ 3.77 in the ^1H NMR spectrum. The saturated methylene section of the allyl moiety appears as triplets at δ 3.64 and δ 3.66. The geminal protons of the vinyl moiety appear as doublet of doublets at δ 5.30 and at δ 5.43 and the methine proton of the vinyl moiety appears as multiplet from δ 6.15 to δ 6.26. The singlet at δ 5.63 indicates the bridgehead proton and the multiplets from δ 7.01 to δ 7.43 represent the aromatic protons. The saturated methylene carbon appears at δ 30.70 in the ^{13}C NMR spectrum of **10b**. The tertiary and quaternary bridgehead carbons appear at δ 50.56 and δ 54.60 respectively. The signals at δ 51.85 and δ 52.33 represent the two methoxy carbon. The aromatic and vinylic carbon are indicated by the signals from δ 122.53 to δ 153.69. The ester carbonyls appear at δ 163.92 and δ 167.38. In the FAB mass spectrum, the signal of the molecular ion peak appears at m/z 361 ($M^+ + 1$).

Compound **10c** exhibits the two carbonyl peaks at 1708 and 1732 cm^{-1} .

The two methoxy groups appear as two singlets at δ 3.72 and δ 3.76 in the ^1H NMR spectrum. The bridgehead proton appeared as a singlet at δ 5.69. The vinylic protons appear as doublets at δ 6.98 and 7.08 with a J value of 16.8 Hz and 17.1 Hz respectively, confirming the *E*-geometry of the double bond. The multiplets from δ 7.00-7.63 indicate the aromatic protons. The ^{13}C NMR spectrum showed peaks at δ 50.40 indicating the tertiary bridgehead carbon, peaks at δ 52.22 and δ 52.41 represent the two methoxy carbon and the peak at δ 57.96 representing the quaternary bridgehead carbon. The signals from δ 121.00 to 156.53 represent the aromatic and vinylic carbon. The ester carbonyls appear at δ 163.70 and at δ 167.42. The molecular ion peak appears at m/z 423 (M^+) in the FAB mass spectrum.

The ester carbonyls of **10d** appear at 1703 and 1731 cm^{-1} and the absorption of the α,β -unsaturated carbonyl group lies embedded in the ester carbonyl peak. The singlets at δ 2.53, δ 3.77 and δ 5.71 in the ^1H NMR spectrum represent the three protons of methyl group, the six protons of methoxy group and the bridgehead methine proton respectively. The vinylic protons appear as doublets at δ 6.69 and at δ 7.71 with a coupling constant value of 16.8 Hz. The aromatic protons appear as multiplets from δ 7.05 to δ 7.45. The signal at δ 28.02 in the ^{13}C NMR spectrum represent the methyl carbon. The peak of the tertiary bridgehead carbon appears at δ 50.46, the two methoxy carbons appear at δ 52.46 and δ 52.68 and the quaternary bridgehead carbon appears at δ 57.53. The ester carbonyl appears at δ 163.58 and δ 167.09, while the α,β -unsaturated carbonyl group appears at δ 197.51. The FAB-MS signal at m/z 389 (M^+), confirms the identity of **10d**.

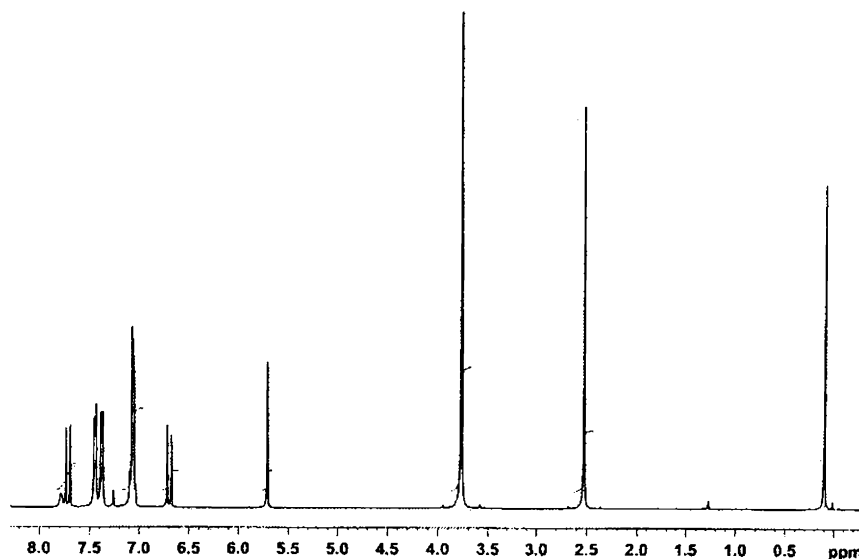
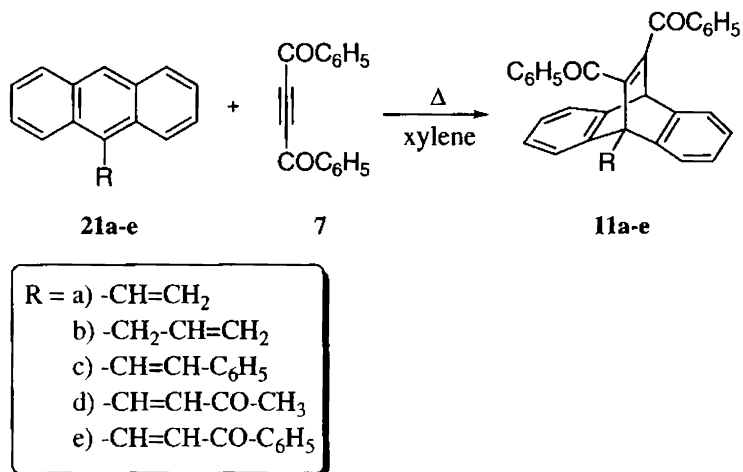


Figure 1: ^1H NMR Spectrum of 10d

For 10e, the α,β -unsaturated carbonyl stretching peak appears at 1673 cm^{-1} and the ester carbonyls appear at 1724 and 1736 cm^{-1} . In the ^1H NMR spectrum, the methoxy protons appear as two singlets at δ 3.71 and δ 3.77. The bridgehead methine proton appears as a singlet at δ 5.72. The multiplets from δ 7.07 to δ 8.10 represent the aromatic protons. The doublets at δ 7.46 and at δ 7.56 represent the vinylic protons with coupling constants of 17.7 Hz and 19.5 Hz respectively, establishing the *E*-geometry of the olefinic bond. The signals at δ 50.42 in the ^{13}C NMR spectrum, indicate the tertiary bridgehead carbon. The signals at δ 52.44 and δ 52.52 represent the methoxy carbons and that at δ 58.00 representing the quaternary bridgehead carbon. The two signals at δ 163.50 and δ 167.21 represent the ester carbonyls and the signal at δ 189.39 indicates the α,β -unsaturated carbonyl group. The signal of the molecular ion peak appears at m/z 451 ($M^+ + 1$) in the FAB mass spectrum.

3.3.2. Diels-Alder Reaction of 9-Alkenylanthracenes (21a-e) with Dibenzoylacetylene (DBA)

The Diels-Alder reaction of 9-alkenylanthracenes **21a-e** with dibenzoylacetylene **6** by refluxing in xylene, yielded the corresponding olefin appended dibenzobarrelenes **11a-e** in good yields (Scheme 5).



Scheme 5

The structural identity of dibenzobarrelenes **11a-e** were established through literature precedence and spectral and analytical data. The IR spectrum of **11a**, exhibits the carbonyl stretching peak at 1651 cm^{-1} . In the ^1H NMR spectrum of **11a**, the vinylic, geminal protons appear as doublets at δ 5.48 and δ 5.95. The bridgehead methine proton appears at δ 5.54. The methine proton of the olefin appears as a multiplet from δ 6.57 to δ 6.65. The aromatic protons appear as multiplets from δ 7.10 to δ 7.58. The signals at δ 53.25 and δ 59.51 in the ^{13}C NMR spectrum represent the tertiary and quaternary bridgehead carbon respectively. The carbonyls appear at δ 193.94 and δ 195.99. In the FAB mass spectrum, the molecular ion peak appears at

m/z 439 ($M^+ + 1$), confirming the structure of **11a**.

The benzoyl carbonyl stretching peak of **11b** appear at 1667 cm^{-1} in the IR spectrum. In the ^1H NMR spectrum, the doublet at δ 3.65 implies the saturated geminal methylene protons of the allyl moiety. The doublet of doublets at δ 5.04 and δ 5.24 with coupling constants of 10.5 Hz and 17.0 Hz respectively, represents the geminal protons of the unsaturated methylene of the allyl moiety. The bridgehead proton appears as a singlet at δ 5.51. The vinylic methine proton of the olefin, appears as a multiplet from δ 5.93 to δ 6.01. The multiplets from δ 7.10 to δ 7.51 represent the aromatic protons of **11b**. The saturated methylene carbon appears at δ 30.70 in the ^{13}C NMR spectrum. The signals at δ 53.22 and δ 55.54 indicate the two bridgehead carbon. The signals at δ 194.21 and δ 195.31 represent the carbonyl functionalities. The signal of the molecular ion in the FAB mass spectrum of **11b** appears at m/z 454 ($M^+ + 2$).

The peak at 1662 cm^{-1} , in the IR spectrum of **11c** represents the carbonyl stretching frequency. The singlet of the bridgehead proton appears at δ 5.58 in the ^1H NMR spectrum. The vinylic protons appear as doublets at δ 6.83 and δ 6.91 with coupling constant values of 17 Hz. The aromatic protons appear as multiplet from δ 7.06 to δ 7.59. The ^{13}C NMR spectrum shows peaks at δ 53.21 and δ 58.92 indicating the two bridgehead carbon. The signals at δ 193.92 and δ 196.02 represent the two carbonyl functionalities. In the FAB mass spectrum of **11c**, the molecular ion peak appears at m/z 515 ($M^+ + 1$).

The peak of the α,β -unsaturated carbonyl group of **11d** appears at 1672 cm^{-1} and the dibenzoyl carbonyls appear at 1655 cm^{-1} . The ^1H NMR spectrum of **11d**, exhibits a singlet at δ 2.53, which represents the methyl protons. The

bridgehead proton appears as a singlet at δ 5.62. The doublets at δ 6.51 and δ 7.64 indicate the vinylic protons with the coupling constant of 16 Hz. The aromatic protons appear as multiplets from δ 7.15 to δ 7.56. The signal at δ 27.38 in the ^{13}C NMR spectrum signifies the methyl group. The signals at δ 53.32 and δ 58.41 denote the tertiary and quaternary bridgehead carbon respectively. The benzoyl carbonyl moieties appear at δ 193.85 and at δ 195.24. The α,β -unsaturated carbonyl group appears at δ 197.65. The signal of the molecular ion peak at m/z 481 (M^+), confirms the structure of **11d**.

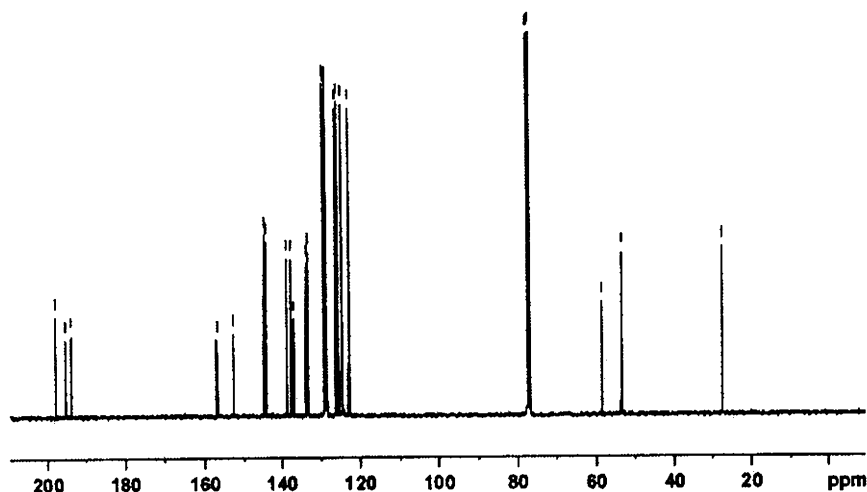


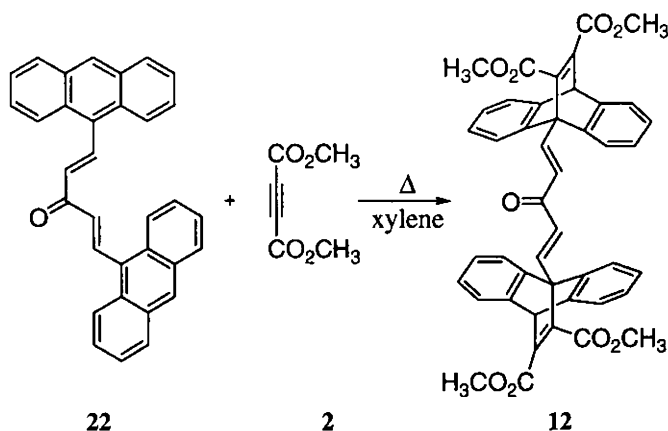
Figure 2: ^{13}C NMR Spectrum of **11d**

The IR absorption peaks of **11e** appear at 1650 and 1665 cm^{-1} indicating the stretching frequency of the benzoyl carbonyl moiety and of the α,β -unsaturated carbonyl group respectively. The bridgehead proton appears at δ 5.58 in the ^1H NMR spectrum. The aromatic protons and a vinylic proton appear as multiplets from δ 7.13 to δ 7.56. The doublet at δ 7.89 indicate the other vinylic proton with a coupling constant value of 16.5 Hz. In the ^{13}C

NMR spectrum, the bridgehead tertiary and quaternary carbons appear at δ 53.21 and δ 58.90 respectively. The signal at δ 189.62, indicates the α,β -unsaturated carbonyl group at the bridgehead position, whereas the signals at δ 193.73 and at δ 195.57 represents the benzoyl carbonyl groups. The molecular ion peak of **11e** appears at m/z 543 (M^+), in the FAB mass spectrum.

3.3.3. Diels-Alder Reaction of Bisanthracenes (**22,24**) with Dimethyl acetylenedicarboxylate (DMAD)

The novel bisdibenzobarrelenes **12** and **13**, were synthesised via the tandem Diels-Alder reaction of the bisanthracenes **22** and **24** with the dienophile DMAD **2**. The bisadducts were isolated in appreciable yield (Schemes 6 and 7).



Scheme 6

The structure of the bismoieties **12** and **13** were unequivocally established through the comparison of its spectral data with that of the monodibenzobarrelenes and via analytical data. The IR spectrum of **12**

exhibits the stretching frequency of the ester carbonyls at 1717 cm^{-1} and at 1744 cm^{-1} . The stretching frequency of the carbonyl group of the dienone moiety appears at 1668 cm^{-1} . The singlets at $\delta\ 3.77$ and $\delta\ 3.78$ in the ^1H NMR spectrum, depicts the methoxy protons. The bridgehead proton appears at $\delta\ 5.71$. The aromatic protons and a vinylic proton, appear as multiplets from $\delta\ 7.05$ to $\delta\ 7.51$. A doublet at $\delta\ 8.04$ signifies a vinylic proton with a coupling constant of 16.5 Hz , indicating *E*-configuration of the vinylic protons of the dienone moiety. The ^1H NMR spectrum depicts an olefin appended monodibenzobarrelene spectrum, but the m/z value of 741.1 ($M^+ + \text{Na}$) from the EI-MS spectrum, indisputably establishes the bisdibenzobarrelene structure of **12**.

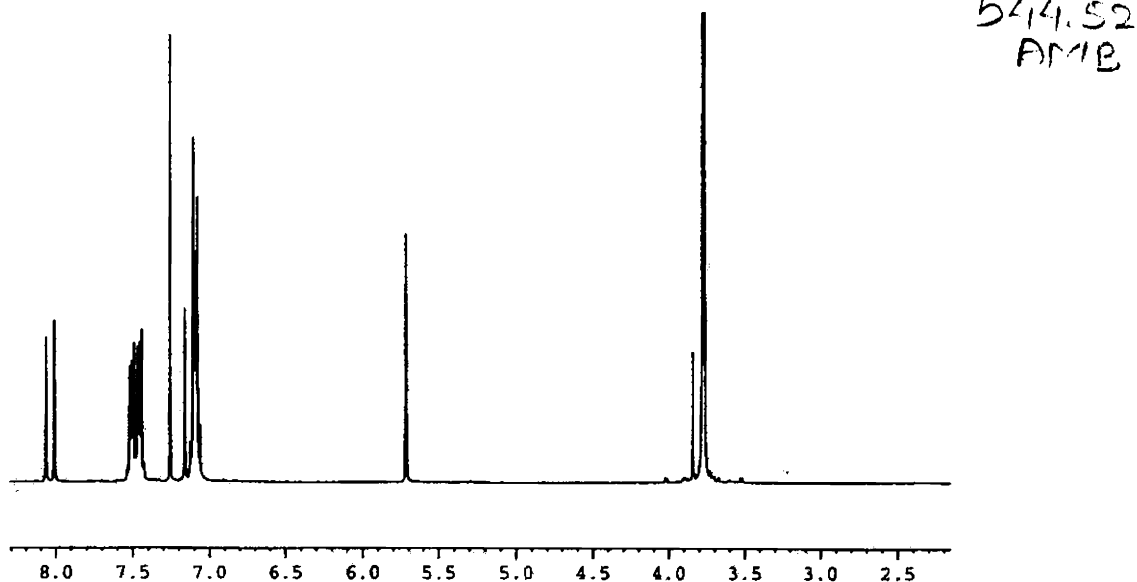
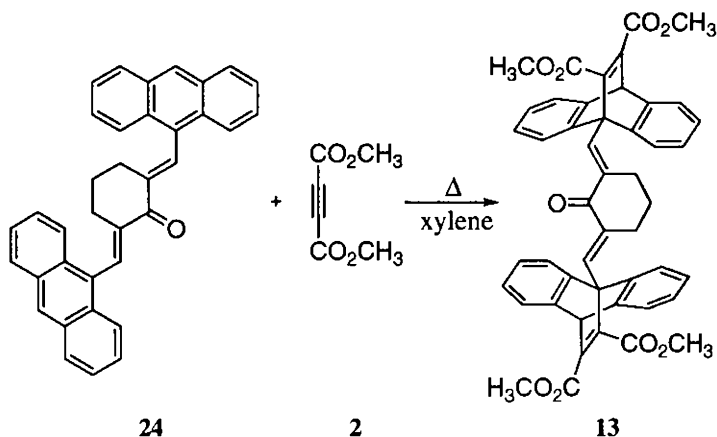


Figure 3: ^1H NMR Spectrum of **12**

The signals at $\delta\ 50.52$ and $\delta\ 57.83$ in the ^{13}C NMR spectrum of **12**, indicates the tertiary and quaternary bridgehead carbons. The methoxy carbons appear

at δ 52.54. The signals of the ester carbonyl functionalities appear at δ 163.53 and at δ 167.13. The signal at δ 188.39 signifies the dienone keto group.



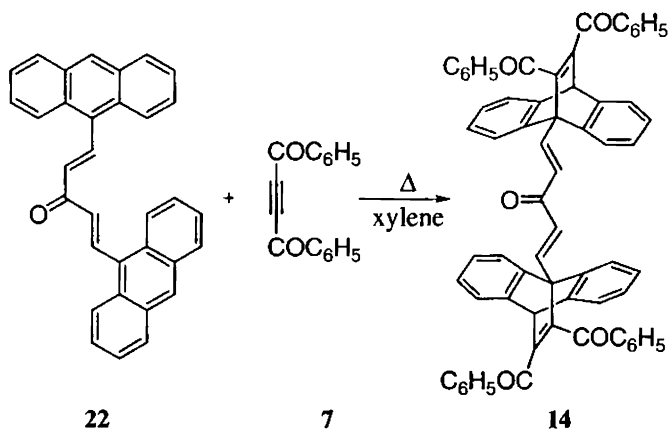
Scheme 7

In the IR spectrum of **13**, the absorption peak of the ester carbonyls appear at 1719 cm^{-1} and at 1725 cm^{-1} . The stretching frequency of the cyclohexanone moiety gets embedded in the ester carbonyl region. The multiplet at δ 1.23 in the ^1H NMR spectrum of **13**, indicates the two geminal hydrogens at the 4-position of the cyclohexanone moiety. The four geminal hydrogens at 3 and 5 positions of cyclohexanone appear as a triplet at δ 2.31. The methoxy protons appear as a singlet at δ 3.76. The singlet at δ 5.70 signifies the bridgehead proton. The vinylic and aromatic protons appear as multiplets from δ 7.08 to δ 7.52. In the ^{13}C NMR spectrum, the saturated carbon atoms of the cyclohexanone moiety appear at δ 28.93 and at δ 31.83. The signals of the methoxy carbon appear at δ 52.63 and at δ 52.74. The two bridgehead carbon appear at δ 50.81 and at δ 58.45. The signals from δ 123.62 to δ 144.49 denote the aromatic and vinylic carbon. The signals of the ester carbonyl groups appear at δ 163.87 and at δ 167.17. The cyclohexanone

carbonyl signal appears at δ 189.34. The peak at m/z 759 ($M^+ + 1$) in the FAB-MS spectrum, ascertains the bis identity of the molecule.

3.3.4. Diels-Alder Reaction of Bisanthracenes (22,24) with Dibenzoylacetylene (DBA)

The Diels-Alder reaction of the bisanthracenes **22** and **24** with DBA **7** led to the formation of the novel bisdibenzobarrelenes **14** and **15** respectively, in good yields (Scheme 8 and 9). The structural identity of the compounds were established through spectral and analytical data.



Scheme 8

The IR spectrum of **14**, showed the carbonyl stretching frequencies at 1653 cm^{-1} and at 1665 cm^{-1} , indicating the carbonyls of the dienone and benzoyl functionalities respectively. The singlet at δ 5.56, in the ^1H NMR spectrum, indicates the bridgehead proton. The vinylic protons appear as doublets at δ 6.70 and at δ 7.75 with coupling constants 16.5 Hz and 17 Hz respectively, signifying the *E*-configuration of the olefinic protons. The aromatic protons appear as multiplets from δ 7.07 to δ 7.49. The two

bridgehead carbons appear at δ 53.29 and δ 58.63 in the ^{13}C NMR spectrum. The carbonyl group of the dienone moiety appears at δ 188.16. The carbonyls of the benzoyl group appear at δ 193.82 and at δ 195.10. The NMR spectrums of **14**, point towards an olefin appended monodibenzobarrelene. It is due to the highly symmetric structure of the bisentity. The FAB-MS provided the m/z value of 904 ($M^+ + 2$) for the molecular ion peak, which proves the structure of **14** as a bisdibenzobarrelene.

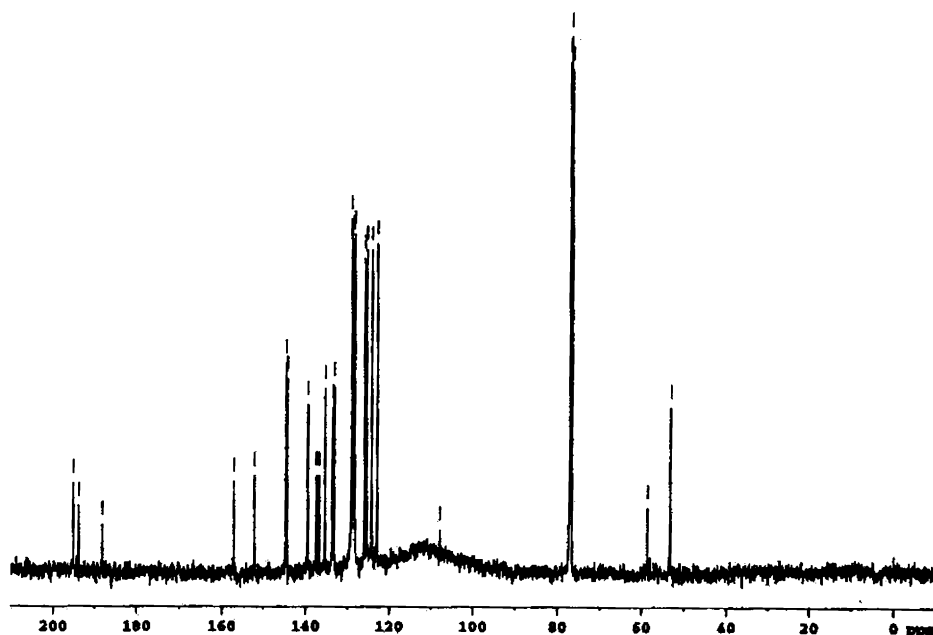
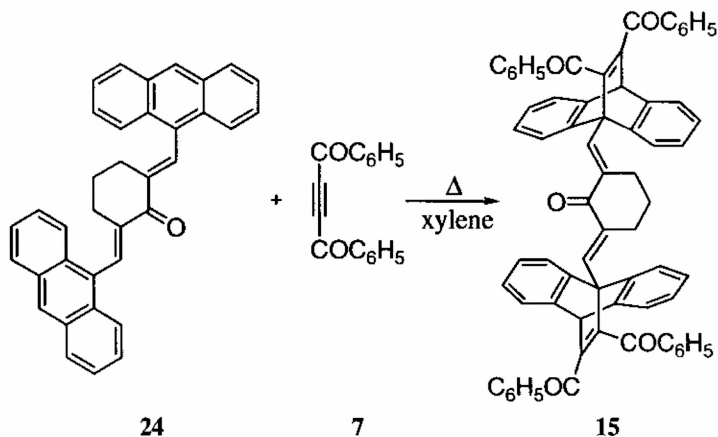


Figure 4: ^{13}C NMR Spectrum of **14**

The benzoyl carbonyl functionality of **15** appears at 1663 cm^{-1} in the IR spectrum. In the ^1H NMR spectrum, the multiplets at δ 1.26 and at δ 2.25 depict the protons of the cyclohexanone moiety. The bridgehead proton appears as a singlet at δ 5.51. The vinylic and aromatic protons appear as multiplet from δ 7.14 to δ 7.64. In the ^{13}C NMR spectrum, the saturated

cyclohexanone carbons appear at δ 31.60 and at δ 29.07. The two bridgehead carbon appears at δ 53.68 and at δ 58.10.



Scheme 9

The signals of the aromatic and vinylic carbon appear from δ 123.49 to δ 144.32. The cyclohexanone carbonyl signal appears at δ 188.75. The benzoyl carbonyl group appears at δ 194.39. The FAB-MS m/z value of 943 ($M^+ + 1$) for the molecular ion peak further confirms the structural identity of 15.

3.4. Experimental

3.4.1. General Procedures

All melting points are uncorrected and were determined on a Neolab melting point apparatus. All reactions and chromatographic separations were monitored by thin layer chromatography (TLC). Aluminium sheets coated with silica (Merck) were used for thin layer chromatography. Visualisation was achieved by exposure to iodine vapour or UV radiation. Column chromatography was carried out with slurry-packed silica (Qualigens 60-120 mesh). Absorption spectra were recorded using Shimadzu 160A spectrometer

and infrared spectra were recorded using ABB Bomem (MB series) FT-IR spectrophotometer respectively. The ^1H and ^{13}C NMR spectra were recorded at 300 and 75 MHz on a Bruker FT-NMR spectrometer with tetramethylsilane (TMS) as internal standard. Chemical shifts are reported in parts per million (ppm) downfield of tetramethylsilane. FAB mass spectra were recorded on a JOEL SX 102/DA-6000 using argon/xenon as the FAB gas, at Central Drug Research Institute (CDRI), Lucknow. Elemental analysis was performed on Elementar Systeme (Vario ELIII) at Regional Sophisticated Instrumentation Centre (STIC), Kochi.

3.4.2. Starting Materials: Dimethyl acetylenedicarboxylate (DMAD) was purchased from Sigma-Aldrich and was used as received.

3.4.2.1. Dibenzoylacetylene (7): Prepared by a known procedure (75%, mp 110-111 °C).³⁴

3.4.3. Synthesis of 9-Alkenyldibenzobarrelenes (10a-e) and Bisdibenzobarrelenes (12,13)

3.4.3.1. Synthesis of 10a: A sample of **21a** (1.02 g, 5mmol) was dissolved in minimum quantity of dry xylene and DMAD **2** (1.58 g, 11mmol) was added. Monitoring the reaction progress through thin layer chromatography, the reaction mixture was refluxed for 12 h. The solvent was removed under reduced pressure and the residue obtained was purified by column chromatography. Elution with 1:1 hexane-dichloromethane mixture yielded **10a** and on further elution with methanol some polymeric material was obtained. **10a** was further purified by recrystallisation from a mixture of dichloromethane and hexane (2:1).

Compound 10a: (62%); mp 180 °C; IR ν_{max} (KBr) 1712, 1732 (C=O, ester)

cm^{-1} ; UV λ_{max} (CH_3CN) 230 (ϵ 11,620), 257 (ϵ 5,290), 300 nm (ϵ 480); ^1H NMR (CDCl_3) δ 3.75 (3H, s, OCH_3), 3.80 (3H, s, OCH_3), 5.66 (1H, dd, $J_{\text{trans}} = 20$ Hz, $J_{\text{gem}} = 2$ Hz, vinylic), 5.67 (1H, s, methine), 6.09 (1H, dd, $J_{\text{cis}} = 10$ Hz, $J_{\text{gem}} = 2$ Hz, vinylic), 6.71-6.81 (1H, m, vinylic), 7.02-7.55 (8H, m, aromatic); ^{13}C NMR (CDCl_3) δ 50.54, 52.09, 52.13, 58.35, 122.75, 123.73, 123.94, 124.92, 125.46, 129.99, 141.75, 144.54, 144.54, 145.13, 156.28, 163.73, 167.46; FAB-MS m/z 347 ($M^+ + 1$), 287 ($M^+ - \text{CO}_2\text{CH}_3$) and other peaks. Anal. Calcd for $\text{C}_{22}\text{H}_{18}\text{O}_4$: C, 76.29; H, 5.24. Found: C, 76.62; H, 5.29.

3.4.3.2. Synthesis of 10b: A sample of **21b** (1.08 g, 5mmol) was dissolved in minimum quantity of dry xylene and DMAD **2** (1.06 g, 7.5mmol) was added and the mixture was refluxed for about 8 h, following the progress of the reaction through TLC. The solvent was removed under reduced pressure and the residue obtained was purified by column chromatography. Trace amounts of **21b** was separated upon elution with 4:1 hexane-dichloromethane mixture and **10b** was obtained upon elution with 2:3 hexane-dichloromethane mixture. **10b** was further purified by recrystallisation from a mixture of dichloromethane and hexane (2:1).

Compound 10b: (56%); mp 128 °C; IR ν_{max} (KBr) 1713, 1728 (C=O, ester) cm^{-1} ; UV λ_{max} (CH_3CN) 253 (ϵ 4,520), 300 nm (ϵ 260); ^1H NMR (CDCl_3) δ 3.73 (3H, s, OCH_3), 3.77 (3H, s, OCH_3), 3.64 (1H, t, methylene), 3.66 (1H, t, methylene), 5.30 (1H, dd, $J_{\text{cis}} = 10.5$ Hz, $J_{\text{gem}} = 1.8$ Hz, vinylic), 5.43 (1H, dd, $J_{\text{trans}} = 17.1$ Hz, $J_{\text{gem}} = 1.8$ Hz, vinylic), 5.63 (1H, s, methine), 6.15-6.26 (1H, m, vinylic), 7.01-7.43 (8H, m, aromatic); ^{13}C NMR (CDCl_3) δ 30.70, 50.56, 51.85, 52.33, 54.60, 118.38, 122.53, 123.73, 124.96, 125.19, 134.07, 143.18, 144.88, 145.90, 153.69, 163.92, 167.38; FAB-MS m/z 361 ($M^+ + 1$), 301 ($M^+ - \text{CO}_2\text{CH}_3$) and other peaks. Anal. Calcd for $\text{C}_{23}\text{H}_{20}\text{O}_4$: C, 76.65; H, 5.59. Found:

C, 76.87; H, 4.96.

3.4.3.3. Synthesis of 10c: A sample of **21c** (1.40 g, 5mmol) was dissolved in minimum quantity of dry xylene and DMAD **2** (1.77 g, 12.5mmol) was added and the mixture was refluxed for 10 h, by monitoring the reaction progress through TLC. The solvent was removed under reduced pressure and the residue obtained was purified by column chromatography. Trace amounts of unreacted **21c** was separated upon elution with 4:1 hexane-dichloromethane mixture and **10c** was obtained upon elution with 2:3 hexane-dichloromethane mixture and further purified by recrystallisation from a mixture of dichloromethane and hexane (2:1).

Compound 10c: (87%); mp 176 °C; IR ν_{\max} (KBr) 1708, 1732 (C=O, ester) cm^{-1} ; UV λ_{\max} (CH₃CN) 253 (ϵ 7,650), 300 nm (ϵ 340); ¹H NMR (CDCl₃) δ 3.72 (3H, s, OCH₃), 3.76 (3H, s, OCH₃), 5.69 (1H, s, methine), 6.98 (1H, d, J_{AX} =16.8 Hz, vinylic), 7.08 (1H, d, J_{AX} =17.1 Hz, vinylic), 7.00-7.63 (13H, m, aromatic); ¹³C NMR (CDCl₃) δ 50.40, 52.22, 52.41, 57.96, 121.00, 122.80, 123.96, 124.94, 125.46, 126.48, 128.34, 128.82, 136.68, 138.33, 141.56, 144.87, 145.09, 156.53, 163.70, 167.42; FAB-MS m/z 423 (M^+ +1), 363 (M^+ -CO₂CH₃) and other peaks. Anal. Calcd for C₂₈H₂₂O₄: C, 79.60; H, 5.25. Found: C, 80.01; H, 5.45.

3.4.3.4. Synthesis of 10d: A sample of **21d** (0.90 g, 3.6mmol) was dissolved in minimum quantity of dry xylene and DMAD **2** (1.72 g, 12mmol) was added and the mixture was refluxed for about 10 h, following the progress of the reaction through TLC. The solvent was removed under reduced pressure and the residue obtained was purified by column chromatography. Trace amounts of unreacted **21d** was separated upon elution with 1:1 hexane-dichloromethane mixture and **10d** was obtained upon elution with 1:4 hexane-dichloromethane

mixture. **10d** was further purified by recrystallisation from absolute ethanol.

Compound 10d: (43%); mp 150-152 °C; IR ν_{\max} (KBr) 1703, 1731 (C=O, ester) cm^{-1} ; UV λ_{\max} (CH₂CN) 230 (ϵ 7,930), 255 (ϵ 3,450), 300 nm (ϵ 290); ¹H NMR (CDCl₃) δ 2.53 (3H, s, CH₃), 3.77 (6H, s, OCH₃), 5.71 (1H, s, methine), 6.69 (1H, d, J_{AX} = 16.8 Hz, vinylic), 7.05-7.46 (8H, m, aromatic), 7.71 (1H, d, J_{AX} = 16.8 Hz, vinylic); ¹³C NMR (CDCl₃) δ 28.02, 50.46, 52.46, 52.68, 57.53, 122.37, 124.34, 125.21, 125.95, 127.27, 133.55, 134.20, 137.29, 137.84, 142.37, 143.49, 144.77, 154.75, 163.58, 167.09, 197.51; FAB-MS m/z 389 (M^+ +1), and other peaks. Anal. Calcd for C₂₄H₂₀O₅: C, 74.21; H, 5.19. Found: C, 74.56; H, 5.42.

3.4.3.5. Synthesis of 10e: A sample of **21e** (1.10 g, 3.6mmol) was dissolved in minimum quantity of dry xylene and DMAD **2** (1.32 g, 9.3mmol) was added and the mixture was refluxed for about 10 h, following the progress of the reaction through TLC. The solvent was removed under reduced pressure and the residue obtained was purified by recrystallisation from a mixture of dichloromethane and hexane (2:1) to give **10e**.

Compound 10e: (75%); mp 166 °C; IR ν_{\max} (KBr) 1724, 1736 (C=O, ester), 1673 (C=O, ketone) cm^{-1} ; UV λ_{\max} (CH₃CN) 254 (ϵ 5,150), 300 nm (ϵ 230); ¹H NMR (CDCl₃) δ 3.71 (3H, s, OCH₃), 3.77 (3H, s, OCH₃), 5.72 (1H, s, methine), 7.07-8.10 (13H, m, aromatic), 7.46 (1H, d, J_{AX} = 17.7 Hz, vinylic), 7.56 (1H, d, J_{AX} = 19.5 Hz, vinylic); ¹³C NMR (CDCl₃) δ 50.42, 52.44, 52.52, 58.00, 122.39, 124.18, 125.17, 125.80, 128.78, 128.86, 132.51, 133.43, 137.35, 138.80, 142.08, 143.75, 144.77, 155.14, 163.50, 167.21, 189.39; FAB-MS m/z 451 (M^+ +1), 391 (M^+ -CO₂CH₃) and other peaks. Anal. Calcd for C₂₉H₂₂O₅: C, 77.32; H, 4.92. Found: C, 77.19; H, 5.08.

3.4.3.6. Synthesis of 12: A sample of **22** (1.00 g, 2.3mmol) was dissolved in minimum quantity of dry xylene and DMAD **2** (1.31 g, 9.2mmol) was added and the mixture was refluxed for about 12 h, following the progress of the reaction through TLC. The solvent was removed under reduced pressure and the residue obtained was purified by recrystallisation from a mixture of dichloromethane and methanol (2:1) to give **12**.

Compound 12: (84%); mp 260 °C; IR ν_{\max} (KBr) 1717, 1744 (C=O, ester), 1668 (C=O, ketone) cm^{-1} ; UV λ_{\max} (CH_2Cl_2) 215 (ϵ 11,530), 254 (ϵ 4,320), 290 nm (ϵ 450); ^1H NMR (CDCl_3) δ 3.77, (3H, s, OCH_3), 3.78 (3H, s, OCH_3), 5.71 (1H, s, methine), 7.05-7.51 (9H, m, aromatic and vinylic), 8.01 (1H, d, $J_{\text{AX}}=16.5$ Hz, vinylic); ^{13}C NMR (CDCl_3) δ 50.52, 52.54, 57.83, 122.33, 124.27, 125.28, 125.91, 135.11, 139.22, 142.29, 143.62, 144.79, 154.88, 163.53, 167.13, 188.39; EI-MS m/z 741.1 ($M^++\text{Na}$) and other peaks. Anal. Calcd for $\text{C}_{45}\text{H}_{34}\text{O}_9$: C, 75.20; H, 4.77. Found: C, 75.91; H, 5.11.

3.4.3.7. Synthesis of 13: A sample of **24** (0.83 g, 1.7mmol) was dissolved in minimum quantity of dry xylene and DMAD **2** (2.04 g, 14.3mmol) was added and the mixture was refluxed for about 20 h, following the progress of the reaction through TLC. The solvent was removed under reduced pressure and the residue obtained was purified by recrystallisation from a mixture of dichloromethane and hexane (2:1) to give **13**.

Compound 13: (52%); mp >280 °C; IR ν_{\max} (KBr) 1719, 1730 (C=O, ester) cm^{-1} ; UV λ_{\max} (CH_2Cl_2) 258 (ϵ 10,680), 300 nm (ϵ 870); ^1H NMR (CDCl_3) δ 1.23 (2H, m, methylene), 2.31 (4H, t, methylene), 3.76 (6H, s, OCH_3), 5.70 (1H, s, methine), 7.08-7.52 (9H, m, aromatic and vinylic); ^{13}C NMR (CDCl_3) δ 28.93, 31.83, 50.81, 52.63, 52.74, 58.45, 123.62, 124.42, 124.87, 125.48, 125.63, 125.94, 127.91, 128.36, 129.00, 131.93, 142.84, 143.58, 144.29,

144.49, 163.87, 167.17, 189.34; FAB-MS m/z 759 (M^+ +1) and other peaks. Anal. Calcd for $C_{48}H_{38}O_9$: C, 75.98; H, 5.05. Found: C, 76.33; H, 5.35.

3.4.4. Synthesis of 9-Alkenyldibenzobarrelenes (11a-e) and Bisdibenzobarrelenes (14,15)

3.4.4.1. Synthesis of 11a: A sample of **21a** (0.50 g, 2.5mmol) was dissolved in minimum quantity of dry xylene and DBA **7** (0.86 g, 3.7mmol) was added and the mixture was refluxed for 10 h, following the progress of the reaction through TLC. The solvent was removed under reduced pressure and the residue obtained was purified by column chromatography. Trace amounts of DBA **7** was separated upon elution with 4:1 hexane-dichloromethane mixture and **11a** was obtained upon elution with 1:1 hexane-dichloromethane mixture. **11a** was further purified by recrystallisation from a mixture of dichloromethane and hexane (2:1).

Compound 11a: (93%); mp 152 °C; IR ν_{max} (KBr) 1651 (C=O, ketone) cm^{-1} ; UV λ_{max} (CH_3CN) 256 (ϵ 12,080), 300 (ϵ 2,320); 1H NMR ($CDCl_3$) δ 5.48 (1H, d, J_{trans} = 18.16 Hz, vinylic), 5.54 (1H, s, methine), 5.95 (1H, d, J_{cis} = 11.52 Hz, vinylic), 6.57-6.65 (1H, m, vinylic), 7.10-7.58 (18H, m, aromatic); ^{13}C NMR ($CDCl_3$) δ 53.25, 59.51, 123.29, 124.03, 124.13, 125.13, 125.65, 128.28, 128.49, 128.64, 128.83, 129.17, 130.13, 133.02, 133.42, 137.01, 137.57, 145.11, 145.33, 151.38, 159.00, 193.94, 195.99; FAB-MS m/z 439 (M^+ +1), 333 (M^+ -COPh) and other peaks. Anal. Calcd for $C_{32}H_{22}O_2$: C, 87.65; H, 5.06. Found: C, 87.79; H, 5.35.

3.4.4.2. Synthesis of 11b: A sample of **21b** (0.55 g, 2.5mmol) was dissolved in minimum quantity of dry xylene and DBA **7** (0.88 g, 3.8mmol) was added and the mixture was refluxed for 8 h, following the progress of the reaction

through TLC. The solvent was removed under reduced pressure and the residue obtained was purified by recrystallisation from a mixture of dichloromethane and hexane (2:1) to give **11b**.

Compound 11b: (82%); mp 172 °C; IR ν_{\max} (KBr) 1667 (C=O, ketone) cm^{-1} ; UV λ_{\max} (CH₃CN) 257 (ϵ 11,090), 300 nm (ϵ 2,450); ¹H NMR (CDCl₃) δ 3.65 (2H, d, methylene, $J_{\text{vic}}=5.5$ Hz), 5.04 (1H, dd, $J_{\text{cis}}=10.5$ Hz, $J_{\text{gem}}=1.5$ Hz, vinylic), 5.24 (1H, dd, $J_{\text{trans}}=17.0$ Hz, $J_{\text{gem}}=1.5$ Hz, vinylic), 5.51 (1H, s, methine), 5.93-6.01 (1H, m, vinylic), 7.10-7.51 (18H, m, aromatic); ¹³C NMR (CDCl₃) δ 30.70, 53.22, 55.54, 119.10, 122.99, 123.73, 124.35, 125.08, 125.26, 128.16, 128.26, 128.71, 129.02, 132.91, 133.10, 134.43, 137.08, 137.74, 145.39, 145.87, 152.56, 155.84, 194.21, 195.31; FAB-MS m/z 454 (M^++2), 347 ($M^+-\text{COPh}$) and other peaks. Anal. Calcd for C₃₃H₂₄O₂: C, 87.58; H, 5.35. Found: C, 88.01; H, 5.09.

3.4.4.3. Synthesis of 11c: A sample of **21c** (0.50 g, 1.8mmol) was dissolved in minimum quantity of dry xylene and DBA **7** (0.63 g, 2.7mmol) was added and the mixture was refluxed for 6 h, following the progress of the reaction through TLC. The solvent was removed under reduced pressure and the residue obtained was purified by recrystallisation from a mixture of dichloromethane and hexane (2:1) to give **11c**.

Compound 11c: (91%); mp 190 °C; IR ν_{\max} (KBr) 1662 (C=O, ketone) cm^{-1} ; UV λ_{\max} (CH₃CN) 256 (ϵ 12,200), 300 (ϵ 2,310); ¹H NMR (CDCl₃) δ 5.58 (1H, s, methine), 6.83 (1H, d, $J_{\text{AX}}=17$ Hz, vinylic), 6.91 (1H, d, $J_{\text{AX}}=17$ Hz, vinylic), 7.06-7.59 (23H, m, aromatic); ¹³C NMR (CDCl₃) δ 53.21, 58.92, 121.65, 123.35, 124.02, 125.11, 125.63, 126.38, 128.10, 128.23, 128.41, 128.63, 128.76, 129.15, 129.79, 132.98, 133.31, 136.68, 136.95, 137.56, 138.54, 145.02, 145.72, 151.57, 159.09, 193.92, 196.02; FAB-MS m/z 515

($M^+ + 1$), 409 ($M^+ - \text{COPh}$) and other peaks. Anal. Calcd for $\text{C}_{38}\text{H}_{26}\text{O}_2$: C, 88.69; H, 5.09. Found: C, 89.10; H, 5.31.

3.4.4.4 Synthesis of 11d: A sample of **21d** (0.50 g, 2.0mmol) was dissolved in minimum quantity of dry xylene and DBA **7** (0.70 g, 3.0mmol) was added and the mixture was refluxed for 10 h, following the progress of the reaction through TLC. The solvent was removed under reduced pressure and the residue obtained was purified by column chromatography. Trace amounts of unreacted **21d** was separated upon elution with 4:1 hexane-dichloromethane mixture and **11d** was obtained upon elution with 2:3 hexane-dichloromethane mixture, which was further purified by recrystallisation from a mixture of dichloromethane and methanol (2:1).

Compound 11d: (78%); mp 186-188 °C; IR ν_{max} (KBr) 1655, 1672 (C=O, ketone) cm^{-1} ; UV λ_{max} (CH_3CN) 250 (ϵ 11,000), 300 nm (ϵ 3,000); ^1H NMR (CDCl_3) δ 2.35 (3H, s, CH_3), 5.62 (1H, s, methine), 6.51 (1H, d, $J_{\text{AX}} = 16.0$ Hz, vinylic), 7.15-7.56 (18H, m, aromatic), 7.64 (1H, d, $J_{\text{AX}} = 16.0$ Hz, vinylic); ^{13}C NMR (CDCl_3) δ 27.38, 53.32, 58.41, 122.78, 124.34, 125.36, 126.05, 128.35, 128.64, 128.75, 129.07, 133.25, 133.71, 136.78, 137.48, 137.61, 138.73, 144.20, 144.66, 152.47, 156.72, 193.85, 195.24, 197.65; FAB-MS m/z 481 ($M^+ + 1$), 376 ($M^+ - \text{COPh}$) and other peaks. Anal. Calcd for $\text{C}_{34}\text{H}_{24}\text{O}_3$: C, 84.98; H, 5.03. Found: C, 85.16; H, 5.47.

3.4.4.5. Synthesis of 11e: A sample of **21e** (0.50 g, 1.6mmol) was dissolved in minimum quantity of dry xylene and DBA **7** (0.56 g, 2.4mmol) was added and the mixture was refluxed for 10 h, following the progress of the reaction through TLC. The solvent was removed under reduced pressure and the residue obtained was purified by column chromatography. Trace amounts of unreacted **21e** was separated upon elution with 4:1 hexane-dichloromethane

mixture and **11e** was obtained upon elution with 3:2 hexane-dichloromethane mixture, which was further purified by recrystallisation from a mixture of dichloromethane and hexane (2:1).

Compound 11e: (86%); mp 120 °C; IR ν_{\max} (KBr) 1650, 1665 (C=O, ketone) cm^{-1} ; UV λ_{\max} (CH_3CN) 254 (ϵ 12,330), 300 (ϵ 3,900); ^1H NMR (CDCl_3) δ 5.58 (1H, s, methine), 7.13-7.77 (24H, m, aromatic and vinylic), 7.89 (1H, d, J_{AX} =16.5 Hz, vinylic); ^{13}C NMR (CDCl_3) δ 53.21, 58.90, 122.81, 124.20, 125.37, 125.93, 128.31, 128.65, 128.78, 129.12, 133.02, 133.15, 133.65, 136.74, 137.26, 139.36, 144.58, 144.74, 151.67, 157.65, 189.62, 193.73, 195.57; FAB-MS m/z 543 (M^++1), 437 ($M^+-\text{COPh}$) and other peaks. Anal. Calcd for $\text{C}_{39}\text{H}_{26}\text{O}_3$: C, 86.32; H, 4.83. Found: C, 86.54; H, 5.34.

3.4.4.6. Synthesis of 14: A sample of **22** (0.70 g, 1.6mmol) was dissolved in minimum quantity of dry xylene and DBA **7** (0.57 g, 2.4mmol) was added and the mixture was refluxed for 10 h. The solvent was removed under reduced pressure and the residue obtained was purified by recrystallisation from a mixture of dichloromethane and hexane (2:1) to give **14**.

Compound 14: (85%); mp 176-178 °C; IR ν_{\max} (KBr) 1653, 1665 (C=O, ketone) cm^{-1} ; UV λ_{\max} (CH_2Cl_2) 256 (ϵ 10,560), 300 (ϵ 4,300); ^1H NMR (CDCl_3) δ 5.56 (1H, s, methine), 6.70 (1H, d, J_{AX} =16.5 Hz, vinylic), 7.07-7.49 (18H, m, aromatic), 7.75 (1H, d, J_{AX} =17 Hz, vinylic); ^{13}C NMR (CDCl_3) δ 53.29, 58.63, 122.86, 124.19, 125.41, 125.93, 128.30, 128.55, 128.72, 129.08, 133.16, 133.56, 135.27, 136.73, 137.37, 139.42, 144.35, 144.64, 152.12, 157.06, 188.16, 193.82, 195.10; FAB-MS m/z 904 (M^++2), 798 ($M^+-\text{COPh}$) and other peaks. Anal. Calcd for $\text{C}_{65}\text{H}_{42}\text{O}_5$: C, 86.45; H, 4.69. Found: C, 87.16; H, 5.12.

3.4.4.7. Synthesis of 15: A sample of **24** (0.70 g, 1.5mmol) was dissolved in minimum quantity of dry xylene and DBA **7** (2.3 g, 9.8mmol) was added and the mixture was refluxed for 16 h. The solvent was removed under reduced pressure and the residue obtained was purified by recrystallisation from a mixture of dichloromethane and hexane (2:1) to give **15**.

Compound 15: (60%); mp >280 °C; IR ν_{\max} (KBr) 1663 (C=O, ketone) cm^{-1} ; UV λ_{\max} (CH_2Cl_2) 280 (ϵ 10,600), 300 nm (ϵ 3,200); ^1H NMR (CDCl_3) δ 1.26 (2H, m, methylene), 2.25 (4H, m, methylene), 5.51 (1H, s, methine), 7.14-7.64 (19H, m, aromatic and vinylic); ^{13}C NMR (CDCl_3) δ 29.07, 31.60, 53.68, 58.10, 123.49, 124.24, 125.08, 125.84, 128.34, 128.40, 128.87, 128.95, 129.60, 129.82, 130.09, 132.19, 133.20, 133.37, 136.79, 137.06, 144.32, 188.75, 194.39; FAB-MS m/z 943 (M^+ +1) and other peaks. Anal. Calcd for $\text{C}_{68}\text{H}_{46}\text{O}_5$: C, 86.60; H, 4.92. Found: C, 86.99; H, 5.50.

References

1. Diels, O.; Alder, K. *Ann.* **1928**, *460*, 98.
 2. Diels, O.; Alder, K. *Justus Liebigs Ann. Chem.* **1926**, *450*, 237.
 3. Sauer, J. *Angew. Chem. Int. Ed.* **1966**, *5*, 211.
 4. Diels, O.; Blom, J. H.; Koll, W. *Ann.* **1925**, *443*, 242.
 5. Martin, J. G.; Hill, R. K. *Chem. Rev.* **1961**, *61*, 537.
 6. Diels, O.; Alder, K. *Ber.* **1929**, *62*, 2087.
 7. Alder, K.; Stein, G. *Angew. Chem.* **1937**, *50*, 510.
 8. Diels, O.; Alder, K. *Ann.* **1931**, *486*, 191.
 9. Sauer, J. *Angew. Chem. Int. Ed.* **1967**, *6*, 16.
 10. Alder, K.; Stein, G.; Rolland, E. *Ann.* **1936**, *525*, 247.
 11. Woodward, R. B.; Katz, T. J. *Tetrahedron* **1959**, *5*, 70.
 12. Alder, K.; Stein, G.; Buddenbrock, R. V.; Eckardt, W.; Frecks, W.; Schneider, S. *Ann.* **1934**, *514*, 1.
 13. Lowry, T. H.; Richardson, K. S. *Mechanism and Theory in Organic Chemistry*; 3rd ed.; Addison-Wesley, New York, 1998, p 919.
 14. Kloetzel, M. *Organic Reactions* **1967**, *4*, 1.
 15. Corey, E. J. *Angew. Chem. Int. Ed.* **2002**, *41*, 1650.
 16. Holmes, H. L. *Organic Reactions* **1948**, *4*, 60.
 17. Sauer, J. *Angew. Chem. Int. Ed.* **1967**, *6*, 16.
 18. Spino, C.; Rezaei, H.; Dory, Y. L. *J. Org. Chem.* **2004**, *69*, 757.
 19. Sauer, J.; Sustmann, R. *Angew. Chem., Int. Ed. Engl.* **1980**, *19*, 779.
 20. Alder, K. *Newer Methods of Preparative Organic Chemistry*, Vol.1, Wiley-Interscience: New York, **1948**, p 381.
 21. Nicolaou, K. C.; Snyder, S. A.; Montagnon, T.; Vassilikogiannakis, G. *Angew. Chem. Int. Ed.* **2002**, *41*, 1668.
 22. Brieger, G.; Bennett, J. N. *Chem. Rev.* **1980**, *80*, 63.
-

23. Needleman, S. B.; Changkuo, M. C. *Chem. Rev.* **1962**, *62*, 405.
 24. Asano, T.; le Noble, W. *Chem. Rev.* **1978**, *78*, 407.
 25. Kagan, H. B.; Riant, O. *Chem. Rev.* **1992**, *92*, 1007.
 26. Cativiela, C.; Garcia, J. I.; Mayoral, J. A.; Salvatella, L. *Chem. Soc. Rev.* **1996**, 209.
 27. Paquette, L. A.; Bay, E. *J. Am. Chem. Soc.* **1984**, *106*, 6693.
 28. Paddick, R. G.; Richards, K. E.; Wright, G. J. *Aust. J. Chem.* **1976**, *29*, 1005.
 29. Kumar, S. A.; Rajesh, C. S.; Das, S.; Rath, N. P.; George, M. V. *J. Photochem. Photobiol. A.* **1995**, *86*, 177.
 30. Kumar, S. A.; Ramaiah, D.; Eldho, N. V.; Das, S.; Rath, N. P.; George, M. V. *J. Photochem. Photobiol. A.* **1997**, *103*, 69.
 31. Sajimon, M. C.; Ramaiah, D.; Muneer, M.; Rath, N. P.; George, M. V. *J. Photochem. Photobiol. A.* **2000**, *136*, 209.
 32. Murthy, B. A. R. C.; Pratapan, S.; Kumar, C. V.; Das, P. K.; George, M. V. *J. Org. Chem.* **1985**, *50*, 2533.
 33. Sajimon, M. C.; Ramaiah, D.; Ajayakumar, S.; Rath, N. P.; George, M. V. *Tetrahedron* **2000**, *56*, 5421.
 34. (a) Lutz, R. E. In *Organic Synthesis*, Horning, E. C., Ed.; Collect. Vol. 3; Wiley: New York, **1995**, p 248. (b) Lutz, R. E.; Smithy, W. R. *J. Org. Chem.* **1951**, *16*, 648.
-

Preliminary Time-Resolved Fluorescence Studies of Some Olefin appended Dibenzobarrelenes and Bisdibenzobarrelenes Employing TCSPC Technique

4.1. Abstract

To understand the primary and secondary physicochemical processes in a photochemical reaction it is necessary to characterise the excited states and the transient intermediates during their short lifetime. A number of methods developed on the basis of the physical properties of the transient species are available for their detection. Time-correlated single-photon counting technique has been utilised in the present study of the excited states of olefin appended dibenzobarrelenes and bisdibenzobarrelenes.

4.2. Introduction

Fluorescence spectroscopy¹ is a powerful technique to investigate the structural and dynamic properties of molecules. The excited states of fluorophores are very sensitive to the changes in their environment, which can result in a shift of the absorption or emission wavelength, or an intensity variation. Alternatively, when time-resolved measurements are performed, the different decay rates of fluorescence intensity or the polarization anisotropy can be recorded. The former stems from the fact that many dynamic events can deactivate the excited state² and hence influence the lifetime.

Time-resolved measurements are widely used in fluorescence spectroscopy, particularly for studies of biological macromolecules and for cellular imaging.³ Time-resolved measurements contain more information

than is available from the steady-state data. One can distinguish static and dynamic quenching using lifetime measurements. The time-resolved donor decays are highly informative about the purity of the sample as well as the donor-to-acceptor distance.

The studies presented in this chapter focuses on the aspect of time-resolved fluorescence. In this method, the fluorophores are excited by a sudden pulse of light, which results in population of excited states. Then this population decays through two channels: 1) random deactivation through fluorescence emission and nonradiative processes⁴, 2) quenching⁵ due to energy transfer. In the case of the novel bisdibenzobarrelenes, there might be chances of excimer^{6,7} formation.

Fox *et al.*^{8,9} as a case study for the design of donor-acceptor compounds with tailor-made properties, has conducted an INDO/S level molecular orbital investigation of organic molecules where aromatic donors are rigidly linked to a maleic ester group via a barrelene-type bridge. The study indicates that dibenzobarrelene with dicarbomethoxy ester groups resemble a bridged donor-acceptor molecule, where the aromatic residues act as electron donors and the dicarbomethoxy ester groups act as electron acceptors.¹⁰ The INDO/S calculations yielded a low-lying state with definite charge-transfer characteristics.

The fluorescence quantum yields (ϕ_f^s) were determined by comparing the integrated fluorescence spectra of the sample with that of the reference,^{11,12} while keeping the excitation wavelength equal. Equation 1 was used for the determination of fluorescence quantum yield (ϕ_f^s).

$$\phi_f^s = \phi_f^r x \frac{A_f^s}{A_f^r} x \frac{OD^r}{OD^s} x \frac{(\eta^s)^2}{(\eta^r)^2} \quad (1)$$

where A_f^s and A_f^r are the area under the fluorescence spectra of the sample and the reference respectively and OD^s and OD^r are the respective optical densities of the sample and the reference solutions at the wavelength of excitation. A correction was applied for the variation of the refractive indices of the solvents. n^s and n^r are the respective refractive indices of the sample solution and reference solution. These measurements were carried out to characterise the excited singlet (S_1) state.

Time dependent fluorescence measurement is an important method to investigate the dynamics of the singlet (S_1) state of the molecules. If the S_1 state is involved in some complex photochemical processes, such behaviour will be reflected in the fluorescence decay and the analysis of decay curves reveals the mechanistic details of the processes undergone by the S_1 state.¹ In majority of the cases it is seen that the fluorescence decay can be expressed as a sum of exponentials as,

$$F(t) = \sum F_i(0) \exp(-t/\tau_i) \quad (2)$$

where, $F_i(0)$ is the fluorescence intensity of the i^{th} component at time zero. The time dependent fluorescence of a molecule can be measured by a number of methods. Time-correlated single-photon counting spectrometer has been used in the present work and is described here in great detail.

4.2.1. Basic Principles of the Fluorescence Life Time Measurements by Time-Correlated Single-Photon Counting (TCSPC) Technique¹³⁻¹⁵

Fluorescence lifetimes were measured using a time domain fluorescence spectrometer Model EI-199 (Edinburgh Instrument, U.K.). The schematic diagram of the set up is shown in Figure 1. The instrument operates

on the principle of time-correlated single-photon counting (TCSPC). This technique relies on the concept that the probability distribution of a single photon emission after an excitation event represents the fluorescence intensity variation with time. An optical excitation pulse from a flash lamp is split into two parts, one part is used to excite the sample which is kept in the sample chamber and the other part is used to generate a start pulse in a start PMT. The optical signal at the start PMT generates an electrical START pulse which is routed through a Constant Fraction Discriminator (CFD) to the START input of the Time to Amplitude Converter (TAC) to initialise its charging operation. The part of the optical pulse which excites the sample effectively gives emission photons, which are then detected by a stop PMT (at the right angle to the direction of excitation) to generate a STOP pulse. The STOP pulse is also routed to TAC through another CFD and variable delay. On receiving the STOP signal, TAC stops its charging operation and generates an electrical output (TAC-output) having amplitude proportional to the time differences (Δt) between the START and STOP pulses reaching the TAC. The TAC output pulse is then fed to the input of a Multichannel Analyzer (MCA) through an analog to digital converter (ADC). The ADC generates a numerical value corresponding to the TAC output pulse and thus selects an appropriate address (channel) of the MCA and a count is added to this address. The above cycle (from excitation to data storage) is repeated large number of times and as a result a histogram of counts against the channel number of the MCA is generated. It represents exactly the fluorescence decay curve only when the collection rate of emission of the photon by the stop PMT is very low usually <0.02 photon/excitation pulse, and is illustrated by statistical treatment.¹³ Fluorescence lifetime of the samples are calculated from such curves after proper time calibration of the MCA channels.

4.2.2. Detailed Description of the Time Domain Fluorimeter (EI-199):

(a) **Coaxial Flash Lamp:** Low pressure, gated, thyatron-triggered coaxial flash lamp of high repetition rate is used for excitation. The lamp compartment and the thyatron are housed together in a large metal box, where the thyatron is coaxial with thoriated tungsten electrodes. The pulse repetition rate of the lamp can be adjusted by means of an oscillator, driving the thyatron pulser.

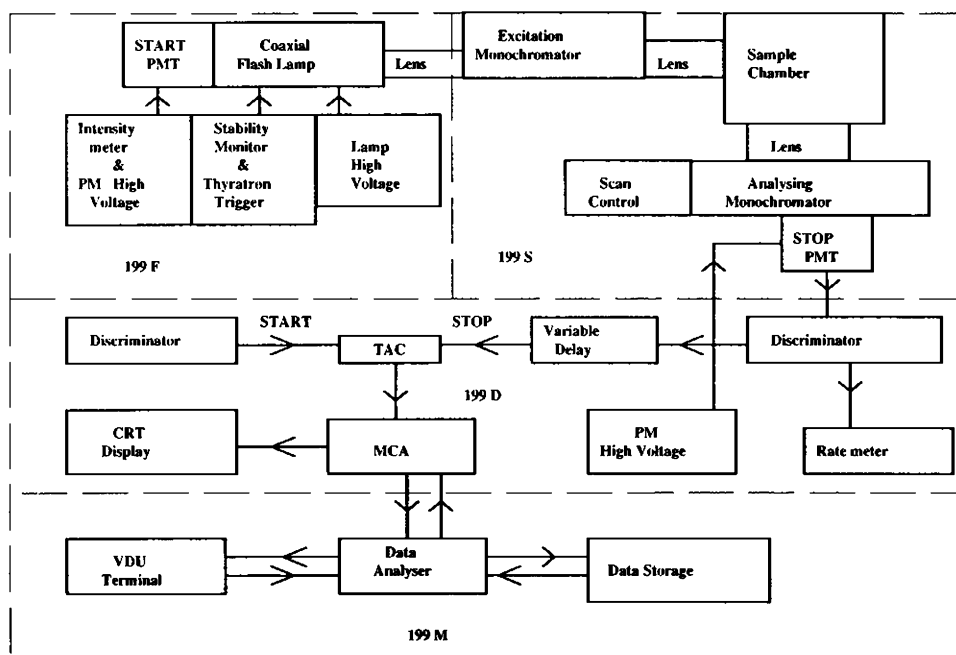


Figure 1. Schematic diagram of the Time-Correlated Single-Photon Counting Fluorescence Spectrometer, EI-199. 199F, the Flash lamp with control units; 199s, the spectrometer part; 199D, the SPC detection system and 199M, the data analyser.

Hydrogen gas is used at ~ 0.5 atm. Pressure in the lamp chamber and

the gap between the two electrodes is kept ~ 0.7 mm. The typical discharge voltage is applied about 6 to 8 kV and repetition rate for the lamp pulsing is kept ~ 30 kHz. Using the above parameters, ~ 1 ns (FWHM) pulses from D_2 lamp can be obtained.

The most important development for TCSPC since 2000 is the introduction of pulsed-laser diodes (LDs) and pulsed light-emitting diodes (LEDs) as simple solid-state sources. These devices consume little power, are easy to operate and require almost no maintenance.

(b) Discriminator: The signals from the PMT are routed through the discriminator in order to improve the signal to noise ratio (S/N) and to get correct timing information. As simple leading edge discriminator is always associated with timing errors, the Constant Fraction Discriminators (CFD) are used in SPC instruments. A threshold level is set on the front panel of the CFD to filter out low amplitude noises from the input pulses.¹³

(c) Variable Delay Lines: A variable delay line is incorporated in the path of the STOP signal between the CFD and the TAC to trigger the TAC-MCA combination in such a way that an optimum placement of the decay curve can be obtained in the MCA channels.

(d) Time to Amplitude Converter (TAC): The time correlation between excitation and emission events is carried out by the TAC unit and is called the heart of the SPC instrument. After receiving the START pulse and after a fixed delay, a timing capacitor is charged linearly from a constant current source. The charging is discontinued on the arrival of a STOP pulse and as a result an output pulse is generated equivalent to the amplitude of the final charge in the capacitor. Since charging ramp of the capacitor is linear with time, the TAC output signal height is proportional to the time differences (Δt) between the START and the STOP pulses.

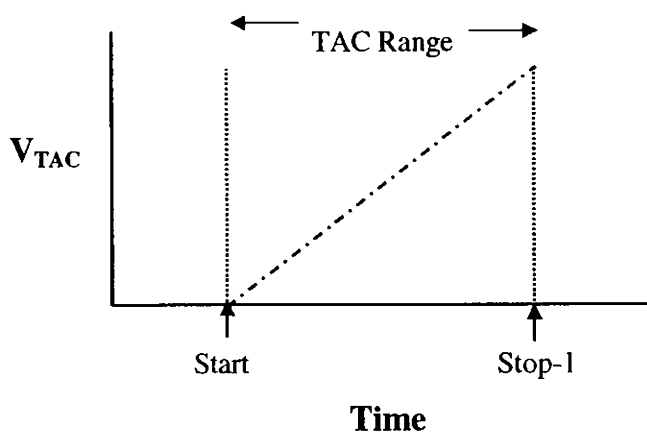


Figure 2. Functioning of TAC

(e) Multichannel Analyzer (MCA): The MCA used in the EI-199 is equipped with an AD-converter, a memory consisting of 1024 channels or multiple of this to store the time correlated data and a CRT screen. MCA can be operated either in Pulse Height Analysis (PHA) mode or in Multichannel Scaling (MCS) mode. For fluorescence lifetime measurements MCA is operated in PHA mode. The data stored in MCA channels are transferred to the computer for analysis.

(f) The Start PMT: As the light intensity detected by the Start PMT is quite high, an ordinary PMT with medium gain and reasonably low transit time can be used. IP-28 PMT (Hamamatsu) is used in EI-199 spectrometer.

(g) The Stop PMT: The spread in transit time (the time difference between the emission of a photoelectron and its arrival to the anode) has a pronounced effect on the time resolution of an SPC instrument. As the transit time becomes shorter the spread also becomes shorter and thus the time resolution increases. Thus a fast PMT is suitable for TCSPC measurements. As the detected light level is very low the gain of the Stop PMT should also be very high. To get better gain one has to increase the number of dynodes, as a result

transit time increases in the process.¹³ For this purpose specially designed 12-stage Philips XP-2020Q end-on PMT is used as Stop PMT, which is having a high gain (3×10^7 at 2.2 kV) and reasonably lower transit time (~28 ns). The cathode material of XP-2020 Q is bi-alkali KCsSb with spectral response from 200-650nm. The dark current is so low that one can work at room temperature.

4.2.3. Time Calibration in EI-199 Spectrometer:

Time Calibration of the MCA channels of EI-199 is done using a number of accurately calibrated delay lines.⁷ For this purpose the stop signal is split into two parts, one is fed to the START input of the TAC and the other is routed through the precisely calibrated delay lines and then fed to the STOP input of the TAC. As the same STOP signal is used for both the START and STOP input of the TAC, counts will be collected at a single channel of the MCA depending on the TAC range used and delay introduced in the path of the STOP pulse. For different delays, counts are collected at different channels of the MCA. MCA data are then processed in a computer and the time calibration is done using suitable program.

4.2.4. Data Analysis:

Since the excitation pulses used for practical purposes have a finite time width and the detection system has also a finite response time, the observed decay curve $I(t)$ is a convolution of the true decay curve $G(t)$ and the effective time profile of the excitation pulse, $P(t)$. Observing $I(t)$ and $P(t)$ experimentally and assuming a proper decay function $G(t)$, a convoluted function $Y(t)$ can be calculated and compared with the experimentally observed decay curve $I(t)$. Hence, $Y(t)$ can be expressed as

$$Y(t) = \int_0^t P(t') G(t - t') dt' \quad (3)$$

For mathematical analysis, the function $G(t)$ is assumed to be a sum of exponentials, such that

$$G(t) = \sum B_i \exp(-t/\tau_i) + A \quad (4)$$

Where, B_i is the pre-exponential factor for the i th component, τ_i is the corresponding fluorescence lifetime and A is a correction term for constant background. The mathematical procedure is used to calculate the function $Y(t)$ and then $G(t)$ is extracted out from $Y(t)$ by the nonlinear least square iterative reconvolution method and is assumed to be either a monoexponential or biexponential or multiexponential function and the best $G(t)$ is selected from the reduced chi-square (χ_r^2) value and distribution of weighted residuals.

(a) Reduced Chi-square value: The reduced chi-square (χ_r^2) value is defined as

$$\chi_r^2 = \frac{\sum_{i=n_1}^{n_2} W_i \{Y(i) - I(i)\}^2}{(n_2 - n_1 + 1 - p)} \quad (5)$$

Where, $W_i \{= 1/I(i)\}$, is the weighting factor of the counts in the i th channel, n_1 and n_2 are the first and last channels of the section of the analysed decay curve, and p is number of degrees of freedom for the particular fitting (namely, three for single exponential fitting, i.e. B , τ and A and so on). In the actual analysis the function $G(t)$ is assumed to be either a monoexponential or a biexponential or a triexponential function and for each of these cases the parameter B_i , τ_i and A are varied as long as a minimum (χ_r^2) value is obtained.

When the decay curve with its peak channel having 5-10 thousand counts, is considered to be having a suitable precision, the number of counts in

each channel $I(i)$, follows a Poission distribution with a standard deviation σ_i , given by

$$\sigma_i = \sqrt{I(i)} \quad (6)$$

Thus, the best selection of $G(t)$ will be the one for which the (χ_r^2) value is very close to unity.

(b) Distribution of Weighted Residuals: The weighted residual for the i th channel is defined as

$$r_i = W_i \{Y(i) - I(i)\} \quad (7)$$

For a good fit the weighted residuals among the data channels should be randomly distributed about zero and should follow a Gaussian distribution, i.e. 68%, 95%, 99.7% and 100% of the weighted residuals should be within 1, 2, 3 and 4 respectively.

4.2.5. Overview of Fluorescence Spectroscopy

Fluorescence spectroscopy can be applied to a wide range of problems in the chemical and biological sciences. The measurements can provide information on a wide range of molecular processes, including the interactions of solvent molecules with fluorophores, rotational diffusion of biomolecules, distances between sites in biomolecules, conformational changes and binding interactions. The usefulness of fluorescence is being expanded by advances in technology for cellular imaging and single-molecule detection. Fluorescence spectroscopy will continue to contribute to rapid advances in biology, biotechnology and nanotechnology.

4.3. Results and Discussion

We chose the dibenzobarrelenes **1a-d** and the bisdibenzobarrelenes **1e-h** (Chart 1) for the time-resolved studies employing TCSPC (Time-Correlated Single-Photon Counting) Technique. The absorption spectra of **1a-h** was recorded in dichloromethane at room temperature, is depicted in Figure 3. Dibenzobarrelene **1a** was chosen as the reference for our study.

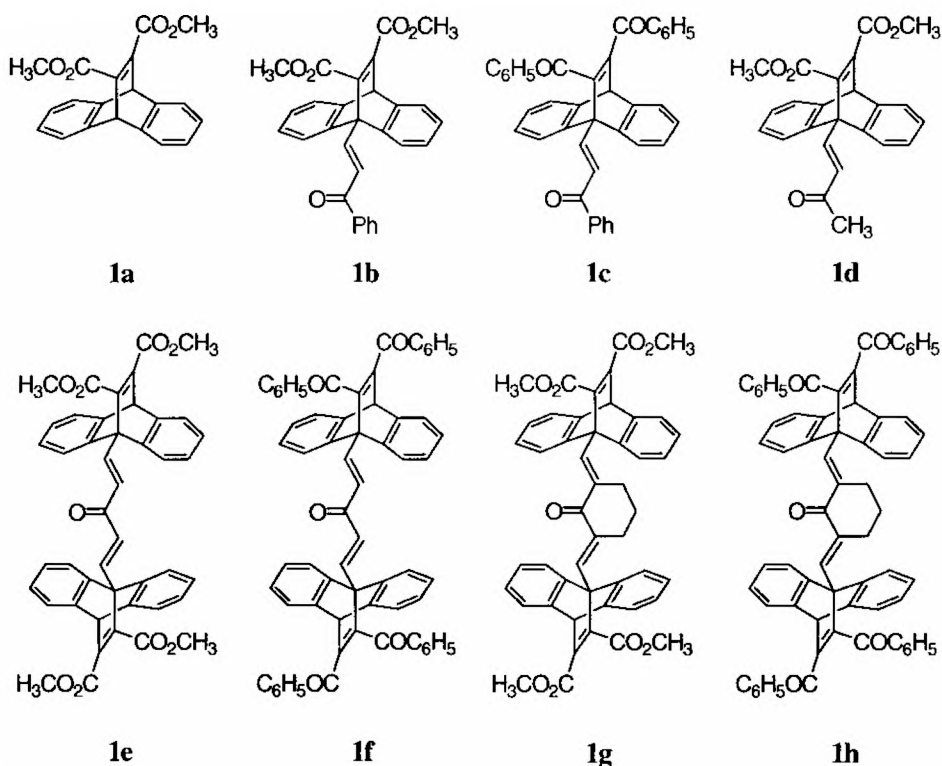


Chart 1

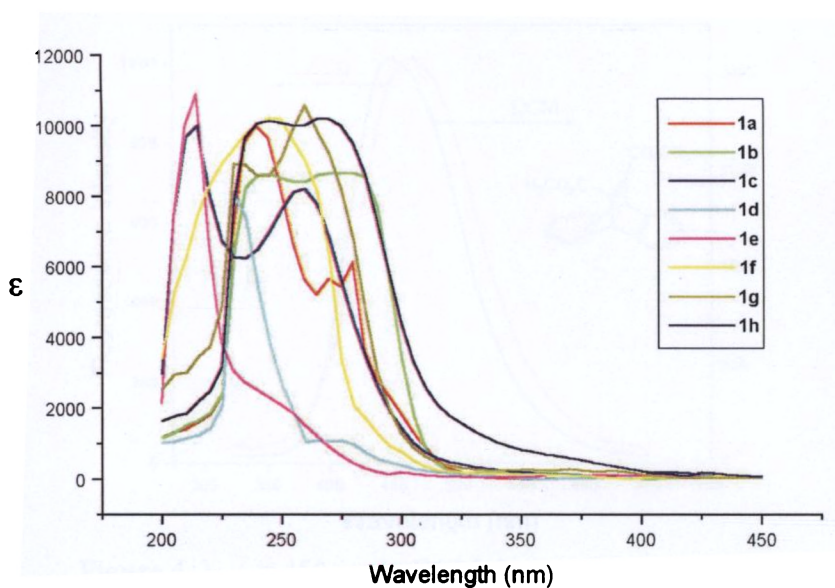


Figure 3. Absorption spectra of **1a-h** at room temperature in 10^{-5} M dichloromethane

In the case of dibenzobarrelene type molecular systems, the absorption band with peak intensity at 280 nm, is attributed to the O-O transition of $S_0 \rightarrow S_1$.⁹

The fluorescence spectrum of the selected molecules taken in acetonitrile (ACN) and dichloromethane (DCM) is shown in Figures 4 to 10.

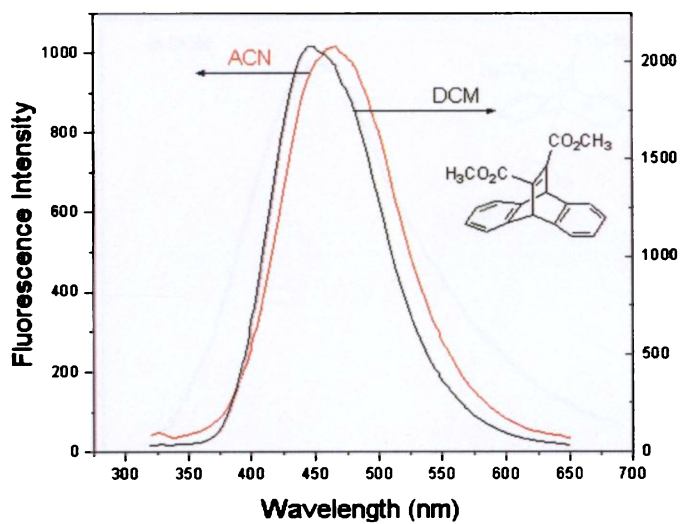


Figure 4. $\lambda_{\text{max}} = 450 \text{ nm}$ in DCM; $\lambda_{\text{max}} = 465 \text{ nm}$ in ACN

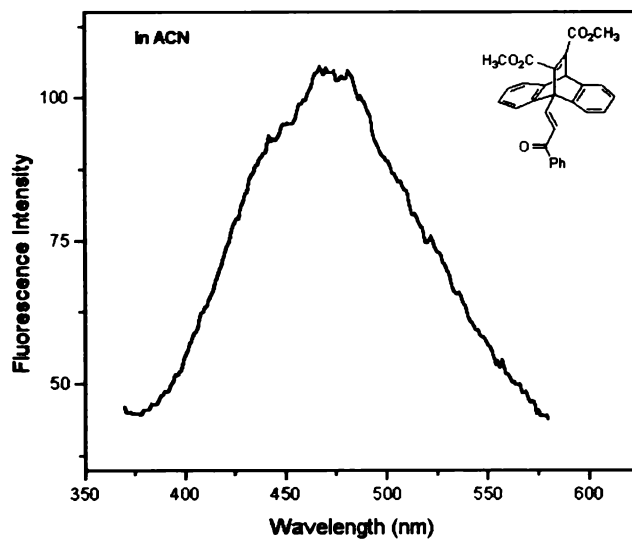


Figure 5. $\lambda_{\text{max}} = 470 \text{ nm}$ in ACN

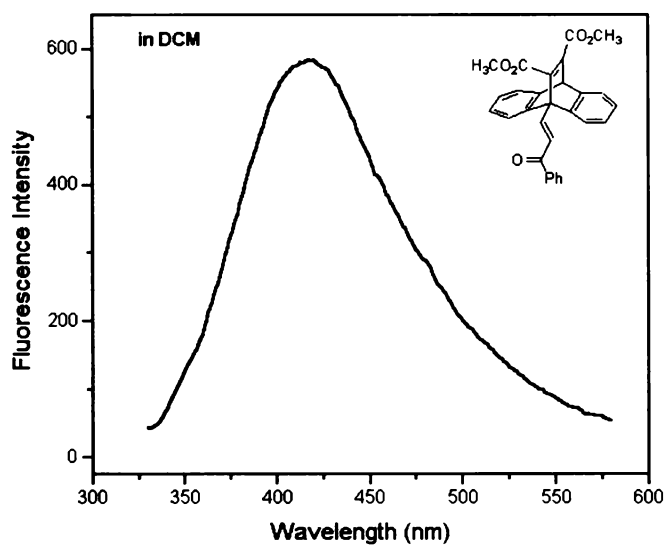


Figure 6. $\lambda_{\text{max}} = 425$ nm in DCM

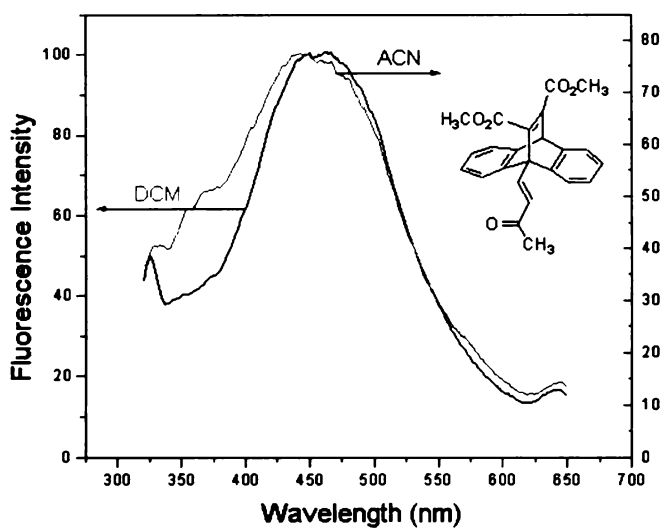


Figure 7. $\lambda_{\text{max}} = 473$ nm in DCM; $\lambda_{\text{max}} = 445$ nm in ACN

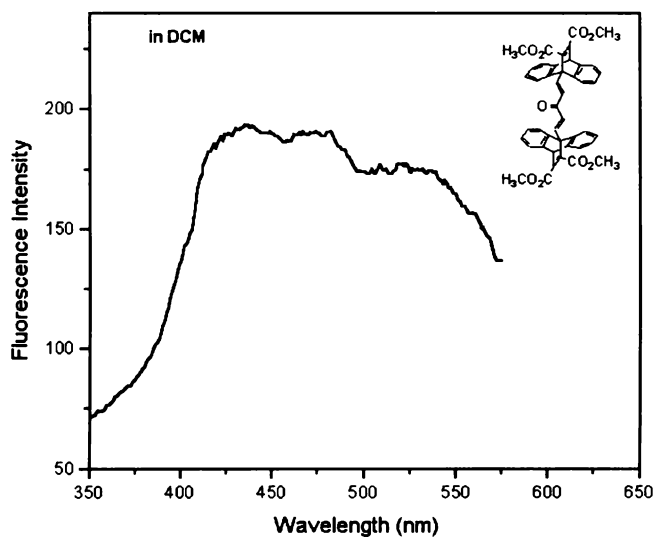


Figure 8. $\lambda_{\text{max}} = 435$ nm in DCM

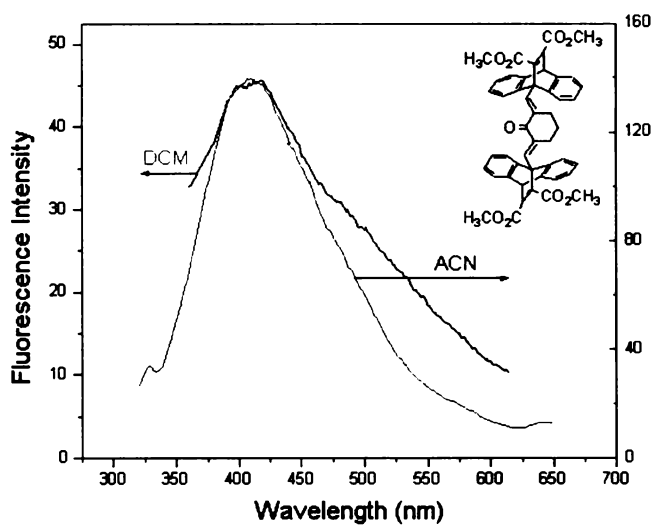


Figure 9. $\lambda_{\text{max}} = 415$ nm in DCM; $\lambda_{\text{max}} = 425$ nm in ACN

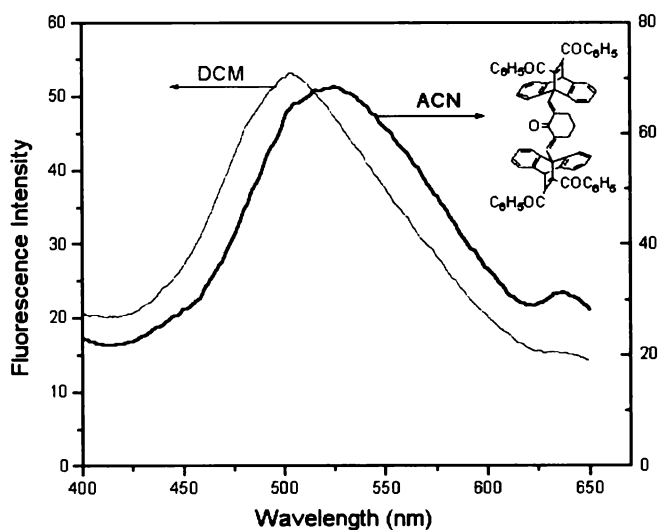


Figure 10. $\lambda_{\text{max}} = 505$ nm in DCM; $\lambda_{\text{max}} = 527$ nm in ACN

Of the selected molecules, **1c** and **1f** were non-fluorescent. It might be due to large rate of internal conversion or a slow rate of emission.¹

The fluorescence λ_{max} of **1a-h** showed marked sensitivity to solvent polarity. This behaviour can be explained through the Jablonski diagram shown in Figure 11. The processes that occur between the absorption and emission of light are usually illustrated by the Jablonski¹⁶ diagram. These diagrams are used in a variety of forms, to illustrate various molecular processes that occur in excited states.

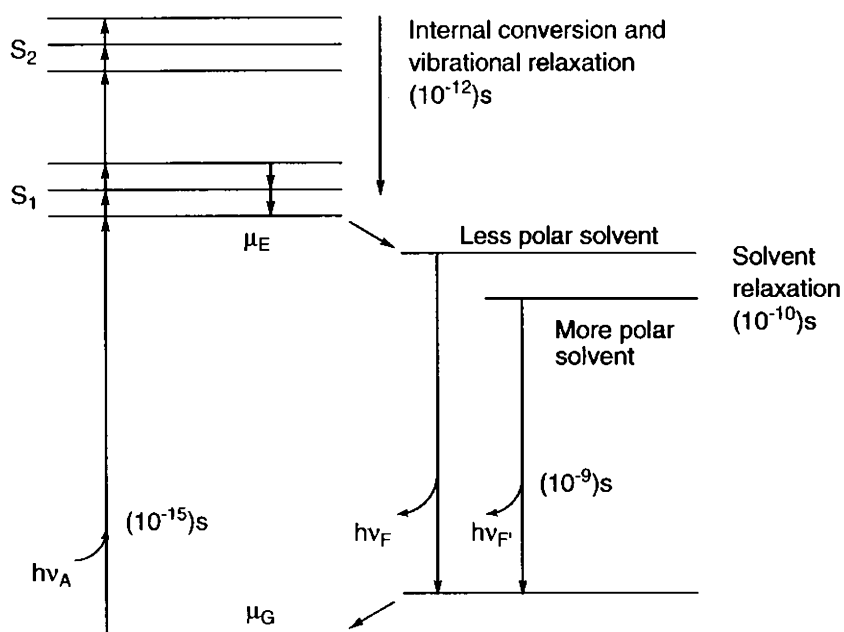


Figure 11. Jablonski diagram for fluorescence with solvent relaxation¹

Emission from fluorophores generally occurs at wavelengths that are longer than those at which absorption occurs. This loss of energy is due to a variety of dynamic processes that occur following light absorption as shown in Figure 11. The fluorophore is typically excited to the first singlet state (S_1), usually to an excited vibrational level within S_1 . The excess vibrational energy is rapidly lost to the solvent. If the fluorophore is excited to the second singlet state (S_2), it rapidly decays to the S_1 state in 10^{-12} s due to internal conversion. Solvent effects shift the emission to still lower energy due to stabilisation of the excited state by the polar solvent molecules. Typically, the fluorophore has a larger dipole moment in the excited state (μ_E) than in the ground state (μ_G). Following excitation, the solvent dipoles can reorient or relax around μ_E , which lowers the energy of the excited state. As the solvent polarity is increased, this effect becomes larger, resulting in emission at lower

energies or longer wavelengths. In general, only fluorophores that are themselves polar display a large sensitivity to solvent polarity. Nonpolar molecules, such as unsubstituted aromatic hydrocarbons, are much less sensitive to solvent polarity.

The marked difference in the fluorescence absorption maximum of the molecules in acetonitrile and dichloromethane, point towards the formation of an internal charge transfer state (ICT).¹⁷ Cortes *et al.*¹⁰ has shown that dibenzobarrelene with dicarbomethoxy ester groups resemble a bridged donor-acceptor molecule, where the aromatic residues act as electron donors and the dicarboxy ester groups act as electron acceptors. Fluorophores possessing electron-donating and electron-accepting groups, upon excitation undergoes an increase in charge separation within the molecule.

The fluorescence emission spectrum of **1e** in Figure 8, shows a broad, structureless emission band, characteristic of an excimer emission. But the non-gaussian nature of the curve and the curve being interrupted due to the second harmonic function of the flash lamp, does not confirm an excimer formation. The fluorescence emission spectra of **1g** and **1h** shows no excimer formation.

4.3.1. Fluorescence Lifetimes

The fluorescence lifetime is one of the most important characteristics of a fluorophore. The lifetime of a fluorophore is the average time between its excitation and return to the ground state and moreover it determines the time available for the fluorophore to interact with or diffuse in its environment, and hence the information available from its emission.

In the excited singlet states, the electron in the excited orbital is paired to the second electron in the ground-state orbital. Consequently, return to the ground state is spin allowed and occurs rapidly by emission of a photon. The

emission rates of fluorescence are typically 10^8 s^{-1} , so that a typical fluorescence lifetime is near 10 ns ($10 \times 10^{-9} \text{ s}$). Due to the short timescale of fluorescence, measurement of the time-resolved emission requires sophisticated optics and electronics. In spite of the added complexity, time-resolved fluorescence is widely used because of the increased information available from the data, as compared with steady-state measurements.

The intensity decay for samples **1a-h**, is shown in Figures 12 to 22. The curve L in the figures is the instrument response function, i.e. the response of the instrument to a zero lifetime sample. This curve is typically collected using a dilute scattering solution such as colloidal silica (Ludox) and no emission filter. This decay represents the shortest time profile that can be measured by the instrument.

The measured intensity decay of the various samples is shown as a histogram of dots. The height of the dots on the y-axis represents the number of photons that were detected within the time interval t_k to $t_k + \Delta t$, where Δt is the width of the timing channel. In the case of **1a** in ACN (Figure 12), the largest number of counts has recorded approximately 3000 photons.

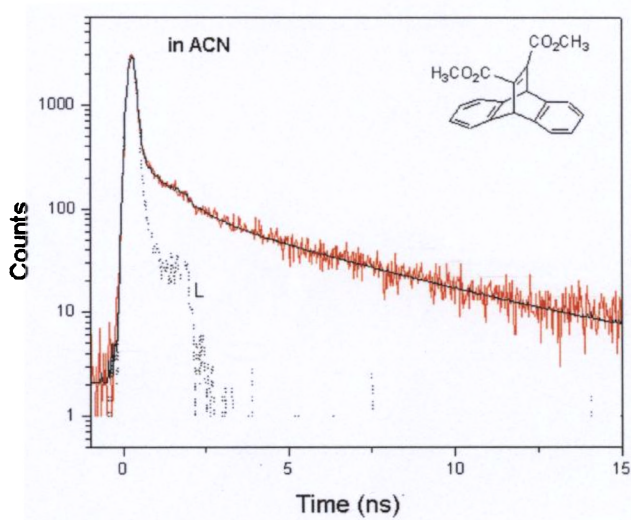


Figure 12

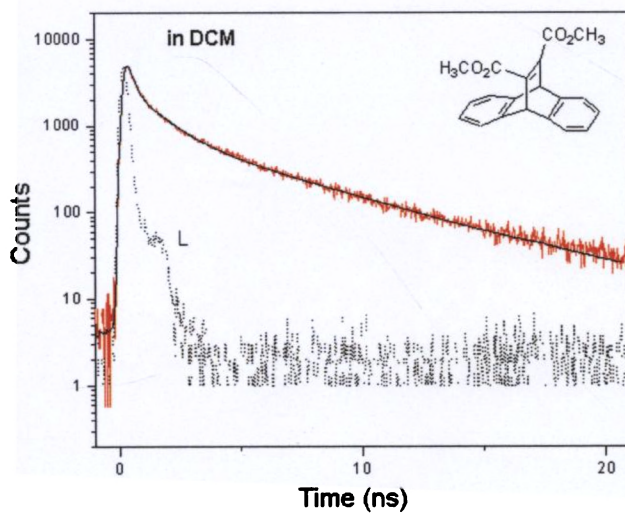


Figure 13

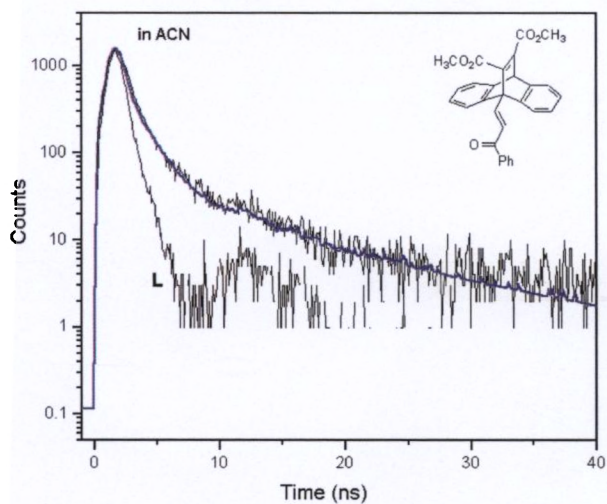


Figure 14

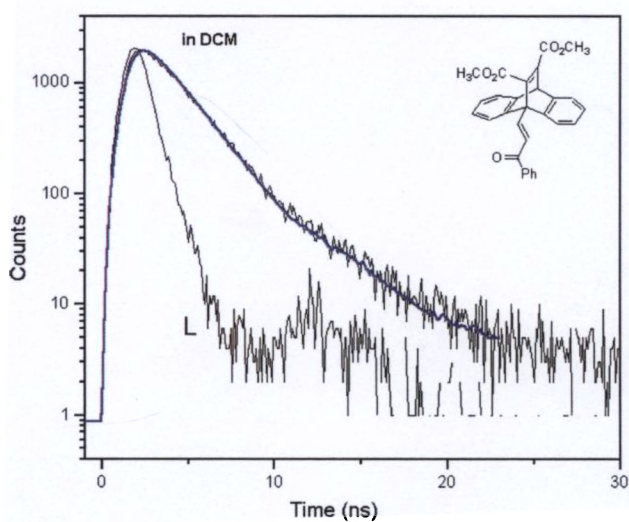


Figure 15

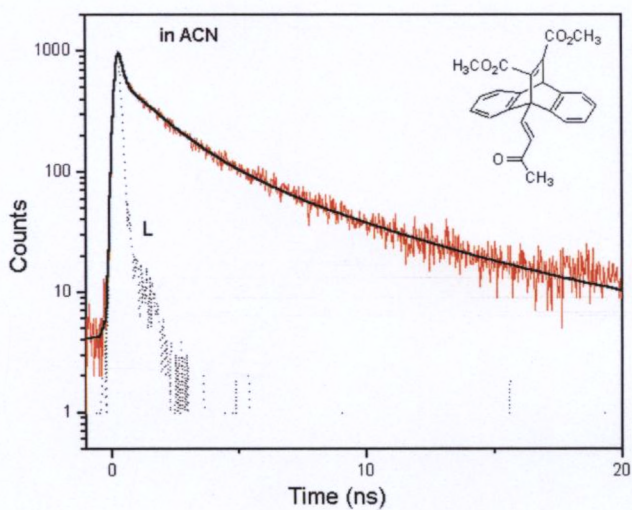


Figure 16

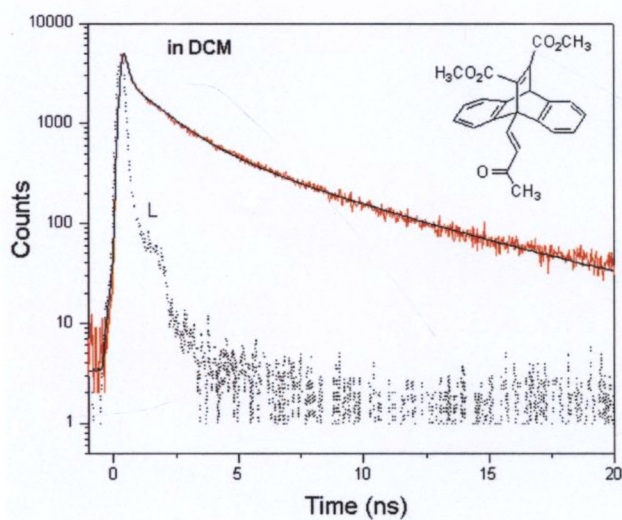


Figure 17

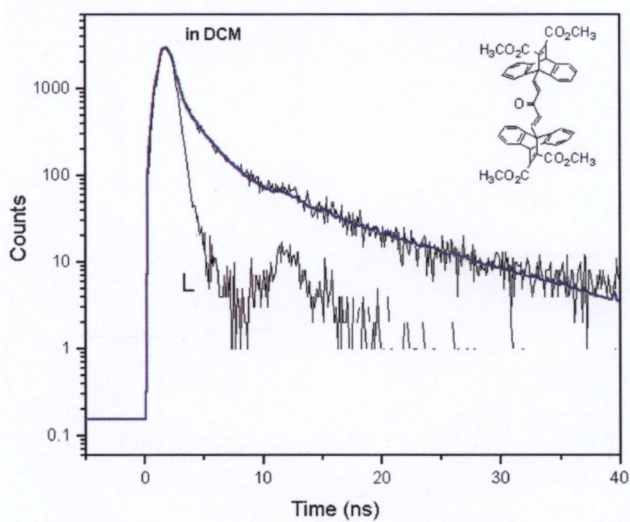


Figure 18

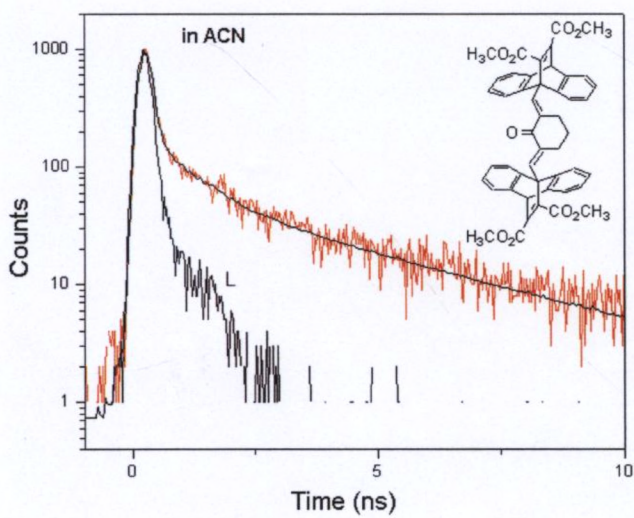
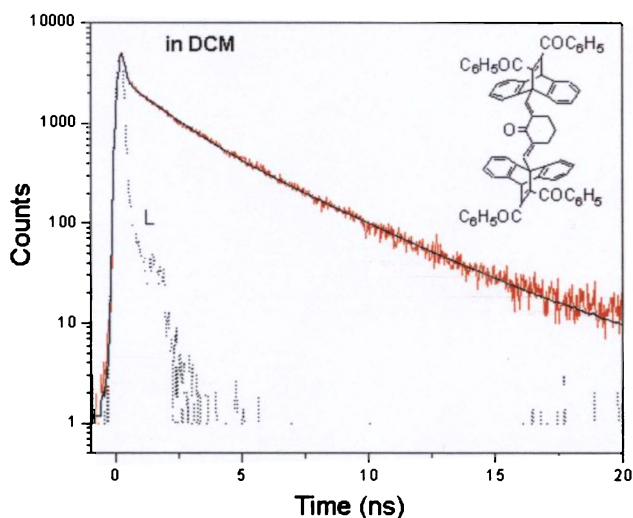


Figure 19

**Figure 22**

A general property of fluorescence is that the same fluorescence emission spectrum is generally observed irrespective of the excitation wavelength. This is known as Kasha's rule.¹⁸ In this study, hydrogen flash lamp emitting 290 nm radiation and diode lasers emitting 408 nm radiation were utilised.

An important concept is that the lifetime is a statistical average and fluorophores emit randomly through out the decay. The fluorophores do not all emit at a time delay equal to the lifetime. For a large number of fluorophores some will emit quickly following the excitation, and some will emit at times longer than the lifetime. This time distribution of emitted photons is the intensity decay.

Compound	λ_{exc} (nm)	Solvent	τ_1	τ_2	τ_3
1a	408	ACN	16 ps (77%)	1 ns (6%)	5 ns (17%)
		DCM	235 ps (19%)	1.2 ns (28%)	5.5 ns (53%)
1b	290	ACN	357 ps (75%)	3.1 ns (25%)	-
		DCM	2.1 ns (100%)	-	-
1d	408	ACN	108 ps (13%)	1.7 ns (37%)	6 ns (50%)
		DCM	110 ps (16%)	1.5 ns (36%)	5.9 ns (50%)
1e	290	DCM	288 ps (63%)	3.14 ns (37%)	-
1g	408	ACN	24 ps (66%)	747 ps (9%)	3.8 ns (25%)
		DCM	35 ps (54%)	1 ns (17%)	4.3 ns (29%)
1h	408	ACN	60 ps (14%)	1.2 ns (19%)	5.5 ns (67%)
		DCM	79 ps (15%)	1.6 ns (31%)	4 ns (54%)

Table 1

Table 1 depicts the lifetimes of the excited species of **1a-h**. The biexponential and triexponential decay of the excited species of these molecules, suggest complex processes involved in their deactivation,¹ which could be explained only through further mechanistic investigations.

4.3.2. Fluorescence Quantum Yield

Quantum yield, one of the most important characteristics of a fluorophore, is defined as the number of emitted photons relative to the

number of absorbed photons. Substances with the largest quantum yields, approaching unity, such as rhodamines, display the brightest emissions.

The quantum yield exhibited by the selected molecules **1a-h** is illustrated in Table 2. The measurements were carried out using dimethyl aminobenzonitrile (DMABN) in acetonitrile as standard, with its quantum yield as 0.03. It was used because the excitation wavelength of DMABN matched with those of the samples.

Sample	Fluorescence Quantum Yield (ϕ_f^s)	
	In CH ₃ CN	In CH ₂ Cl ₂
1a	0.015	0.03
1b	0.001	0.0006
1c	0.0004	0.0006
1d	0.002	0.002
1e	0.002	0.003
1f	0.001	0.001
1g	0.0006	0.005
1h	0.001	0.002

Table 2

The dibenzobarrelene moiety without an olefin appendage at the bridgehead position, exhibited the largest quantum yield. The rest of the samples, having olefin moieties at the bridgehead position, showed very low

quantum yields, which might be due to the interactions between the olefin moieties and the dibenzobarrelene. Studies have shown that low values of ϕ_f suggests a "flexible" molecule for which a rapid radiationless deactivation may occur via a twisting motion about a carbon-carbon double bond.² It might also be due to quenching processes or might be the result of competing $S_1 \rightarrow T_1$ intersystem crossing.

4.4. Conclusion

The preliminary photophysical study of the dibenzobarrelenes **1a-d** and the bisdibenzobarrelenes **1e-h** were conducted utilising Time-Correlated Single-Photon Counting (TCSPC) Technique. The molecules **1a**, **1b**, **1d**, **1e**, **1g** and **1h** exhibited the formation of an internal charge transfer state upon excitation. **1c** and **1f** were non-fluorescent, which might be due to a large rate of internal conversion or a slow rate of emission. The biexponential and triexponential fluorescence decay, suggests complex processes involved in their deactivation. The excited state interaction between the bridgehead olefin appendages and the dibenzobarrelene moiety is confirmed through the very low fluorescence quantum yield.

References

1. Lakowicz, J. R. *Principles of Fluorescence Spectroscopy*, 3rd ed.; Springer, USA.
 2. Turro, N. J. *Modern Molecular Photochemistry*, The Benjamin/Cummings Publishing Co. Menlo Park, California, 1978.
 3. Lakowicz, J. R. *Encyclopedia of Molecular Biology and Molecular Medicine*, R. A. Meyers ed. VCH Publishers, New York, 1995, p. 294.
 4. Lowry, T. H.; Richardson, K. S. *Mechanism and Theory in Organic Chemistry*; 3rd ed.; Addison-Wesley, New York, 1998.
 5. Lamola, A. A.; Turro, N. J. in *Energy Transfer and Organic Photochemistry*, Vol. XIV, Interscience Publishers, New York, 1969.
 6. Itagaki, H.; Obukata, N.; Okamoto, A.; Horie, K.; Mita, I. *J. Am. Chem. Soc.* **1982**, *104*, 4469.
 7. Chandross, E. A.; Dempster, C. J. *J. Am. Chem. Soc.* **1970**, *92*, 3586.
 8. Fox, T.; Kotzian, M.; Rosch, N. *J. Chem. Phys.* **1993**, *97*, 11420.
 9. Fox, T.; Rosch, N.; Cortes, J.; Heitele, H. *Chem. Phys.* **1993**, *175*, 357.
 10. Cortes, J.; Heitele, H.; Jortner, J. *J. Chem. Phys.* **1994**, *98*, 2527.
 11. Birks, J. B. *Photophysics of Aromatic Molecules*, Wiley Interscience, New York, 1970.
 12. Becker, R. S. *Theory and Interpretation of Fluorescence and Phosphorescence*, Wiley Interscience, New York, 1969.
 13. O'Connor, D. V.; Phillips, D. *Time Correlated Single Photon Counting*, Academic Press, New York, 1984.
 14. Demas, J. N. *Excited State Life Time Measurements*, Academic Press, New York, 1983.
 15. Ware, W. R. *Creation and Detection of the Excited State*, Marcel Dekker, New York, 1971.
-

16. Jablonski, A. *Z. Phys.* **1935**, *94*, 38.
17. Rettig, W. *Angew. Chem., Int. Ed. Engl.*, **1986**, *25*, 971.
18. Kasha, M. *Disc. Faraday Soc.* **1950**, *9*, 14.

Photochemistry of Olefin appended Dibenzobarrelenes and Bisdibenzobarrelenes

5.1. Abstract

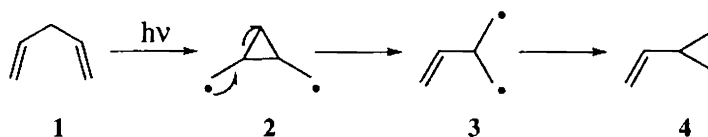
Dibenzocyclooctatetraene and dibenzosemibullvalene are the photoproducts obtained respectively through the singlet excited state and the triplet excited state of dibenzobarrelenes. Chemical literature shows evidences of the photoreactivity of dibenzobarrelenes generating both the singlet and triplet mediated photoproducts, in a single photoreaction. Our research target in synthesising various bridgehead olefin appended dibenzobarrelenes and bisdibenzobarrelenes, was based on the perception that olefins are efficient triplet quenchers, thereby quenching intramolecularly the triplet excited state of the barrelenes. A π -moiety at the bridgehead position of the dibenzobarrelene, creates a tetra π -methane system, which similar to a di- π or tri- π -methane systems, could be the fertile ground for interesting photochemical rearrangements. Our attempts in deciphering the photochemistry of the olefin appended dibenzobarrelenes and bisdibenzobarrelenes is the substance of this chapter.

5.2. Introduction

5.2.1. An Overview on the Theoretical Aspects of Di- π -methane Rearrangement

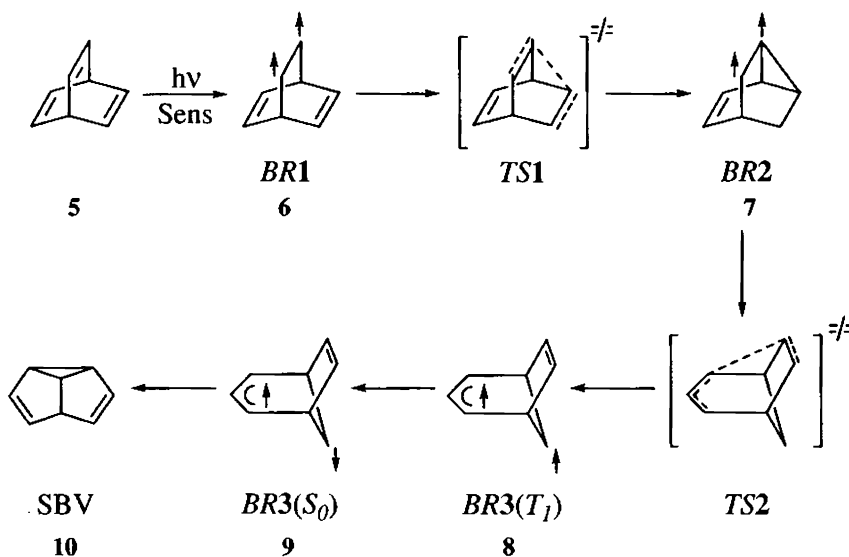
Di- π -methane rearrangement takes place when a molecule with two vinyl groups or equivalent π -moieties (i.e., aryl groups) linked to the same sp^3 carbon atom is irradiated to yield a vinylcyclopropane. The mechanism of di-

π -methane rearrangement illustrated in Scheme 1 depicts the 1,4- and 1,3-biradicals (**2** and **3**, respectively) as reaction intermediate species.



Scheme 1

The irradiation of barrelene in the presence of a triplet sensitizer leads to the formation of semibullvalene, the di- π -methane rearrangement product with a high yield,¹ while the direct photolysis of the molecule follows a pericyclic reaction, leading to the formation of cyclooctatetraene.² Theoretical studies on the photoreactivity of barrelene by direct as well as triplet-sensitized irradiation, has strongly proved the existence of the biradicals. The reaction takes place in four steps (Scheme 2).



Scheme 2

A schematic potential energy surface (PES) depicting the regions of T_1

and S_0 involved in the sensitised di- π -methane rearrangement, is shown in Figure 1.³ In the first step, after the triplet-sensitised excitation, the barrelene on T_1 yields the 1,2-biradical (BR1). An intersystem crossing (ISC) point T_1/S_0 , is located 39 kcal/mol above the BR1 in the PES. Therefore, due to its instability, this ISC is not an effective channel of deactivation to the ground state, which would otherwise have led to the recovery of the barrelene.

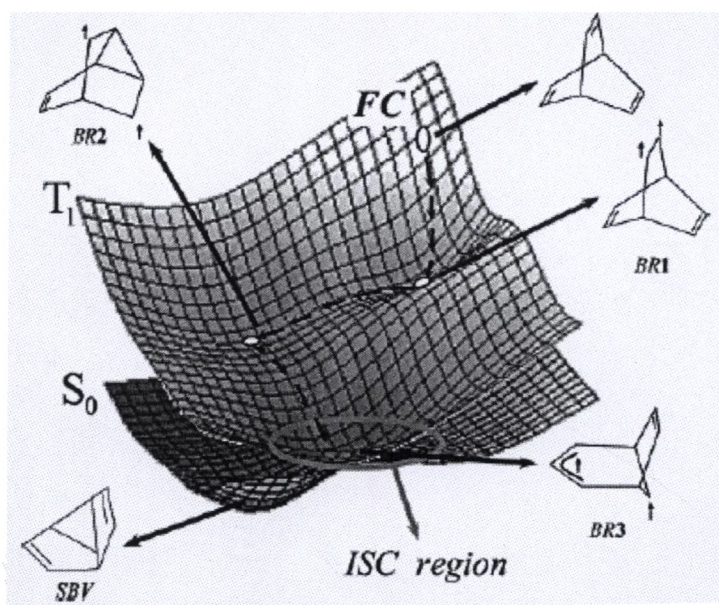
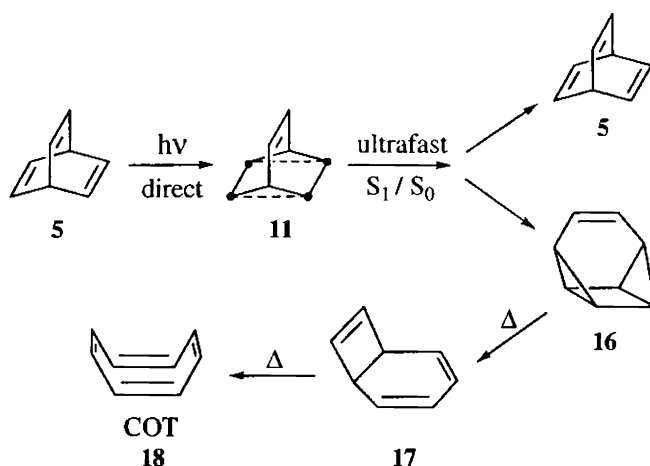


Figure 1

Any biradical species would tend to adopt a structure that minimises electron repulsion, so the formation of BR1 paves way to formation of the 1,3-biradical (BR2) and thereafter to the most stable biradical (BR3), a 1-allyl-1,3-biradical. As the system enters the 1,3-biradical region, the energy of T_1 and S_0 becomes very close, giving rise to a quasi-degenerate situation. The two half-filled orbitals containing the unpaired electrons in BR3 are nearly

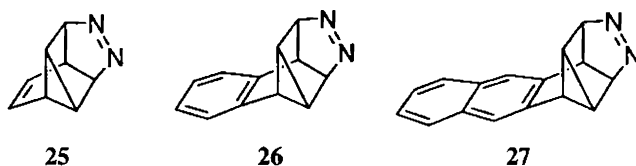
perpendicular, while those in BR2 are parallel. This could result in a much higher ISC rate for BR3 than for BR2, due to the angular dependence of the spin-orbit coupling (SOC) energy. So the surface crossing to the ground state would be clearly much more efficient at the BR3 region, not only because this is the most stable species, but also because of the enhanced SOC. Since the biradical BR3 is not a stable intermediate on the S_0 surface, the fast pairing of the two electrons finally yields semibullvalene as the only reaction product.



Scheme 3

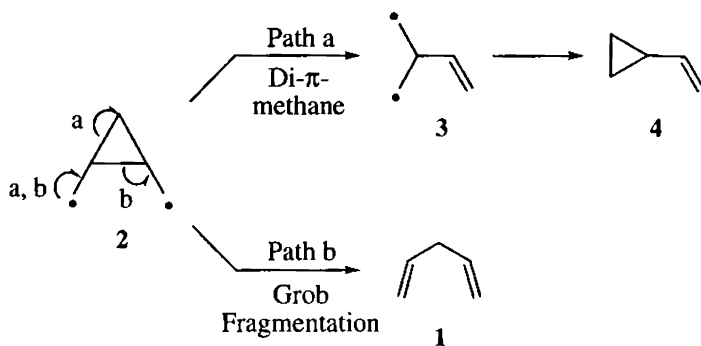
In the case of direct irradiation of barrelene into the first absorption band at 239 nm, the Franck-Condon (FC) excitation occurs and the system relaxes vibrationally, reaching a conical intersection region (CoInR), rather than a conical intersection point (CoIn), corresponding to the [2+2] cycloaddition CoIn topology.⁴ No intermediate is reached in the relaxation on S_1 , and the $S_1 \rightarrow S_0$ radiationless transition occurs via a CoIn in the time scale of a few molecular vibrations, supporting the ultrafast character of this reaction. Passing the CoInR, the system evolves on the ground state through

In an attempt to understand the behaviour of independently generated cyclopropyldicarbonyl diradical species, which is proposed as involved in the di- π -methane rearrangement of barrelenes to semibullvalenes, Zimmerman⁸ used the three azo compounds which are formal homo Diels-Alder adducts of nitrogen to barrelene **25**, benzobarrelene **26** and 2,3-naphthobarrelene **27** (Scheme 6).



Scheme 6

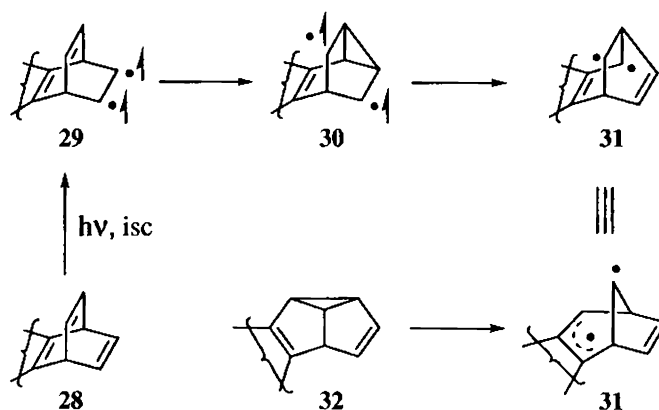
The thermal reactions of these azo compounds afforded exclusively the corresponding barrelenes. No semibullvalene or cyclooctatetraene could be discerned. Studies have shown that cyclopropyldicarbonyl diradical species **2** in the S_0 state undergoes a 1,4-(2,3)-fragmentation i.e. a Grob fragmentation⁹ leading to the starting reactant **1**, while the S_1 diradical species proceeds along the excited hypersurface towards the di- π -methane product **4**. Scheme 7 depicts the alternative modes of cyclopropyldicarbonyl diradical reactivity.



Scheme 7

In contrast, the photochemical reactions of **25**, **26** and **27** using sensitizers led to the formation of triplet excited state (T_1) which paved way for semibullvalenes, whereas the direct irradiations gave the corresponding barrelenes through the singlet excited state (S_1). The reasons for the semibullvalene formation from T_1 and the greater tendency of S_1 to give barrelenes were explained on the basis of potential energy hypersurfaces.

As shown in Figure 2, the excited state minima corresponds to cyclopropyldicarbonyl diradical **30** and the allylic diradical **31** (Scheme 8). The first minimum is directly above ground-state surface leading back to barrelene. The second excited state minimum is poised over a ground-state minimum which has a barrier leading onward to semibullvalene. This barrier is lower than the barrier leading backwards to barrelene. Hence, in the chemistry of triplet diradicals there seems to be an accumulation of allylic diradicals **31** and decay to product semibullvalenes. But in the chemistry of S_1 there is formation of cyclopropyldicarbonyl diradicals **30**, which then decay to barrelenes.



Scheme 8

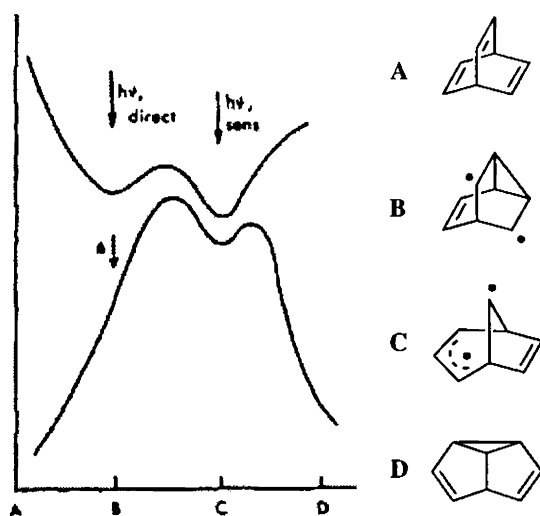
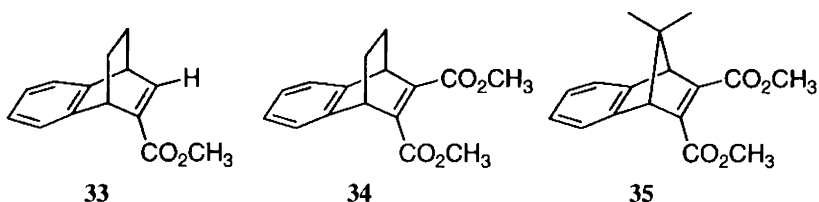


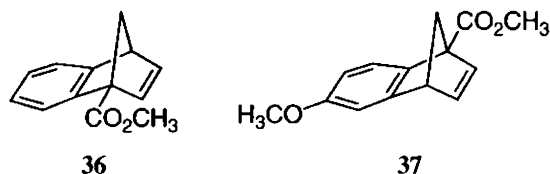
Figure 2

The studies on the substituent effects in some dihydrobenzobarrelenes and 7,7-dimethylbenzonorbornadienes¹⁰ performed by Hemetsberger *et al.*, has assisted in understanding the role of the substituents in di- π -methane rearrangement. It was found out that the acetone-sensitised irradiation of carbomethoxy-substituted system **33**, failed to rearrange, though the dicarbomethoxy substituted system and carbomethoxydibenzobarrelene⁵ could be isomerised. The dicarbomethoxy-substituted systems **34** and **35**, also do not rearrange at all. The reason for the inefficiency was interpreted in terms of spin-orbit coupling,^{11,12} which enhances the rate of intersystem crossing to starting material (Scheme 9).



Scheme 9

Paquette *et al.* had explored the effects of substituents in benzenorbornadienes,¹³ found that on introducing carbomethoxy at the bridgehead position of the benzenorbornadiene **36**, reduces the photoisomerisation efficiency considerably. The inefficiency is repeated in **37**, where a methoxy group is substituted on an aryl position and the carbomethoxy occupying the bridgehead position (Scheme 10).



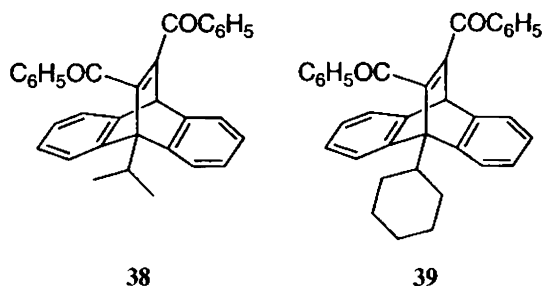
Scheme 10

Three causative factors were outlined for **36**. One possibility considered was the reduced rates of energy transfer from the sensitiser to the photoreactant. Another probable reason would be an increase in the decay or intersystem crossing. Yet another reason would be that, these particular electron-withdrawing substituents may introduce a competitive electron-transfer mode that reduces overall efficiency.

The scenario in **37** is such that, the internal transmission of excitation energy between the two pendant groups reaches a maximum. This leads to the onset of donor-acceptor interaction and triplet state deactivation.

George *et al.* have reported the reluctance of a few dibenzobarrelenes to undergo the barrelene-semibullvalene rearrangement under steady-state irradiation.¹⁴ The dibenzobarrelenes, 11,12-dibenzoyl-9,10-dihydro-9-isopropyl-9,10-ethenoanthracene **38** and 9-cyclohexyl-11,12-dibenzoyl-9,10-dihydro-9,10-ethenoanthracene **39** (Scheme 11), upon irradiation reverted almost quantitatively to the starting material along with the formation of a

small amount of dibenzocyclooctatetraene. Laser flash photolysis studies revealed the unusually short lifetimes of the triplets of **38** and **39**, which undergo fast decay to metastable intermediates, eventually reverting to reactant ground states.



Scheme 11

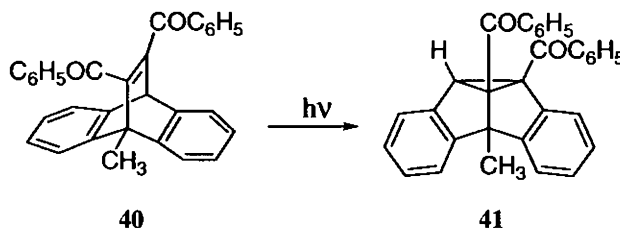
5.3. Results and Discussion

The photochemical studies were performed in a Rayonet Photochemical Reactor employing 300nm lamps. The criterion for the selection of 300 nm lamps for irradiation, was based on a simple Beer-Lambert calculation which reveals that for bulk reactivity, photolysis wavelength near the absorption tail should be used or else the incident radiation will be absorbed near the surface.⁷ Moreover the $S_0 \rightarrow S_1$ transition in dibenzobarrelenes takes place at 280 nm.¹⁵ Due to the solubility of the dibenzobarrelenes in benzene, and its transparency at the 300 nm region, led us to opt benzene as the ideal solvent for photochemical studies. Studies have shown that sensitizers transfer their triplet energy to the acceptor dibenzobarrelene, thereby quenching the singlet excited state of the substrate and promoting triplet mediated pathway.¹⁶ As the function of a sensitizer contradicted our target of quenching triplet excited states, sensitizers were not used in our studies.

An intramolecular quenching process outweighs the criteria of diffusion dependence, solvent effects, temperature etc of intermolecular quenching process, thereby making it more acceptable to photochemists. George *et al.* have performed studies on the intermolecular quenching process of some selected dibenzobarrelenes by triplet quenchers.¹⁷

Our investigations were based on the photochemistry exhibited by dimethyl 9-methyl-9,10-dihydro-9,10-ethenoanthracene-11,12-dicarboxylate **22a** and 9-methyl -11,12-dibenzoyl-9,10-dihydro-9,10-ethenoanthracene **40**. Scheme 5 illustrates the photochemical behaviour of **22a** upon direct irradiation in solution and in solid state. Both cyclooctatetraene (COT) and the di- π -methane rearrangement product semibullvalene are formed. The COT formed was that derived from 1,4-biradical fragmentation rather than [2+2] photocycloaddition.

George *et al.* demonstrated that irradiation of **40** in benzene, acetone or methanol gave the semibullvalene **41** and a small amount of benzoic acid (Scheme 12).¹⁷



Scheme 12

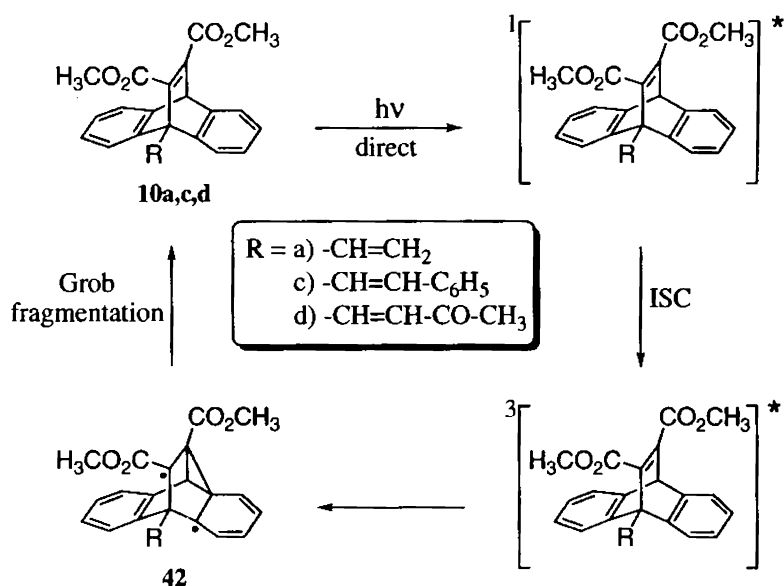
5.3.1 Photochemistry of DMAD adducts of 9-Alkenylantracenes (10a-e)

The irradiation of **10a,c,d** in benzene under nitrogen atmosphere, resulted in the recovery of the starting material with varying amounts of polymeric material. The inability to agitate the solution under irradiation, in

the Rayonet Photochemical Reactor might have contributed to the formation of polymeric residues. The characterisation of the polymeric residues was not successful through spectral methods, as the spectra showed broad featureless peaks. Instances of polymeric residues are reported in the works of Hemmetsberger¹⁸ and Richards.¹⁹ The photochemically unreactive behaviour of **10a,c,d** could be clarified through the photochemical studies conducted on various dicarbomethoxy substituted systems, by some eminent photochemists.

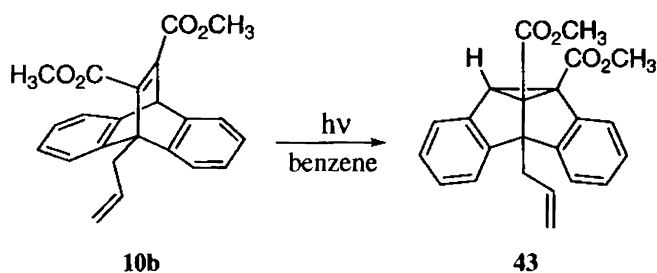
According to Zimmerman, the 1,4-biradicals formed during the photorearrangement might undergo Grob fragmentation²⁰ leading to the reactant. Theoretical works on di- π -methane rearrangement has shown that the 1,4-diradical (T_1) of barrelene, on intersystem crossing will lead to the (S_0) 1,4-singlet diradical, which is known to revert to the corresponding barrelene. The works of Hemmetsberger¹⁰ has shown that dicarbomethoxy substituted systems undergo spin-orbit coupling, which leads to enhanced rate of intersystem crossing to starting material, driving the photoisomerisation completely inefficient.

In the UV-visible absorption spectra of the synthesized dibenzobarrelenes, a broad shoulder is observed at about 290 nm ($\epsilon = 400 \text{ mol}^{-1} \text{ cm}^{-1}$) at the red end. Based on the studies conducted on dibenzobarrelene-dicarboxymethylester,¹⁵ Fox *et al.* have suggested that this shoulder absorption indicates the existence of a new first excited state due to a significant interaction between the aromatic donor moiety and the electron accepting ester groups. The donor-acceptor interaction could have led to the triplet state deactivation in the dibenzobarrelenes as suggested by Paquette *et al.*¹³



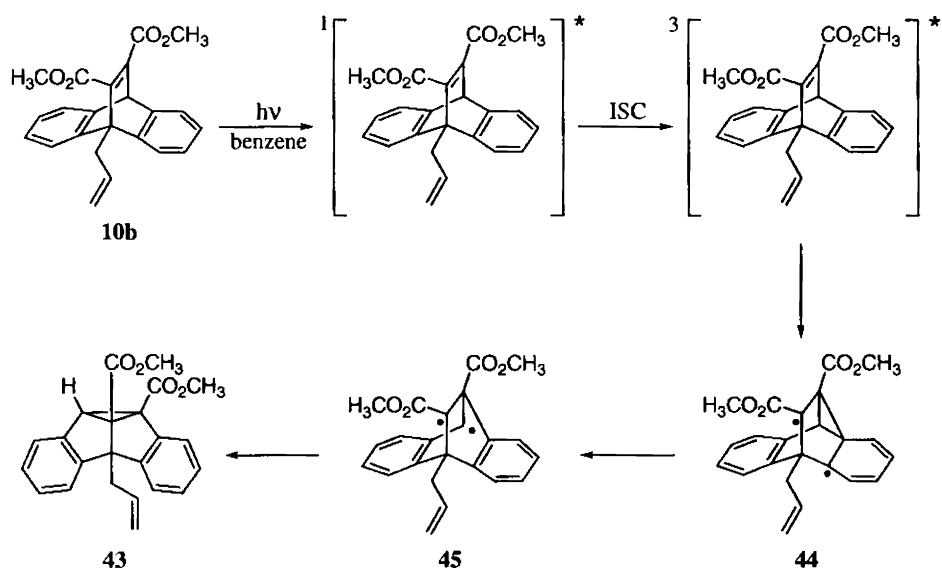
Scheme 13

Chemical literature reveals that carbomethoxy groups have an enhanced rate of intersystem crossing.¹⁰ A triplet mediated photoisomerisation, in the case of **10a,c,d** could have resulted in the reversion of the 1,4-biradicals **42** to the ground state dibenzobarrelenes **10a,c,d** (Scheme 13).



Scheme 14

The irradiation of **10b**, gave a 4b-substituted semibullvalene **43** as the photoproduct (Scheme 14).



Scheme 15

A remote olefin moiety, behaved in a similar manner to a methyl substituent, not interfering in the photochemistry of the bridgehead allyl appended dibenzobarrelene. The mechanism of the photoreaction is depicted in Scheme 15.

As the R_f values of **10b** and **43** were very close, their separation through column chromatography on silica gel was not successful. In comparison with previous literature,¹⁷ the ^1H NMR spectrum of the photoproduct mixture (Figure 3), facilitated in identifying the 4b-substituted semibullvalene. The doublets at δ 3.24 and at δ 3.28 represent the two methylene protons of the allyl moiety. The methoxy protons appear as two singlets at δ 3.67 and δ 3.86. The singlet at δ 4.35 ascertains the proton at C-8b of **43**. The two doublet of doublets at δ 5.17 and at δ 5.07, indicate the unsaturated geminal protons of the allyl moiety, with coupling constant values of 12.7 Hz and 7.3 Hz respectively. The unsaturated methine proton of allyl, appears as a multiplet at δ 5.72. The multiplets from δ 7.03 to δ 7.64

represents the aromatic protons.

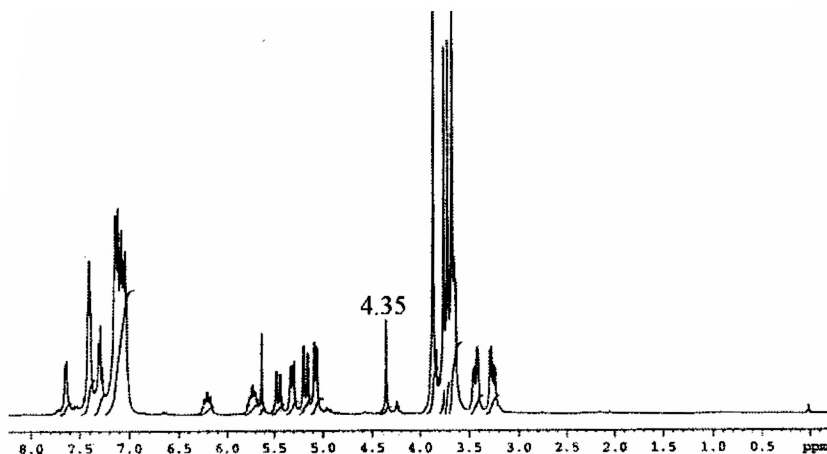
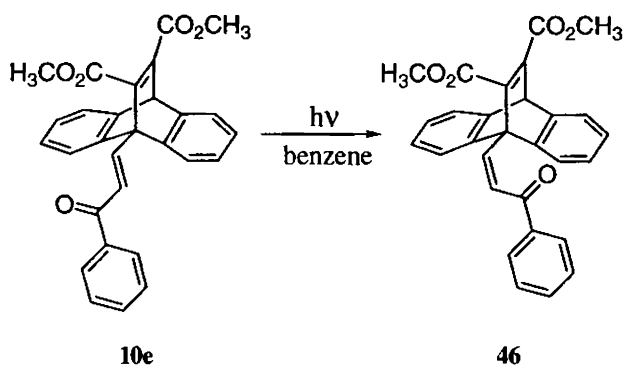
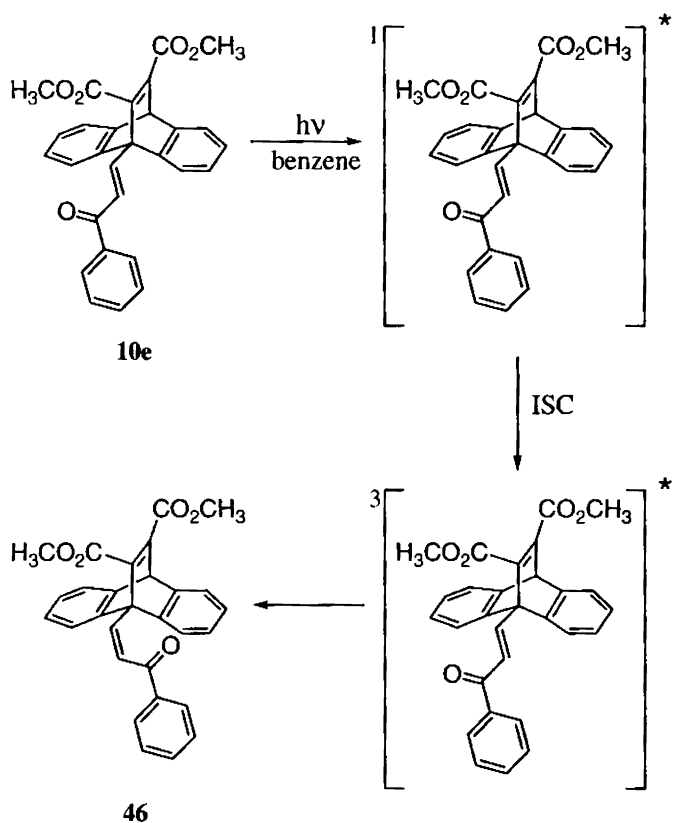


Figure 3: ^1H NMR spectrum of photoproduct mixture of **10b**

Irradiation of **10e** in benzene at 300 nm, led to *cis-trans* isomerisation of the olefinic bond, resulting in **46** as the sole photoproduct (Scheme 16). The triplet energy of the dibenzobarrelene **10e** was dissipated through the *cis-trans* isomerisation of the bridgehead appended 1-phenylprop-2-en-1-one moiety as shown in Scheme 17, thus proving the olefin to be an efficient intramolecular quencher of the triplet excited state of the dibenzobarrelene.



Scheme 16



Scheme 17

The structural identity of **46** was confirmed through spectral and analytical data. In the IR spectrum of **46**, the α,β -unsaturated carbonyl stretching peak appears at 1672 cm^{-1} and the ester carbonyls appear at 1711 and 1726 cm^{-1} . In the ^1H NMR spectrum, the methoxy protons appear as two singlets at δ 3.54 and δ 3.73. The bridgehead methine proton appears as a singlet at δ 5.58. The doublets at δ 6.93 and at δ 7.30 represent the vinylic protons with a coupling constant value of 5.1 Hz, establishing the *Z*-geometry of the olefinic bond. The multiplets from δ 7.00 to δ 7.97 represent the aromatic protons. The signals at δ 51.02 and at δ 58.12 in the ^{13}C NMR

spectrum, indicate the tertiary and the quaternary bridgehead carbon respectively. The signals at δ 52.00 and δ 52.30 represent the two methoxy carbons. The signals of the aromatic and vinylic carbon appear from δ 122.67 to δ 153.58. The two signals at δ 164.54 and δ 166.80 represent the ester carbonyls and the signal at δ 188.53 indicates the α,β -unsaturated carbonyl group.

The single crystal X-ray diffraction analysis conducted on the crystal of **46**, unequivocally confirms the *Z*-geometry of the bridgehead olefin. The ORTEP diagram of compound **46** is shown in Figures 4 and 5.

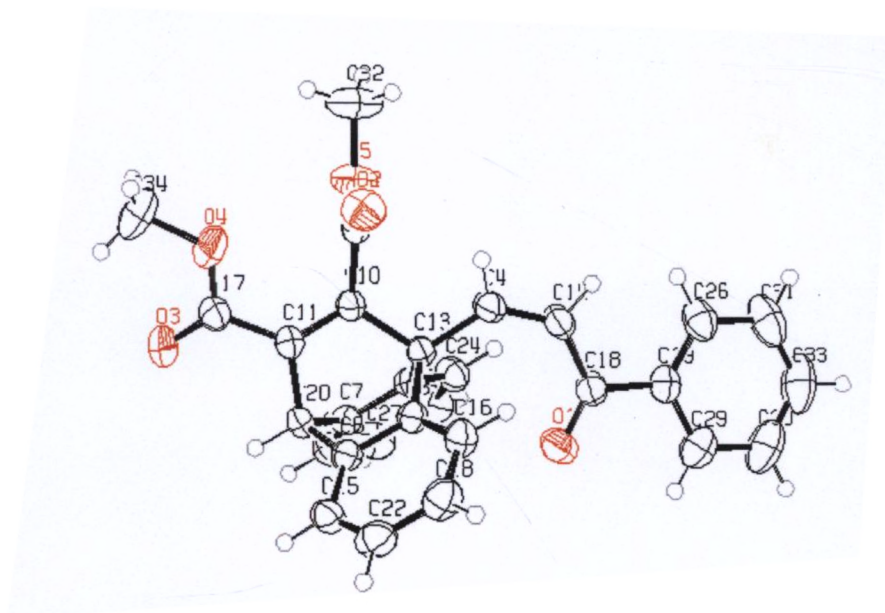


Figure 4. ORTEP diagram of molecular structure of compound **46** in the crystal (side view)

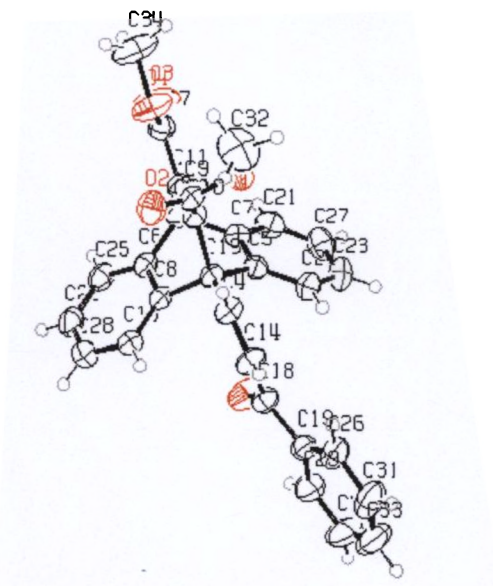
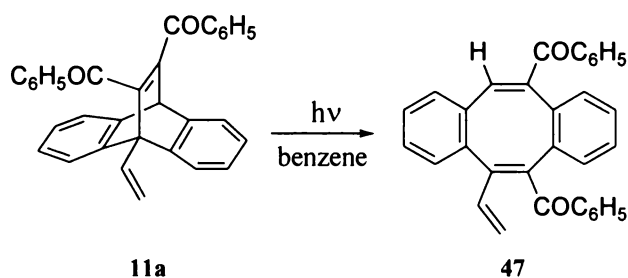


Figure 5. ORTEP diagram of molecular structure of compound **46** in the crystal (front view)

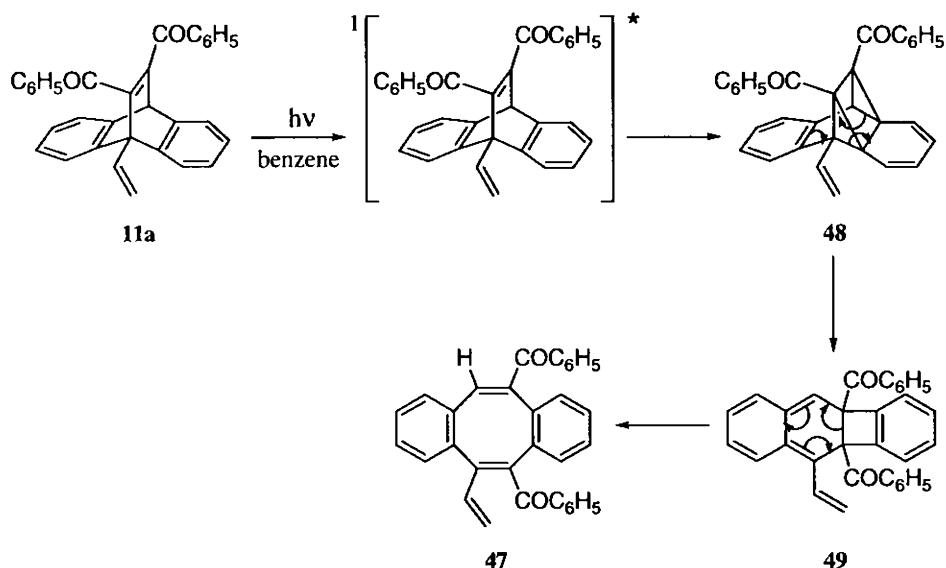
5.3.2. Photochemistry of DBA adducts of 9-Alkenylanthracenes (11a-e)

Photolysis of **11a** in benzene at 300 nm gave the dibenzocyclooctatetraene **47** as the only photoproduct (Scheme 18). Typically, 11,12-dibenzoyldibenzobarrelenes undergo efficient intersystem crossing leading to triplet-mediated products, dibenzosemibullvalenes.



Scheme 18

In spite of the fact that benzoyl group being an efficient intramolecular intersystem crossing catalyst, singlet mediated product is formed. The triplet excited species formed in this scenario, might be too short lived to favour a triplet mediated product. The following mechanism (Scheme 19) is proposed for the photochemical outcome.



Scheme 19

The structural identity of the photoproduct **47** was established through spectral and analytical data. The stretching frequency of the benzoyl carbonyl groups appeared at 1659 cm^{-1} in the IR spectrum of **47**. The bridgehead proton was completely absent in the ^1H NMR spectrum. The doublets at δ 4.96 and at δ 5.26 represent the geminal vinylic protons of the olefin moiety. The multiplet from δ 6.66 to δ 6.73 signifies the methylene proton of the olefin. The signals from δ 7.12 to δ 8.11 indicate the aromatic protons. The vinylic proton of the cyclooctatetraene moiety appears as a singlet at δ 7.64.

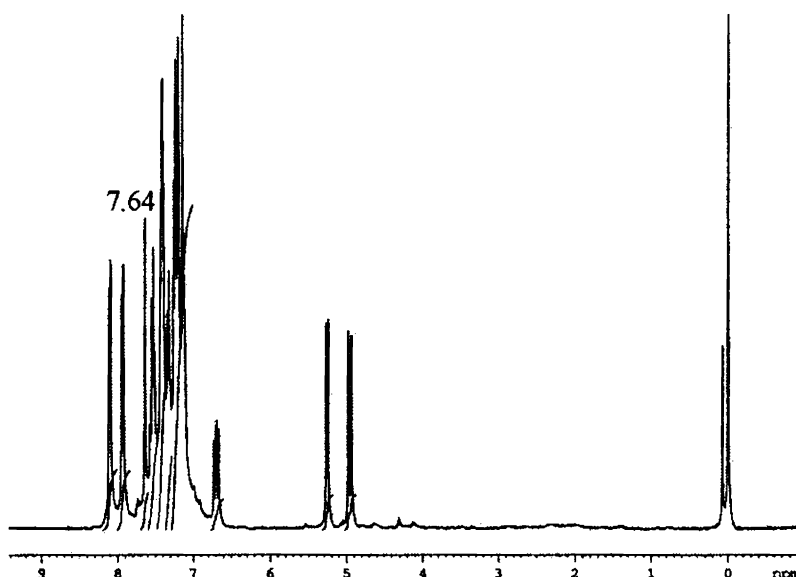
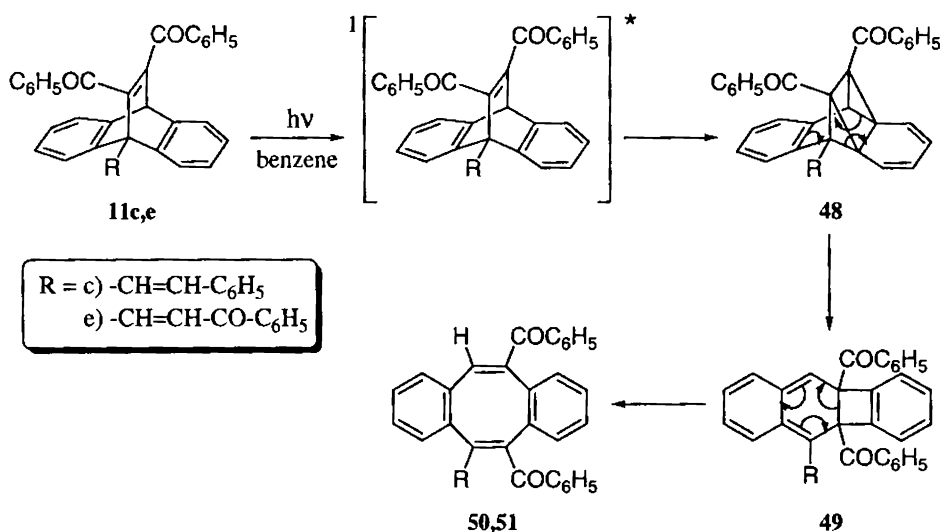


Figure 6: ^1H NMR spectrum of **47**

In the ^{13}C NMR spectrum of **47**, the vinylic and aromatic protons are designated by the signals from δ 121.21 to δ 144.47. The signals at δ 196.12 and at δ 197.66 represent the dibenzoyl carbonyl functionalities.

Quenching of triplet excited state was also observed in the irradiation of **11c** and **11e**, in benzene at 300 nm, resulting in the formation of the dibenzocyclooctatetraene **50** and **51** respectively. Here also there was no trace of dibenzosemibullvalenes, indicating an efficient intramolecular quenching of the triplet excited states of the dibenzobarrelenes by the styryl moiety appended at the bridgehead position in **11c** and by 1-phenylprop-2-en-1-one in **11e**. The mechanism of the formation of photoproducts **50** and **51**, via the singlet mediated pathway is depicted in Scheme 20.



Scheme 20

Through spectral and analytical data, the structural identity of the photoproduct **50** was confirmed. The IR spectrum of **50** showed the carbonyl stretching frequency at 1667 cm^{-1} and the stretching frequency of the olefin part of the styryl moiety appeared at 1655 cm^{-1} . The doublet at $\delta 6.21$ in the ^1H NMR spectrum, indicates a vinylic proton of styryl, having a coupling constant value of 16 Hz. The *E*-geometry of the olefin is retained in the photoproduct. A singlet at $\delta 7.67$ denotes the vinylic proton of the cyclooctatetraene. The multiplets from $\delta 7.10$ to $\delta 8.12$ represent the aromatic and vinylic proton.

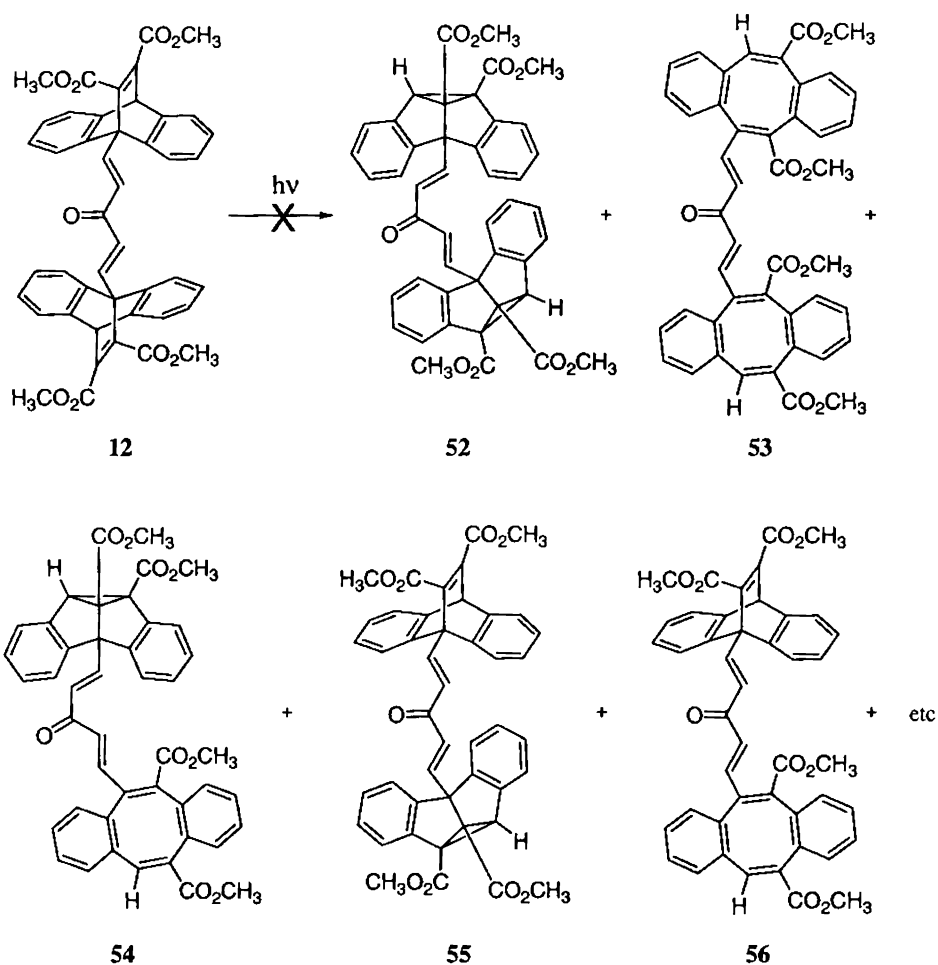
The structural identity of **51** was established through spectral and analytical data. In the IR spectrum, the carbonyl stretching frequency appears at 1664 cm^{-1} . The signals from $\delta 7.12$ to $\delta 7.96$ in the ^1H NMR spectrum, represents the vinylic and aromatic protons. In the ^{13}C NMR spectrum, the signals from $\delta 121.89$ to $\delta 148.07$ represent the vinylic and aromatic carbon. The two benzoyl carbon appear at $\delta 195.29$ and at $\delta 196.80$.

Photolysis of **11b** in benzene at 300nm, gave a complex mixture of photoproducts, which we were unable to isolate and identify.

Irradiation of **11d** in benzene at 300nm, gave a photoproduct having a lactone ring, as identified via the IR spectral analysis indicating the carbonyl stretching peak at 1764 cm^{-1} . The α,β -unsaturated carbonyl group appears at 1677 cm^{-1} . The photoproduct could not be separated and identified due to low yield and its structural identity has not been established.

5.3.3. Photochemistry of Bisdibenzobarrelenes (12-15)

We have synthesised some novel bisdibenzobarrelenes, **12**, **13**, **14** and **15**. Based on literature precedence on the photochemistry of dibenzobarrelenes, the photoproducts depicted in Scheme 21 were anticipated. The solvents, acetone and dichloromethane were used for studying the photochemistry of these novel molecular systems. Contrary to our anticipation of many photoproducts, the photoreaction resulted in polymeric material along with some starting material.



Scheme 21

The inefficiency of bisdibenzobarrelenes towards di- π -methane rearrangement might be due to reversion of the cyclopropyldicarbonyl diradicals to the starting material. Scheme 22 depicts the mechanism of the reversion to the starting compound.

an inert behaviour towards photochemical reactivity.

5.5. Experimental

5.5.1. General Procedures

All melting points are uncorrected and were determined on a Neolab melting point apparatus. All reactions and chromatographic separations were monitored by thin layer chromatography (TLC). Aluminium sheets coated with silica (Merck) were used for thin layer chromatography. Visualisation was achieved by exposure to iodine vapour or UV radiation. Column chromatography was carried out with slurry-packed silica (Qualigens 60-120 mesh). All steady state irradiations were carried out using Rayonet Photochemical Reactor (RPR). Solvents for photolysis were purified and distilled before use. Absorption spectra were recorded using Shimadzu 160A spectrometer and infrared spectra were recorded using ABB Bomem (MB series) FT-IR spectrophotometer respectively. The ^1H and ^{13}C NMR spectra were recorded at 300 and 75 MHz on a Bruker FT-NMR spectrometer with tetramethylsilane (TMS) as internal standard. Chemical shifts are reported in parts per million (ppm) downfield of tetramethylsilane. FAB mass spectra were recorded on a JOEL SX 102/DA-6000 using argon/xenon as the FAB gas, at Central Drug Research Institute (CDRI), Lucknow. Elemental analysis was performed on Elementar Systeme (Vario ELIII) at Regional Sophisticated Instrumentation Centre (STIC), Kochi.

5.5.2. Photochemical Studies of Dibenzobarrelenes (10a-e) and (11a-e)

5.5.2.1. Irradiation of 10a: A degassed solution of **10a** (0.28 g, 0.8 mmol) in benzene (130 mL) was irradiated using RPR 300 nm lamp for 10 h. The progress of the reaction was monitored by TLC. Removal of the solvent under

reduced pressure gave a residual solid, which was chromatographed over silica gel. Elution with a mixture (1:1) of dichloromethane and hexane gave unchanged **10a** (25%, mp 180 °C). Further elution with a mixture (1:9) of methanol and dichloromethane gave a polymeric residue.

5.5.2.2. Irradiation of 10b: A degassed solution of **10b** (0.28 g, 0.8 mmol) in benzene (130 mL) was irradiated using RPR 300 nm lamp for 6 h. The progress of the reaction was monitored by TLC. Removal of the solvent under reduced pressure gave a residual solid, which was chromatographed over silica gel. Elution with a mixture (1:1) of hexane and dichloromethane 0.16 g of **43**. Further elution with a mixture (2:3) of hexane and dichloromethane gave unchanged **10b** (25%, mp 128 °C).

Compound 43: (56%); mixture mp 147 °C; ¹H NMR (CDCl₃) δ 3.24 (1H, d, methylene), 3.28 (1H, d, methylene), 3.67 (3H, s, OCH₃), 3.86 (3H, s, OCH₃), 4.35 (1H, s, 8b-H), 5.07 (1H, dd, $J_{cis}=7.3$ Hz, vinylic), 5.17 (1H, dd, $J_{trans}=12.7$ Hz, vinylic), , 5.72 (1H, m, vinylic), 7.03-7.64 (8H, m, aromatic).

5.5.2.3. Irradiation of 10c: A degassed solution of **10c** (0.33 g, 0.8 mmol) in benzene (130 mL) was irradiated using RPR 300 nm lamp for 10 h. The progress of the reaction was monitored by TLC. Removal of the solvent under reduced pressure gave a residual solid, which was chromatographed over silica gel. Elution with a mixture (2:3) of hexane and dichloromethane gave unchanged **10c** (37%, mp 176 °C). Further elution with a mixture (1:9) of methanol and dichloromethane gave a polymeric residue.

5.5.2.4. Irradiation of 10d: A degassed solution of **10d** (0.27 g, 0.7 mmol) in benzene (130 mL) was irradiated using RPR 300 nm lamp for 4 h. The progress of the reaction was monitored by TLC. Removal of the solvent under reduced pressure gave a residual solid, which was chromatographed over silica

gel. Elution with a mixture (1:4) of hexane and dichloromethane gave unchanged **10d** (40%, mp 150-152 °C). Further elution with a mixture (1:9) of methanol and dichloromethane gave a polymeric residue.

5.5.2.5. Irradiation of 10e: A degassed solution of **10e** (0.35 g, 0.8 mmol) in benzene (130 mL) was irradiated using RPR 300 nm lamp for 2 h. The progress of the reaction was monitored by TLC. Removal of the solvent under reduced pressure gave a residual solid, which was chromatographed over silica gel. Elution with a mixture (3:2) of hexane and ethylacetate gave unchanged **10e** (27%, mp 166 °C). Further elution with a mixture (1:1) of hexane and ethylacetate gave 0.23 g of **46**, which was further purified by recrystallisation from a mixture of hexane and ethylacetate (2:1).

Compound 46: (64%); mp 207-208 °C; IR ν_{\max} (KBr) 1711, 1726 (C=O, ester), 1672 (C=O, ketone) cm^{-1} ; ^1H NMR (CDCl_3) δ 3.54 (3H, s, OCH_3), 3.73 (3H, s, OCH_3), 5.58 (1H, s, methine), 6.93 (1H, d, J_{AX} = 5.1 Hz, vinylic), 7.30 (1H, d, J_{AX} = 5.1 Hz, vinylic), 7.00-7.97 (13H, m, aromatic); ^{13}C NMR (CDCl_3) δ 51.02, 52.00, 52.30, 58.12, 122.67, 123.88, 124.46, 125.32, 128.37, 128.68, 128.77, 133.02, 137.82, 138.14, 142.53, 143.12, 143.85, 153.58, 164.54, 166.80, 188.53; FAB-MS m/z 451 (M^+ +1), 391 (M^+ - CO_2CH_3) and other peaks. Anal. Calcd for $\text{C}_{29}\text{H}_{22}\text{O}_5$: C, 77.32; H, 4.92. Found: C, 77.21; H, 5.15.

5.5.2.6. Irradiation of 11a. A degassed solution of **11a** (0.30 g, 0.7 mmol) in benzene (130 mL) was irradiated using RPR 300 nm lamp for 1 h. The progress of the reaction was monitored by TLC. Removal of the solvent under reduced pressure gave a residual solid, which was chromatographed over silica gel. Elution with a mixture (3:2) of hexane and dichloromethane gave 0.20 g of **47**, which was further purified by recrystallisation from a mixture of

dichloromethane and hexane (2:1). Further elution with a mixture (1:1) of hexane and dichloromethane gave unchanged **11a** (27%, mp 152 °C).

Compound 47: (65%); mp 108 °C; IR ν_{\max} (KBr) 1659 (C=O, ketone) cm^{-1} ; ^1H NMR (CDCl_3) δ 4.96 (1H, d, J_{AX} = 16.9 Hz, vinylic), 5.26 (1H, d, J_{AX} = 10.7 Hz, vinylic), 6.66-6.73 (1H, m, vinylic), 7.12-8.11 (18H, m, aromatic), 7.64 (1H, s, vinylic); ^{13}C NMR (CDCl_3) δ 121.21, 126.56, 127.39, 127.44, 127.83, 127.99, 128.24, 128.35, 128.67, 128.88, 129.00, 129.27, 129.70, 129.91, 130.02, 130.62, 130.75, 130.92, 131.26, 132.24, 132.49, 132.75, 133.78, 135.27, 135.69, 136.26, 136.51, 136.77, 137.87, 140.78, 141.03, 141.24, 144.47, 196.12, 197.66. Anal. Calcd for $\text{C}_{32}\text{H}_{22}\text{O}_2$: C, 87.65; H, 5.06. Found: C, 87.12; H, 4.78.

5.5.2.7. Irradiation of 11b: A degassed solution of **11b** (0.36 g, 0.8 mmol) in benzene (130 mL) was irradiated using RPR 300 nm lamp for 2 h. The progress of the reaction was monitored by TLC. Removal of the solvent under reduced pressure gave a residual solid, which gave a complex mixture of products, which we were unable to isolate and identify.

5.5.2.8. Irradiation of 11c: A degassed solution of **11c** (0.30 g, 0.5 mmol) in benzene (130 mL) was irradiated using RPR 300 nm lamp for 3 h. The progress of the reaction was monitored by TLC. Removal of the solvent under reduced pressure gave a residual solid, which was chromatographed over silica gel. Elution with a mixture (3:2) of hexane and chloroform gave 0.16 g of **50**, which was further purified by recrystallisation from a mixture of chloroform and hexane (2:1). Further elution with a mixture (1:1) of hexane and chloroform gave unchanged **11c** (30%, mp 190 °C).

Compound 50: (62%); mp 182 °C; IR ν_{\max} (KBr) 1667 (C=O, ketone), 1655 cm^{-1} ; ^1H NMR (CDCl_3) δ 6.21 (1H, d, J_{AX} = 16.0 Hz, vinylic), 7.10-8.12 (19H,

m, aromatic and vinylic), 7.67 (1H, s, vinylic). Anal. Calcd for $C_{38}H_{26}O_2$: C, 88.69; H, 5.09. Found: C, 89.04; H, 5.55.

5.5.2.9. Irradiation of 11d. A degassed solution of **11d** (0.35 g, 0.7 mmol) in benzene (130 mL) was irradiated using RPR 300 nm lamp for 2 h. The progress of the reaction was monitored by TLC. Removal of the solvent under reduced pressure gave a residual solid, which was chromatographed over silica gel. Elution with a mixture (1:1) of hexane and dichloromethane gave 0.10 g of a photoproduct (30%, mixture mp 110 °C). Further elution with a mixture (2:3) of hexane and dichloromethane gave unchanged **11d** (35%, mp 186-188 °C).

5.5.2.10. Irradiation of 11e. A degassed solution of **11e** (0.35 g, 0.6 mmol) in benzene (130 mL) was irradiated using RPR 300 nm lamp for 1 h. The progress of the reaction was monitored by TLC. Removal of the solvent under reduced pressure gave a residual solid, which was chromatographed over silica gel. Elution with a mixture (7:3) of hexane and dichloromethane gave 0.19 g of **51**, which was further purified by recrystallisation from a mixture of hexane and dichloromethane (1:1).. Further elution with a mixture (3:2) of hexane and dichloromethane gave unchanged **11e** (36%, mp 120 °C).

Compound 51: (58%); mp 170 °C; IR ν_{\max} (KBr) 1664 (C=O, ketone) cm^{-1} ; ^1H NMR (CDCl_3) 7.12-7.96 (26H, m, aromatic and vinylic); ^{13}C NMR (CDCl_3) δ 121.89, 123.64, 124.76, 125.54, 125.87, 126.08, 127.38, 127.68, 127.76, 128.11, 128.25, 128.35, 128.59, 128.80, 128.89, 129.13, 129.15, 129.77, 129.83, 130.14, 130.47, 131.13, 131.86, 132.23, 132.39, 133.56, 136.11, 136.35, 136.64, 137.83, 140.64, 142.88, 143.39, 148.07, 195.29, 196.80. Anal. Calcd for $C_{39}H_{26}O_3$: C, 86.32; H, 4.83. Found: C, 86.99; H, 5.31.

5.5.3. Photochemical Studies of Bisdibenzobarrelenes (12-15)

5.5.3.1. Irradiation of 12: A degassed solution of **12** (0.32 g, 0.4 mmol) in dichloromethane (130 mL) was irradiated using RPR 300 nm lamp for 10 h. The progress of the reaction was monitored by TLC. Removal of the solvent under reduced pressure gave a residual solid, which was chromatographed over silica gel. Elution with a mixture (4:1) of hexane and ethyl acetate gave unchanged **12** (30%, mp >280 °C). Further elution with a mixture (1:1) of hexane and ethyl acetate gave a polymeric residue.

In a repeat run, an acetone solution of **12** was irradiated using RPR 300 nm lamp for 5 h, yielded 33% of unchanged **12** and polymeric residue.

In a repeat run, an acetone solution of **12** was irradiated using RPR 254 nm lamp for 8 h, yielded 26% of unchanged **12** and polymeric residue.

5.5.3.2. Irradiation of 13: A degassed solution of **13** (0.30 g, 0.4 mmol) in dichloromethane (130 mL) was irradiated using RPR 300 nm lamp for 6 h. The progress of the reaction was monitored by TLC. Removal of the solvent under reduced pressure gave a residual solid, which was chromatographed over silica gel. Elution with a mixture (7:3) of dichloromethane and hexane gave unchanged **13** (27%, mp >280 °C). Further elution with a mixture (1:9) of methanol and dichloromethane gave a polymeric residue.

In a repeat run, an acetone solution of **13** was irradiated using RPR 300 nm lamp for 4h, yielded 38% of unchanged **13** and polymeric residue.

5.5.3.3. Irradiation of 14: A degassed solution of **14** (0.27 g, 0.3 mmol) in benzene (130 mL) was irradiated using RPR 300 nm lamp for 10 h. The progress of the reaction was monitored by TLC. Removal of the solvent under reduced pressure gave a residual solid, which was chromatographed over silica gel. Elution with a mixture (7:3) of dichloromethane and hexane gave

unchanged **14** (28%, mp 176-178 °C). Further elution with a mixture (1:9) of methanol and dichloromethane gave a polymeric residue.

In a repeat run, an acetone solution of **14** was irradiated using RPR 300 nm lamp for 5h, yielded 31% of unchanged **14** and polymeric residue.

5.5.3.4. Irradiation of 15: A degassed solution of **15** (0.28 g, 0.3 mmol) in dichloromethane (130 mL) was irradiated using RPR 300 nm lamp for 10 h. The progress of the reaction was monitored by TLC. Removal of the solvent under reduced pressure gave a residual solid, which was chromatographed over silica gel. Elution with a mixture (4:1) of dichloromethane and hexane gave unchanged **15** (36%, mp >280 °C). Further elution with a mixture (1:9) of methanol and dichloromethane gave a polymeric residue.

In a repeat run, an acetone solution of **15** was irradiated using RPR 300 nm lamp for 7h, yielded 29% of unchanged **15** and polymeric residue.

References

1. Zimmerman, H. E.; Binkley, R. W.; Givens, R. S.; Sherwin, M. A. *J. Am. Chem. Soc.* **1967**, *98*, 393.
2. Rabideau, P. W.; Hamilton, J. B.; Friedman, L. *J. Am. Chem. Soc.* **1968**, *90*, 4465.
3. Frutos, L. M.; Sancho, U.; Castano, O. *Org. Lett.* **2004**, *6*, 1229.
4. Olivucci, M.; Bernardi, F.; Ottani, S.; Robb, M. A. *J. Am. Chem. Soc.* **1994**, *116*, 2034.
5. Ciganek, E. *J. Am. Chem. Soc.* **1966**, *88*, 2882.
6. Adam, W.; De Lucchi, O.; Peters, K.; Peters, E-M.; von Schering, H. G. *J. Am. Chem. Soc.* **1982**, *104*, 5747.
7. Chen, J.; Scheffer, J. R.; Trotter, J. *Tetrahedron* **1992**, *48*, 3251.
8. Zimmerman, H. E.; Boettcher, R. J.; Buehler, N. E.; Keck, G. E.; Steinmetz, M. G. *J. Am. Chem. Soc.* **1976**, *98*, 7680.
9. Grob, C. A. *Angew. Chem.* **1969**, *81*, 543.
10. Hemetsberger, H.; Nobbe, M. *Tetrahedron* **1988**, *44*, 67.
11. Kasha, M. *J. Chem. Phys.* **1952**, *20*, 71.
12. Turro, N. J. *Modern Molecular Photochemistry*, The Benjamin/Cummings Publishing Co. Menlo Park, California, **1978**, p 48.
13. Paquette, L. A.; Varadarajan, A.; Burke, L. D. *J. Am. Chem. Soc.* **1986**, *108*, 8032.
14. Pratapan, S.; Ashok, K.; Cyr, D. R.; Das, P. K.; George, M. V. *J. Org. Chem.* **1987**, *52*, 5512.
15. Fox, T.; Roesch, N.; Cortes, J.; Heitele, H. *Chem. Phys.* **1993**, *175*, 357.
16. Cristol, S. J.; Kaufman, R. L.; Opitz, S. M.; Szalecki, W.; Bindel, T. H. *J. Am. Chem. Soc.* **1983**, *105*, 3226.

17. Kumar, C. V.; Murty, B. A. R. C.; Lahiri, S.; Chackachery, E.; Scaiano, J. C.; George, M. V. *J. Org. Chem.* **1984**, *49*, 4923.
18. Hemetsberger, H.; Nispel, F. *Tetrahedron* **1990**, *46*, 3823.
19. Paddick, R. G.; Richards, K. E.; Wright, G. J. *Aust. J. Chem.* **1976**, *29*, 1005.
20. Grob, C. A.; Schiess, P. W. *Angew. Chem.* **1967**, *79*, 1.